HOKKAIDO UNIVERSITY

Title	FUNDAMENTAL STUDIES ON A FISHING BOAT'S POSITION
Author(s)	HIRAIWA, Takashi
Citation	MEMOIRS OF THE FACULTY OF FISHERIES HOKKAIDO UNIVERSITY, 25(1), 1-96
Issue Date	1977-12
Doc URL	http://hdl.handle.net/2115/21864
Type	bulletin (article)
File Information	25(1)_P1-96.pdf

Instructions for use

FUNDAMENTAL STUDIES ON A FISHING BOAT'S POSITION

Takashi Hiraiwa

Faculty of Fisheries, Hokkaido University, Hakodate, Japan

Contents

1. Introduction

When a ship is under way, it is indispensable for a safe voyage to know its position at any time. To know it, several means have been devised for centuries. Position lines have been broadly classified into, by observing the bearing or distance of a terrestrial object, observing the altitude or included angle of a celestial or terrestrial object, and measuring the distance difference of the observer from two stations.

When we come to the means in connection with the used apparatuses, the bearing is measured by a compass or a direction finder or a radar, the angle is measured by a sextant, and the distance difference is measured by Decca, Loran etc.

Besides, let's criticize the utility and the objects of study of these methods. Taking bearings by a direction finder includes night error, coastal error and hull error. Moreover, owing to the development of radar, Loran, this method for determining a ship's position is of little value. A marine radar contributes to the prevention of disaster at sea, and when we determine a position by radar bearings, the character of the position line is similar to that of the compass bearing and radio bearing. Therefore, it is treated in the same way. Hyperbolic navigation by

Decca, Loran etc. is an excellent method as it is not affected by weather, but in this case the confidence of the determined position is the subject of study, because the selectivity based upon limited stations is restricted.

Secondly, whether a ship's position is determined roughly or accurately suggests that there are infinite possibilities. Some are very accurate, such as the hydrographical survey to draw up a chart, and others are not so accurate, such as noon position determined by both anti-meridian and noon sights by the sun when a ship is ocean-going. Hydrographical survey is done carefully on account of its business character. A ship's position, when ocean-going, is not willfully determined by an inaccurate method but restricted by objects and methods which are used for observations. In the case of a fishing boat, especially a trawl-boat or a drifter busy with fishery carried on a continental shelf, a particular method is required to acquire an accurate position; a buoy is anchored artificially to determine the ship's position and the datum point (buoy) is observed exactly on the geographical co-ordinates. Then we can relatively replace each position opposite the datum with the position on the geographical co-ordinates by a relative distance and direction to the point.

Moreover, an officer on duty on a fishing boat in operation has to watch the fishing gear adrift after shooting the salmon gill-net or tuna longline. To do that, he has to know the relative position to the fishing gear.

As mentioned above, the author pointed out the peculiarity of a fishing boat's position from the point of view of the general ship's position. And it follows that the author will describe the problems, history and necessity of study according to their characteristics.

First of all, a fishing boat in operation gets under a particular condition which is called drifting. While a common ship that is drifting loses parts of its driving force and may meet with disaster; so, its position must be indicated on the geographical co-ordinates. Contrarily, a fishing boat stops its driving force after shooting a fishing gear and watches it under the drifting condition. Therefore, the drifting position must be indicated as a relative position to the gear. The watching method which is done nowadays owes much to the crew's efforts. That is to say, even when the ship is drifting, whenever it is necessary for them to confirm the object, they set the engine movement and go up weather-side and continue to watch it. In that routine work, it happens that they are frequently forced to drift for hours to repair the engine, for instance, and that it is difficult for them to confirm the object; however they are required to adopt a prudential policy whatever may happen. In order to cope with such unexpected conditions, if one studies the drift-age of his ship, it will be very effective, from the view-point of labor management and operation efficiency, if he is relieved of so much watching and can reduce his labor by avoiding the repeated sailing and watching. Therefore an easy method conceived by the author will be helpful to men at work.

Up to now, a synthetic study concerning that problem has not been done. The reasons are as follows; drifting is a peculiar condition limited to some kinds of vessel such as a fishing boat, so that few people are interested in that sort of thing, and on a fishing boat that problem has been solved by the crew's efforts. Further-more, when using a flag or a light or a radio buoy as datum points, nobody is able to make experiment on an actual ship because it is impossible for him to determine

its relative position to the object.   Yet as to drifting distances, experimental studies
were reported by Yasui,[1] Kosaka et al.,[2] Saito et al.[3] and Yamaguchi et al.[4]
In these papers, the drifting velocity was indicated as a parameter of wind velocity
and a ship's draught.   Moreover, the author et al.[5] described this problem as a
general expression by parameters of wind velocity, a ship's speed and draught
when the ship was under way and its engine stopped.

Next, as to the drifting direction, the appearance frequency of every bearing
based on statistics, and the classification of the direction were reported.[3][4]
However, they can't regard those reports as reference data to be sure of any
drifting position for the lack of reliable rules.   According to Yamaguchi et al.,[4]
the best way to watch the tuna long line is to sail toward the weather side catching
the wind about two points from the bow on the lee board in the case of planned
drifting and to turn toward the direction in which the fishing implement is stretched
and to drift.   After all, they can easily find the long line after they have drifted
beyond its end and have even lost sight of it, because they must necessarily meet
the implement if they sail into the wind from there.   But this method is based on
the statistic data that the ship has drifted $15° \sim 25°$ ahead from the direction many
times in which the wind blows away.   Therefore if it drifts backward from the
direction in which the wind blows away, it will not meet with the implement even
if it sails in the wind, so that there is a danger of losing the implement.   If there is
any chance to cross at some point of the implement, then from the view-point of
statistics, we can't forecast the crossing point, so that this watching method is not
considered to be an efficient one.   When watching a fishing gear, it is not necessary
to classify mere statistic figures but to estimate the drifting direction and distance
corresponding to the condition of the day based on analyzed results of a ship's
drifting.

As a secondary problem, when we select a fishing-ground, an equal sea
temperature chart, an equal salinity chart, a sea bottom topographical map and
a geological map are used as materials for reference; and whether observation
points are accurate or not, it is closely related with the valuation of those materials.
In the past, if a fisherman set a fishing gear, he could get a good catch, whether
observation points were accurate or not for discussion.   At present, because of
the rationalization of all aspects one cannot discuss fishery without thinking of the
efficiency of a haul of fish.   Take trawling for instance, if one tries to increase its
efficiency by a concentrated casting of fishing implement, charts of water depths,
topographical and geological maps of the sea bottom and other things must be
drawn in detail corresponding to the accurate stations.   From the view-point of
fishery oceanography, the accuracy of the stations must also be studied.   In short,
the results gotten by the analysis of some observations are related to the accuracies
of the observation points.   Not only in the case of closed-space observations on a
coast but also in that of wide-space observations on the ocean, will discussing
about the accuracies of observation positions be required.

Next, if we compare a common ship with a fishing boat, what is the funda-
mental difference between the methods used to determine their positions ?   It is
that in the case of the fishing boat in operation, a datum point can be fixed at
any position as far as possible.   On the other hand, a steamer under way does not

stop, and a navigator looks upon a determined position not as a point but as a position with an error boundary in a wide sense according to the accuracy of a determined method because a determined position is mainly necessary for a safe voyage. Furthermore, it gives a wide berth to a danger zone such as a shoal, or an islet. After all, the valuation of a point need not be done strictly and practically we deal with as such.

Moreover as a special case, the detailed determination of a position in coastal surveying is listed. In such a case, it is carried out by navigation aids; they select basic points by preparing a plan in advance in order to simplify the determination of the surveying ship's position on the sea and prepare ground marks or stations at suitable shore points. On the other hand, in the case of a fishing boat in operation, an officer on duty must determine a ship's position for himself by natural objects on land. Thus, the exact determination of position with natural objects is limited to operating fishing boats, and the generality is scanty, therefore the studies on the method of determination and the reliability have not been made. In addition, it is regrettable that the false understanding from old time has been still inherited and seen in many books. Thinking of them, the author studied how to determine a ship's position when the ship is near the coast and out at sea.

As to the third problem, he studied the confidence regions about determined positions. It is natural that we consider how to get more accurate positions. The determination of the range required for maintaining the required probability about the determined position is one of the methods for representing positions in view of the theory of probability, and also it serves as the scale for evaluating observation points at the time of the data analysis in various observations on the sea. Besides, the exactness of determining method which must be adopted is suggested on the other hand from the range. When we come to this problem, there are two ways to it. One way is that one studies the problem theoretically and solves it. In other words, a practical navigator understands the answer and makes it clear from a pure theoretical view without thinking whether he embodies it or not. The other way is that one studies how to show an error boundary by a simple quantity, briefly from a practical point of view.

From the former standpoint, an error boundary is shown as an ellipse, and from the latter it is expressed as a circle. Sameshima et al.[6] introduced a simultaneous probability law in the error boundaries of a ship's position fixed by astronomical observations, and showed the results by nomographs. Trow et al.[7] indicated the radial error system which does not emphasize the probability theory and looks upon conveniencies as important points; the system was recommended by Anderson[8] and Parker.[9] The author[10] expressed the probability circle system which includes both theoretical foundation and practical convenience, and showed the results by tables and figures. When we discuss about the accuracy of a determined position, the valuation of position ought to be done by probability density, and as to an error boundary the indication must be also done fundamentally by the ellipse system which pursues the equal probability density curve. But in the steps to materialize error boundaries, one must fully consider how to make them practicable so as to be able to construct them.

In regard to these reasons, the author presents the next three subjects for

study.

The first is to predict the direction in which a ship will drift and the distance covered thereby, under the conditions of weather and sea after the ship cast a gill-net or a long line; then an effective point to open a drift will be determined. After the beginning of the drift, by estimating the direction and the distance of the drift corresponding to each condition of time one can use those data effectively to watch the fishing gear.

The second is the method to determine exact positions near the coast and at sea. The positions of trawling grounds where shoals of fish inhabit densely, and the observation points corresponding well enough to the exact water temperatures and salinities are fundamentally different from those of sea-going vessels, and they require a strict valuation as a point. Therefore, to satisfy that aim, a fundamental study is done. The characteristic of measurements of a fishing boat is that if a navigator prepares a datum point artifically and shows each position by a relative point for it when accurate positions are required, he can replace those points with geographical co-ordinates. After all, by using such a method he can get accurate positions easily.

The third is a method to show the accuracy of determined position concretely as a subject of study. Theoretically, probability densities or areas of probability ellipses satisfy this question, but it is very difficult for anyone to draw theoretical answers on a map. Therefore, from the point of view of the real state of things, and also taking into account the probability theory, the author studied how to express the error boundaries of a ship's positions.

Before going further, the author wishes to express his hearty thanks to Proffessors M. Ishida, R. Kawashima, O. Sato and Associate Proffessor T. Suzuki, of the Faculty of Fisheries, Hokkaido University, for their helpful guidance and criticism in regard to the problems discussed in this paper. The author also wishes to express his thanks to the crew members of Oshoro-Maru and Hokusei-Maru for their kind help.

2. Estimation and prediction of the drifting position of a fishing boat

2.1 Purpose of the study

The causes that bring about a ship's drifting are the force of the wind blowing on the upper structure of the ship, the drift current caused by the wind, the rolling caused by the wind, wave and swell, the ocean current and the tidal current. It is necessary to know those phenomena whether the ship is stopped or underway.

The investigation of a ship's drifting when the engine is stopped plays an important part in searching a wrecked ship and in watching the fishing gear (salmon gill-net, tuna long line) of a fishing boat. For a wrecked ship having lost its impellent force, and for a fishing boat whose engine stopped, it is significant to estimate the ship's position in drifting; but how to indicate the position itself differs fundamentally for each one. That is, in the case of the wrecked ship it is necessary to indicate the present position by geographical co-ordinates, estimating all the above-mentioned factors, on the other hand in the case of the fishing boat its drifting position has to be indicated by polar co-ordinates, the fishing gear being

the pole and the wind direction being the primitive line, because the ship in opera-
tion and its fishing gear go adrift almost equally to the ocean current, the tidal
current and the drift current; therefore the ship is affected only by the action of
the wind.   Today, the work of watching a fishing gear is done by the crew.   The
crew would often run the engine even during the drifting, go up to the weather
side, continue to watch in order to keep the object (light, flag, reflector etc.) visible.
However, in that routine work, it might occur that the drifting would go on for
hours while the engine is being repaired; as a result it would be rather difficult to
confirm the object; therefore, it is necessary to adopt a safe policy whatever may
happen.

    Next, in the case of watching by a radio buoy, if the boat drifts continuously
untill it is time to haul in the implement, one can find the direction of the object
but can't know how long it will take to return.   Moreover he must keep in mind
that he has to find out a plan in case the object runs out of order.   Because of
those causes the author selected the next two suggestions as the subject of his
own experimental studies.

    One suggestion is that before drifting, it is better to know in advance the
relative direction in which the ship will drift and distance between the gear and
the ship, under the particular weather and sea conditions at that time.   If it is
possible for him to foresee them, he can foresee the movement of the ship adrift from
beginning to end, so that he can select the beginning point of drifting in order
to drift through a convenient route to watch the gear.

    The other is to estimate a ship's position at a time based on the information
gotten after the ship begins to drift.   If the conditions remain the same, the
foreseen values and estimation will be equal.   On the other hand, since the weather
and sea conditions change constantly, it is necessary to estimate accordingly.   If
one can estimate his ship's position from the gear at any time without any
objects, it is effective for watching the gear in direct, supplementary and
preparatory standpoints.   It goes without saying that a drift is expressed by
parameters with the ship's condition and the wind velocity, but it is almost
impossible to command a drift because there are various problems due to the
influence of the sea conditions on the ship.   As for the fishery, it is necessary that
the method should be simple and satisfy the required accuracy.   Therefore it is
important that each ship investigates and analyzes its own drift, and applies the
findings practically in case of necessity.

2.2 Estimation method of a drifting ship's position

    If a ship suffers the wind and sea force whether it is stopped or under way, the
ship will drift on the lee side.   As the causes of this pushing-away action, the wind
force working on the upper structures, the drift current produced by the wind, the
rolling which is caused by the action of the wave and swell and finally, the ocean
currents and tidal stream currents, are conceivable, and in the phenomenon of
drift they appear synthetically.

    From the standpoint of watching a fishing gear, the drift caused by the wind
action is particularly important.   Therefore it is the aim of this study to pick up
and analyze the direction and the distance in all drifting phenomena.   For the

purpose, either of the following two methods must be adopted, the one is to carry out the experiment which can eliminate those due to other factors, and the other is to grasp these quantities exactly and exclude them from the total, but both methods are difficult problems.

As for that, the author selected the former experimental method, that is, the effect done by the wind action only. When a drifter is in operation, after casting a gill-net, the crew watches the gear under drifting. Then the gear and the ship are affected by the ocean current, the tidal stream current, the drift current in the same way. The corner reflector on the net (which can be several miles long) is not subject to drifting caused by the wind, because the net acts as a sea anchor. The ship is likely to drift, so that its drifting direction and the distance, both caused by the wind, make the difference between the ship's position and that of the gear. For these reasons, in order to measure the wind drift, the author planned an experiment which considers the reflector on the net as a base for observation. And these experiments were carried out by two fishery training ships of the Hokkaido University, the Oshoro-Maru and the Hokusei-Maru. The Oshoro-Maru was selected as large fishing boat model and the Hokusei-Maru was selected as medium-sized boat model; the latter has an anti-rolling tank.

2.2.1 *Ship's motion in drifting*

(1) Co-ordinate system in drifting

(a) Space co-ordinate

On the water-plan, the corner reflector connected on a salmon gill-net is selected as the origin; the direction of the wind is taken as ξ-axis, the direction of the right angle to ξ-axis as η-axis and the direction of the perpendicularity as ζ-axis.

(b) Ship's co-ordinate

On the co-ordinate with the ship's center of gravity as the origin, the x,y,z axes are taken for fore and aft line, side direction and upward direction respectively, and z-axis is parallel to ζ-axis.

(2) Expression of ship's posture

If we consider a ship's drifting as a motion on the ξ, η plan of the space co-ordinate ξ, η, ζ system, and the ship's posture in drifting as a plan motion, the

Fig. 2.1. Co-ordinate system.

ship's drifting is expressed as a function of time having three degrees of freedom that is $\xi(t)$, $\eta(t)$ and $\theta(t)$. In this case, the position of the center of gravity (G) is indicated as $\xi(t)$, $\eta(t)$ and with an expression of angular motion around the z-axis; the angle between the x-axis and the ξ-axis of the ship's co-ordinate is indicated as $\theta(t)$. In practical fishery, a ship's head at the time of opening drift is free toward
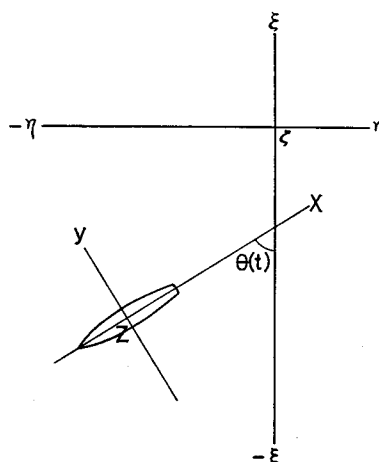
the wind direction and ξ, η, θ indicate the ship's position and posture changing from hour to hour in the space co-ordinate. Hitherto, as an indication of such motion, it has been expressed by drifting velocity and a ship's head towards wind direction.

(3) Motion equation

As external forces acting upon a drifter, the force and the moment of the current, wind, wind wave and swell are considered. And the variation in these external forces appears by way of a swing; however, in this section, it is decided to exclude the varying portion contained in these forces from the consideration, and to give dynamic and deterministic thought.

As a motion in drifting is considered as a plane motion, the motion equations are indicated as follows.

$$M_\xi \frac{\mathrm{d}^2\xi}{\mathrm{d}t^2} = R_{\xi u} + F_{\xi w} + F_{\xi v} + F_{\xi c} \tag{2.1}$$

$$M_\eta \frac{\mathrm{d}^2\eta}{\mathrm{d}t^2} = R_{\eta u} + F_{\eta w} + F_{\eta v} + F_{\eta c} \tag{2.2}$$

$$I \frac{\mathrm{d}^2\theta}{\mathrm{d}t^2} = M_u + M_w + M_v + M_c \tag{2.3}$$

where M_ξ: virtual mass of the ξ-axis direction,

$\quad M_\eta$: virtual mass of the η-axis direction,

$\quad I$: virtual moment of inertia, M: moment, suffixes u, w, v and c indicate water resistance, wind action, wave action and current action respectively.

$\quad R_u$: wave resistance, F_w: wind action, F_v: wave action, F_c: current action, suffixes ξ, η indicate the forces on the ξ-axis and the η-axis directions respectively.

With this problem, the author studies the wind action and wind moment which are considered to produce the greatest effect.

(4) Solution of motion equation

If the wind acts on a ship with constant velocity, the wind pressure is considered to be constant, and if we put the wind pressure force as $P_\xi(W)$, the water resistance as $K_\xi U_\xi^2$, the ocean wave force as D_ξ, in the ξ-axis direction; and the wind pressure force as $P_\eta(W)$, the water resistance as $K_\eta U_\eta^2$, the ocean wave force as D_η, in the η-axis direction, and furthermore the ship's mass as m, $\varDelta m_\xi$ and $\varDelta m_\eta$ as additional mass respectively, moment by wind pressure as $M_w(\theta)$ and moment by water pressure as $M_u(\theta)$, we get the following equations:

$$(m+\varDelta m_\xi)\frac{\mathrm{d}U_\xi}{\mathrm{d}t} = P_\xi(W) - K_\xi U_\xi^2 + D_\xi \tag{2.4}$$

$$(m+\varDelta m_\eta)\frac{\mathrm{d}U_\eta}{\mathrm{d}t} = P_\eta(W) - K_\eta U_\eta^2 + D_\eta \tag{2.5}$$

Now, assuming that $P_\xi(W) \fallingdotseq P_0\xi$, $D_\xi \fallingdotseq D_0\xi$, $P_\eta(W) \fallingdotseq P_0\eta$, $D_\eta \fallingdotseq D_0\eta$ exist, the following relations are derived:

$$(m + \Delta m_\xi) \frac{dU_\xi}{dt} = (P_0\xi + D_0\xi) - K_\xi U_\xi{}^2 \qquad (2.6)$$

$$(m + \Delta m_\eta) \frac{dU_\eta}{dt} = (P_0\eta + D_0\eta) - K_\eta U_\eta{}^2 \qquad (2.7)$$

By solving them

$$U_\xi = \sqrt{\frac{P_0\xi + D_0\xi}{K_\xi}} \cdot \frac{1 - Ce^{-\frac{2\sqrt{(P_0\xi + D_0\xi)K_\xi}\,t}{m + \Delta m_\xi}}}{1 + Ce^{-\frac{2\sqrt{(P_0\xi + D_0\xi)K_\xi}\,t}{m + \Delta m_\xi}}} \qquad (2.8)$$

$$U_\eta = \sqrt{\frac{P_0\eta + D_0\eta}{K_\eta}} \cdot \frac{1 - Ce^{-\frac{2\sqrt{(P_0\eta + D_0\eta)K_\eta}\,t}{m + \Delta m_\eta}}}{1 + Ce^{-\frac{2\sqrt{(P_0\eta + D_0\eta)K_\eta}\,t}{m + \Delta m_\eta}}} \qquad (2.9)$$

According to the result of the wind tunnel experiment, the rotary moment of the above water portion of the ship caused by the action of the wind, and that of the under water portion caused by the water pressure are considered to keep the balance at the angle θ_B, and the ship's rotary motion is kept at that angle or thereabout. So the resistance in proportion to the rotary angular velocity is considered to be in action, and if one puts a small motion around the balanced angle as θ_S, $\theta(t) = \theta_B + \theta_S(t)$, $\dot\theta(t) = \dot\theta_S(t)$, $\ddot\theta(t) = \ddot\theta_S(t)$ is devised, and if $\theta_S(t)$ is expressed by θ_S, the next equation exists:
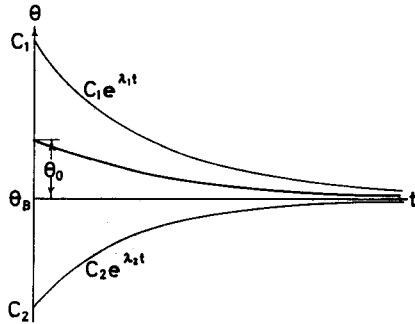

Fig. 2.2 (a). Small motion around the balanced rotary angle θ_B in the case of $C_1 > 0$, $C_2 < 0$, $|C_1| > |C_2|$.
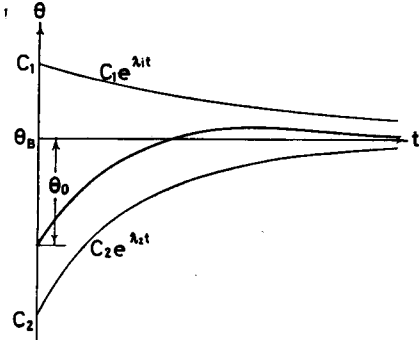
Fig. 2.2 (b). Small motion around the balanced rotary angle θ_B in the case of $C_1 > 0$, $C_2 < 0$, $|C_1| < |C_2|$.

$$(I+\Delta I)\,\frac{\mathrm{d}\theta_S}{\mathrm{d}t} = M_u(\theta_B+\theta_S)-M_w(\theta_B+\theta_S)-K_1\dot{\theta}_S+M_v \qquad (2.10)$$

where $M_u(\theta_B+\theta_S)-M_w(\theta_B+\theta_S)$ can be replaced with $-K_2\theta_S$; accordingly equation (2.10) is expressed as follows.

$$(I+\Delta I)\,\frac{\mathrm{d}^2\theta_S}{\mathrm{d}t^2} +K_1\,\frac{\mathrm{d}\theta_S}{\mathrm{d}t} +K_2\theta_S = M_v \qquad (2.11)$$

Now, assuming that M_v does not exist, in other words, the effect of the ocean wave is negligible, as the solution of equation (2.11)

$$\theta_S = C_1\,e^{\lambda_1 t}+C_2\,e^{\lambda_2 t} \qquad (2.12)$$

is used. Accordingly from the characteristic equation

$$\lambda_1 = \frac{-K_1}{2(I+\Delta I)} + \sqrt{\left[\frac{K_1}{2(I+\Delta I)}\right]^2 - \frac{K_2}{I+\Delta I}} \qquad (2.13)$$

$$\lambda_2 = \frac{-K_1}{2(I+\Delta I)} - \sqrt{\left[\frac{K_1}{2(I+\Delta I)}\right]^2 - \frac{K_2}{I+\Delta I}} \qquad (2.14)$$

is devised. And if one puts $\dot{\theta}_S(t)_{t=0}=0$, $\theta_S(t)_{t=0}=\theta_S$ as the initial condition

$$C_1 = \frac{\lambda_2\theta_0}{\lambda_2-\lambda_1}, \qquad C_2 = \frac{-\lambda_1\theta_0}{\lambda_2-\lambda_1}$$

are devised. And in equation (2.12), the second term becomes asymptotic to $0(\theta_B)$ more quickly than the first term because $0>\lambda_1>\lambda_2$.
In this case, two types exist depending on whether $|C_1|>|C_2|$ or $|C_2|>|C_1|$. First of all, in the case of $C_1>0$, $C_2<0$, $|C_1|>|C_2|$, θ_S gradually becomes asymptotic to the balanced rotary angle θ_B. And the next, when $C_1>0$, $C_2<0$, $|C_1|<|C_2|$, θ_S goes once beyond the balanced rotary angle θ_B and after that, gradually asymptotic to the angle θ_B. If an external force by wave acts on the ship, in other words $\Delta\theta_v(t)$ is added

$$\theta_S = C_1\,e^{\lambda_1 t}+C_2\,e^{\lambda_2 t}+\Delta\theta_v(t)$$

Accordingly, for example, a ship drifts, fluctuating around the balanced angle, in a swell.

2.2.2 Drift analysis of the Oshoro-Maru[11][12]

(1) Aim of the experiment

The Oshoro-Maru is a large fishing boat which can measure internal factors (draught, trim, ship's head) that affect driftage and external elements (wind direction, wind velocity). It also has an equipment for its own recording. By analyzing dirftages in detail the empirical formula which includes whole factors will be utilized. After all, it will be adopted any time and become the only material to estimate the ship's position in relation to its fishing gear.

(2) Principal dimensions of the ship and its conditions

G.T. 1119.66T, L_{oa} 66.70 m, L_{pp} 60.50 m, Beam 11.00 m, Depth 5.40 m, mean draught 3.75 m (max. 3.86 m, min. 3.68 m), trim(=after draught−fore draught) max. 2.07 m, min. 1.10 m, [longitudinal projected area above water line / longitudinal projected area under water line] max. 1.88, min. 1.73.

(3) Sea region and periods of experimentation

The experiments were carried out at 14 points in the Bering Sea from June 11, 1969 till July 24, 1969 and at 11 points from June 11, 1971 till July 5, 1971.

Table 2.1(a). *Relation of wind velocity (W(m/s)), drifting velocity (U(m/s)), ship's head (a(degree)), drifting direction (β (degree)), mean draught (d(m)), angle of cut between wind and swell (γ (degree)) and trim (m).*

W	U	a	β	d	γ	Trim	W	U	a	β	d	γ	Trim
7.0	0.40	123	− 9	3.825	var.	1.65	5.2	0.25	110	− 4	3.765	−49	1.43
7.5	0.40	123	−18	″	″	″	5.0	0.31	108	− 8	″	−48	″
7.5	0.42	120	− 5	″	″	″	3.5	0.29	75	+64	3.735	+44	″
7.0	0.53	123	− 3	″	″	″	3.8	0.34	80	+64	″	+38	″
6.5	0.42	95	+37	3.790	+ 6	1.56	4.2	0.26	90	+21	3.715	+ 1	″
5.8	0.36	90	+33	″	+11	″	4.0	0.19	100	+25	″	−18	″
5.5	0.23	92	+25	3.785	0	1.53	4.5	0.17	104	− 3	″	−24	″
5.7	0.24	96	+20	″	0	″	3.9	0.20	104	−10	″	−18	″
5.7	0.30	97	+20	″	0	″	3.5	0.26	104	−10	″	−19	″
5.8	0.27	96	+23	″	0	″	3.5	0.27	104	−13	″	−21	″
6.0	0.24	97	+22	″	0	″	4.8	0.29	98	− 3	3.680	0	1.44
6.2	0.33	95	+26	″	0	″	4.0	0.28	88	+18	″	0	″
3.5	0.23	80	+76	3.775	+27	1.49	4.0	0.24	95	+27	″	0	″
3.0	0.26	72	+83	″	+33	″	4.0	0.28	92	+10	″	0	″
3.9	0.29	79	+68	″	+28	″	4.1	0.24	95	+ 9	″	0	″
5.5	0.41	85	+32	3.785	+30	1.43	4.0	0.22	92	+23	″	0	″
5.4	0.40	86	+35	″	+31	″	4.1	0.21	98	+17	″	0	″
5.8	0.43	87	+35	″	+24	″	2.0	0.08	112	− 8	3.690	−11	1.42
6.0	0.39	87	+34	″	+26	″	2.5	0.13	97	+53	″	−16	″
5.0	0.36	87	+41	″	+ 1	″	2.6	0.12	93	+47	″	−21	″
4.5	0.38	91	+27	″	− 6	″	2.5	0.12	87	+65	″	−14	″
5.5	0.37	92	+19	″	−11	″	2.5	0.09	87	+35	″	−17	″
5.5	0.48	91	+26	″	− 6	″	2.5	0.09	90	+56	″	−21	″
7.2	0.44	95	+25	3.760	+ 9	1.32	2.5	0.10	90	+50	″	−19	″
7.5	0.42	100	+20	″	+ 1	″	5.0	0.46	90	+23	3.760	− 7	1.18
7.5	0.43	102	+15	″	− 1	″	5.1	0.53	80	+55	″	+15	″
7.2	0.45	100	+21	″	+ 2	″	5.2	0.52	79	+69	″	+24	″
7.2	0.47	100	+19	″	+10	″	5.6	0.58	78	+60	″	+24	″
7.5	0.50	100	+20	″	+ 8	″	6.0	0.58	80	+63	″	+21	″
7.5	0.43	97	+21	″	+10	″	6.5	0.60	78	+65	″	+25	″
7.5	0.49	95	+34	3.745	− 7	1.29	5.0	0.36	108	− 6	3.750	0	1.10
7.0	0.47	95	+34	″	− 3	″	5.0	0.38	122	−16	″	−23	″
6.5	0.48	95	+41	″	−11	″	5.0	0.34	124	−18	″	−28	″
6.0	0.45	80	+53	″	+ 4	″	5.0	0.29	124	−23	″	−22	″
5.5	0.44	75	+70	″	+15	″	5.0	0.23	115	− 8	″	−17	″
4.2	0.23	122	− 9	3.765	−39	1.43	5.0	0.27	109	−20	″	−16	″
4.5	0.28	115	−15	″	−37	″	5.0	0.29	115	−23	″	−21	″
5.2	0.30	112	−13	″	−36	″	5.0	0.27	117	−27	″	−30	″
5.0	0.26	112	− 9	″	−39	″	5.0	0.33	120	−30	″	−35	″
4.5	0.30	110	−18	″	−45	″							

Table 2.1(b). *Relation of wind velocity (W), drifting velocity (U), ship's head (a), drifting direction (β), mean draught (d), angle of cut between wind and swell (γ) and trim.*

W	U	a	β	d	γ	Trim	W	U	a	β	d	γ	Trim
5 2	0.32	110	+28	3.860	−25	1.88	7.2	0.49	101	+34	3.745	− 5	1.97
5.0	0.40	107	+31	″	−25	″	7.2	0.48	101	+31	″	+ 3	″
4.8	0.34	100	+45	″	−16	″	7.2	0.52	102	+31	″	+ 1	″
6.0	0.32	96	+48	″	−11	″	7.0	0.49	100	+33	″	+ 2	″
5.0	0.37	90	+52	″	− 1	″	7.3	0.46	100	+28	″	+ 2	″
4.7	0.37	85	+55	″	+16	″	7.8	0.51	100	+32	″	+ 4	″
7.0	0.47	85	+64	3.825	+17	1.89	7.7	0.51	100	+31	″	+ 1	″
6.0	0.43	90	+61	″	+10	″	7.7	0.50	101	+28	″	− 5	″
6.0	0.42	85	+77	″	+19	″	7.5	0.62	102	+48	3.735	−17	2.07
5.8	0.40	85	+59	″	+28	″	7.5	0.56	101	+45	″	−15	″
5.8	0.46	83	+70	″	+32	″	7.5	0.62	105	+41	″	−19	″
5.8	0.38	83	+64	″	+27	″	7.7	0.55	105	+41	″	−17	″
6.5	0.45	112	+36	3.755	−26	2.07	7.9	0.55	106	+42	″	−19	″
6.5	0.45	118	+ 5	″	−39	″	7.6	0.52	106	+38	″	−20	″
6.5	0.47	114	+ 6	″	−35	″	7.6	0.53	107	+30	″	−23	″
10.0	0 62	110	+21	3.765	−18	2.05	10.1	0.75	102	+43	3.720	− 1	2.04
9.0	0.62	110	+20	″	−17	″	10.1	0.77	102	+41	″	+ 2	″
8.5	0.57	108	+19	″	−21	″	10.0	0.69	106	+35	″	− 1	″
5.8	0.37	98	+12	3.745	+ 4	1.99	10.2	0.66	106	+29	″	− 4	″
5.1	0.37	98	+37	″	+ 7	″	10.1	0.76	107	+44	″	+ 2	″
5.1	0.34	95	+27	″	+ 9	″	9.5	0.74	102	+44	″	+ 9	″
5.1	0.28	93	+23	″	+ 9	″	9.5	0.65	103	+36	″	+ 6	″
5.1	0.38	90	+34	″	+13	″	9.0	0.66	103	+46	″	+12	″
5.1	0.45	92	+33	″	+14	″	6.2	0.34	113	+ 3	3.720	−19	1.98
5.1	0.35	92	+45	″	+22	″	6.0	0.33	112	+12	″	−18	″
5.1	0.39	90	+46	″	+13	″	6.0	0.35	113	+ 8	″	−20	″
5.0	0.31	98	+52	″	+32	″	6.2	0.37	111	+ 5	″	−21	″
5.0	0.27	100	+40	″	+35	″	6.3	0.35	111	+ 3	″	−18	″
6.0	0.33	95	+19	3.750	0	1.90	6.0	0.32	110	+17	″	−13	″
6.3	0.32	92	+30	″	+19	″	5.9	0.36	111	− 1	″	−14	″
6.9	0.40	94	+20	″	+11	″	6.1	0.33	111	+ 4	″	−16	″
7.4	0.43	95	+29	″	+10	″	4.9	0.28	92	+33	3.730	0	1.94
6.9	0.39	92	+38	″	+15	″	5.0	0.28	90	+35	″	− 1	″
6.1	0.41	90	+35	″	+17	″	5.0	0.32	91	+35	″	+ 1	″
7.5	0.53	102	+34	3.745	− 6	1.97	5.0	0.31	95	+36	″	− 3	″
7.0	0.53	102	+36	″	− 5	″	5.0	0.34	100	+27	″	−10	″
7.5	0.50	102	+37	″	− 3	″	5.0	0.32	100	+30	″	−13	″

(4)　Method of experiment

The corner reflector on the gill-net was selected as the datum point for observation and the observers determined the ship's relative positions with regard to that point by checking the directions and distances to the object every 30 minutes. Then the direction of the drift and the distance covered were calculated every 30 minutes. The wind direction and wind velocity are given as the average of numerical values recorded on the anemograph and the direction of the ship's head is also given as the average of course recorder.

(5)　Results

As shown in Fig. 2.3, the ship's direction (a) and the drifting direction (β) for

a given wind direction are measured. The swell is measured as plus when it is affected by the stern-side rather than the wind direction and as minus when it is affected by the bow-side.   And Table 2.1 (a)(b) indicate circumstance conditions, ship's conditions and driftages.

(A) Drifting distance

If it is admitted that a ship drifts to leeward when it suffers the wind on the beam, the following equation is derived under balanced conditions.

$$\frac{1}{2}\rho_a C_a S_a W^2 = \frac{1}{2}\rho_w C_w S_w U^2$$

where W: wind velocity, U: drifting velocity, ρ: density of flud, S: longitudinal projected area, C: resistance coefficient, suffixes a and w indicate above water-line and under water-line respectively.

From this relation, the following equation $U=\sqrt{S_a/S_w}\sqrt{\rho_a C_a/\rho_w C_w}\,W$ exists between the drifting velocity and the wind velocity. Therefore the drifting velocity is generally indicated as $U=K\sqrt{S_a/S_w}\,W$.

Next, when discussing the drifting distance, in order to avoid the lack of unity in the data, corrections were performed adopting data under the condition that mean draught is 3.75 m.   That is to say, on the relation $U=K\sqrt{S_a/S_w}\,W$, to convert any drifting distance into the distance corresponding to

Fig. 2.3. Measurement of a ship's head (α) and its drifting direction (β).

the condition of mean draught (=3.75 m), the ratio of 1.348 (the value of $\sqrt{S_a/S_w}$ when the draught is 3.75 m) to the value of $\sqrt{S_a/S_w}$ in any draught must be multiplied by any drifting distance at any time. The drifting distances in Table 2.1 (a)(b) are values that have been corrected by such a method.

(a) Relation between the drifting coefficient and the ship's head and trim

In the homogeneity of classified data, it is desirable to subdivide them as much as possible. However, in actual experiments with real ships, it is impossible to vary the ship's conditions at will.   When the author thinks of the connection between obtained data and scattering, the data are classified in the following three groups.   The data shown in Table 2.1(a) are classified into two groups: one group is that the trim is 1.10~1.32 m (mean 1.21 m) and the other is that the trim is 1.42~1.65 m (mean 1.47 m).   The trim shown in Table 2.1(b) is treated as one group because it is 1.88~2.07 m (mean 1.98 m).   The author calls the above-mentioned K a "drifting coefficient".   If the relation between each observation $K(=U/\sqrt{S_a/S_w}\,W)$ and the ship's head (α) is shown, each group is in Fig. 2.4 (a)(b) (c).   There is a tendency that if the angle between the ship's head and the wind direction is small the ship drifts easily.   Every swell is small and the classified states are shown in these figures; a striking difference cannot be found between
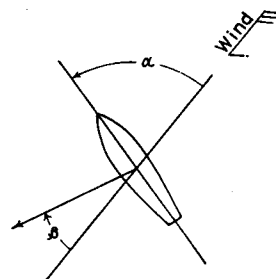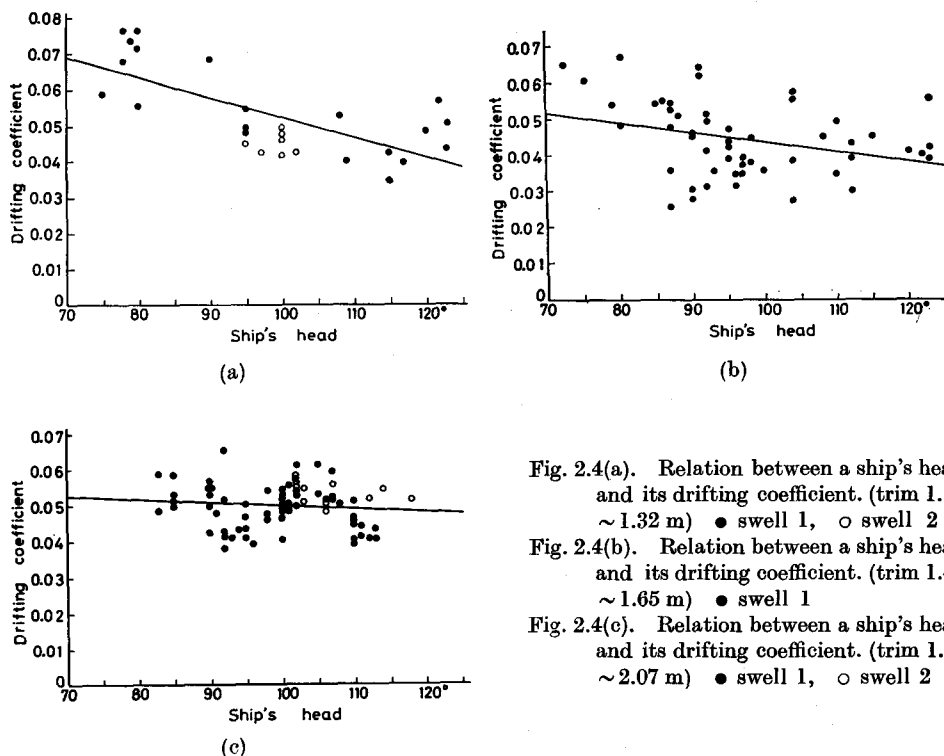
(a)

(b)

(c)

Fig. 2.4(a). Relation between a ship's head and its drifting coefficient. (trim 1.10 ~ 1.32 m) ● swell 1, ○ swell 2

Fig. 2.4(b). Relation between a ship's head and its drifting coefficient. (trim 1.42 ~ 1.65 m) ● swell 1

Fig. 2.4(c). Relation between a ship's head and its drifting coefficient. (trim 1.88 ~ 2.07 m) ● swell 1, ○ swell 2

them. The reason is considered as follows:

Let's consider the case when the drifting force (D_S) by a swell added to the wind pressure force acts upon the above water portion. When discussing the wind and the water resistance acting on a ship, and a ship's velocity in drifting, if one captures them as motions on the drifting route and puts the direction of the tangent as e_t, a small displacement $\varDelta S$ is expressed as $\overrightarrow{\varDelta S} = \varDelta S\,\overrightarrow{e_t}$, that is the velocity on the route is put $\overrightarrow{U_S} = \mathrm{d}S/\mathrm{d}t\,\overrightarrow{e_t}$. Now let's consider the movement on a route and put the virtual mass as M_S, the wind pressure force as P_0 on the S-direction, the following equation is formularized.

$$M_S\,\frac{\mathrm{d}^2 S}{\mathrm{d}t^2} = P_0 - K U_S^2 + D_S$$

About these relations, the same relationship exists as in equations (2.8) (2.9) founded on the same conception as (4) term of 2.2.1, that is

$$U_S = \sqrt{\frac{P_0 + D_S}{K}} \cdot \frac{1 - Ce^{-\frac{2\sqrt{K(P_0 + D_S)}\,t}{Ms}}}{1 + Ce^{-\frac{2\sqrt{K(P_0 + D_S)}\,t}{Ms}}}$$

From this equation, if a constant time elapses $\left(\text{time constant:} \dfrac{M_S}{2\sqrt{K(P_0+D_S)}}\right)$ it turns as follows.

$$U_S = \sqrt{\frac{P_0+D_S}{K}}$$

On this equation, it is possible to put $P_0=\rho_a C_a S_a W^2/2$, $K=\rho_w C_w S_w/2$, so the following equation exists.

$$U_S = \sqrt{\frac{0.5\rho_a C_a S_a W^2+D_S}{0.5\rho_w C_w S_w}} = \sqrt{\frac{\rho_a C_a S_a}{\rho_w C_w S_w}}\ W\left(1+\frac{2D_S}{\rho_a C_a S_a W^2}\right)^{1/2}$$

where, if assuming that $2D_S/\rho_a C_a S_a W^2$ is smaller than 1, the equation is changed as follows by Taylor's expansion.

$$U_S = \sqrt{\frac{\rho_a C_a S_a}{\rho_w C_w S_w}}\ W\left\{1+\frac{D_S}{\rho_a C_a S_a W^2}-\frac{1}{8}\left(\frac{2D_S}{\rho_a C_a S_a W^2}\right)^2-\frac{1}{16}\left(\frac{2D_S}{\rho_a C_a S_a W^2}\right)^3\cdots\right\}$$

The drifting force by rolling is expressed as follows.[13]

$$D_S = (\pi^2 H_w \cdot \theta \cdot M \cdot GM \cdot \gamma / L_w^2)\sin \varepsilon$$

where H_w: wave height, L_w: wave length, θ: amplitude, M: hull weight, γ: effective wave slope coefficient, ε: phase difference between forced moment by wave and ship's rolling.

From the equation, $D_S=1.17\times10^7\theta\ H_w/L_w^2$ is obtained by substituting $\gamma \doteqdot 0.7$, $M=1470$ ton, $GM=1.15$ m, $\sin\varepsilon \doteqdot 1$. As θ, W, the respective mean values in the statement of the experiments are adopted that is $\theta=2°3$, $W=5.9$ m/sec, and as ρ_a, C_a, S_a, 0.129 kg·sec^2/m^4, 1.219, 365 m^2 are substituted respectively, and it results in $D_S/\rho_a C_a S_a W^2=234\ H_w/L_w^2$. Now, with regard to the dimensions of the swell, the following combinations are assumed that is, $H_w=1$ m, $L_w=100$ m; $H_w=2$ m, $L_w=100$ m; $H_w=2$ m, $L_w=200$ m, then $D_S/\rho_a C_a S_a W^2$ are calculated as 0.023, 0.047, 0.012 respectively and each value is small. Accordingly

$$U_S \doteqdot \sqrt{\frac{\rho_a C_a S_a}{\rho_w C_w S_w}}\ W\left(1+\frac{D_S}{\rho_a C_a S_a W^2}\right)$$

is put approximately, and by this equation, the difference between the effect by the swell and the drifting velocity is negligible regardless of its magnitude. Generally, the effect by the swell is large when the wind velocity is weak and the swell is short in length but high in height.

If the relation is smoothed by the equation $K=a-b\alpha$, each is expressed as follows:

    group of trim$=1.10\sim1.32$m (number of data is 27) $K=0.108-0.00056\alpha$
    group of trim$=1.42\sim1.65$m (number of data is 52) $K=0.071-0.00027\alpha$
    group of trim$=1.88\sim2.07$m (number of data is 74) $K=0.059-0.00009\alpha$

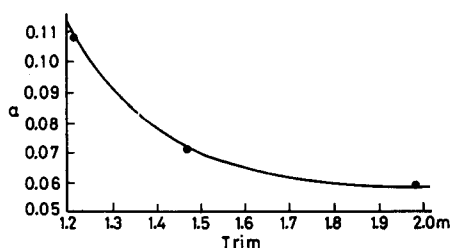If the mean trims 1.21m, 1.47m and 1.98m in each group represent the group,

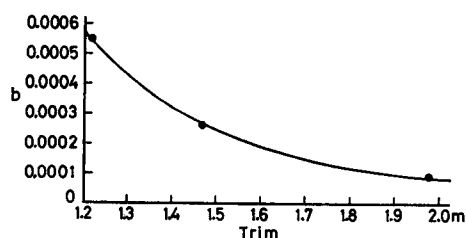Fig. 2.5(a). a-curve of the drifting coefficient.

Fig. 2.5(b). b-curve of the drifting coefficient.

coefficients (a, b) are shown in Fig. 2.5(a)(b) in relation to the trim. If they are smoothed by equations $a=c+de^{-nt}$, $b=c'+d'e^{-n't}$, they are indicated as follows. (where t is trim)

$$a = 0.058+24.2e^{-5.14t} , \quad b = 0.00005+0.022e^{-3.14t}$$

Therefore as an experimental equation of drifting velocity,

$$U= \{0.058+24.2e^{-5.14t}-(0.00005+0.022e^{-3.14t})a\} \sqrt{\frac{S_a}{S_w}} \, W$$

is obtained. (where the units of U, t, a, W are m/s, m, degree, m/s)

(b) Relation between the direction of the ship's head and the trim
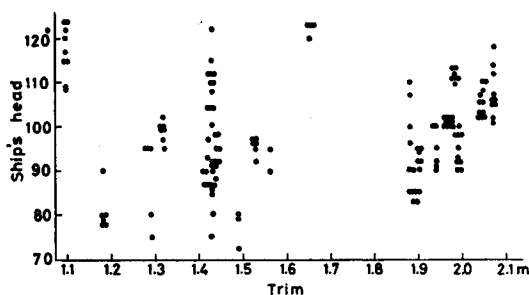
Fig. 2.6. Relation between ship's head and trim.

The above-mentioned equation is obtained by looking upon the drifting coefficient as trim and the ship's head as parameters and we tried to find out whether there is any connection between the trim and the ship's head (drifting posture) or not. The relation between the two is shown in Fig. 2.6, and there are few correlations. Therefore as for the experimental equation, it is adequate to treat a and t as independent variables.

(B) Drifting direction

As in the case of drifting distances, the relation of the ship's head to the drifting direction in regard to the three groups is shown in Fig. 2.7 (a)(b)(c). In
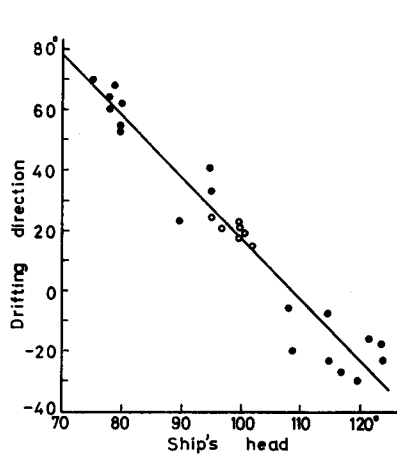
(a)
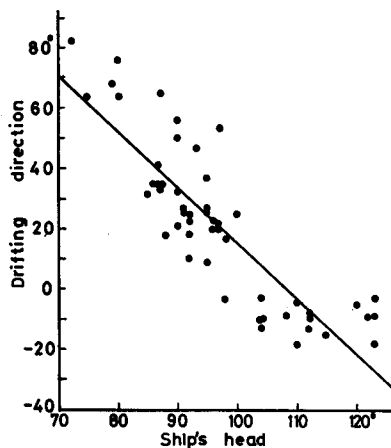
(b)

Fig. 2.7(a). Relation between ship's head and
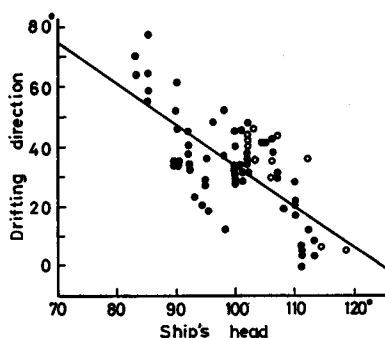drifting direction. (trim 1.10~1.32 m)
● swell 1,   ○ swell 2
Fig. 2.7(b). Relation between ship's head and
drifting direction. (trim 1.42~1.65 m)
● swell 1
Fig. 2.7(c). Relation between ship's head and
drifting direction. (trim 1.88~2.07 m)
● swell 1,   ○ swell 2

(c)

each case, a linear relation exists between the ship's head (a) and the drifting
direction (β).   If it is expressed by the equation $\beta=a-ba$, each will be indicated as
follows: that is

group of trim=1.10~1.32 m $\beta=220°6-2.027a$
group of trim=1.42~1.65 m $\beta=198°9-1.830a$
group of trim=1.88~2.07 m $\beta=169°9-1.360a$

these a, b corresponding to mean trims are shown in Fig. 2.8(a)(b) and linear
relations exist.   They are indicated as follows:

$$a = 293°4 - 62.6t, \qquad b = 3.117 - 0.886t$$

In the end, as an experimental equation of drifting direction,

$$\beta = (293.4-62.6t)-(3.117-0.886t)\,a$$
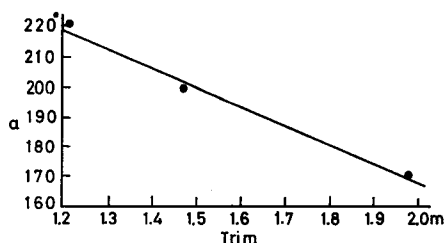
was obtained.

Fig. 2.8(a). c-line of the drifting direction.   Fig. 2.8(b). d-line of the drifting direction.
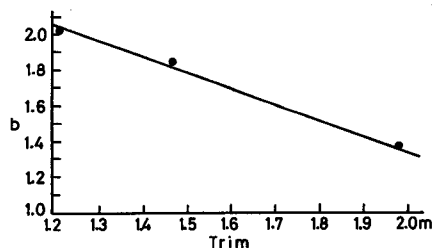
(6) Discussion

The results obtained from the actual experiment of the Oshoro-Maru were mentioned before. The author will now discuss the accuracy of the method and the results.
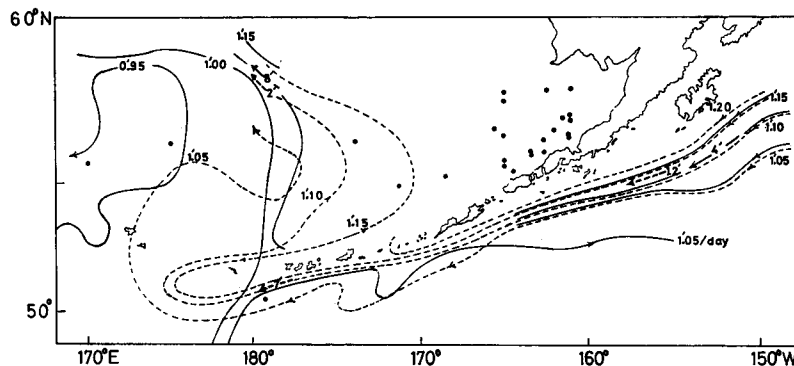
(a) Drift of datum point by wind action

It is important to fix the reflector on the water exactly since it is to be used as a basic point for observations. For about seven hours between casting the net and hauling it in, it was estimated that the total drift was less than 0.1 mile because of its length and the angle of bend. So, for thirty-minute observations, we thought drifts of datum point were not needed at all.

Furthermore the experiments to verify the fact were carried out by the Hokusei-Maru, so the method and results will be described in 2.2.3.

(b) Effect of currents

In the experimental sea area, the velocity of the ocean current was somewhat less than 0.05 knot, as shown in Fig. 2.9.[14]   As the distance between the ship and the reflector was less than 5 miles, both the ship and the reflector were influenced by ocean currents in the same way.   The speed of the drift current was $2 \sim 4$ per cent of the wind velocity at the sea surface, decreasing with the depth, and the direction also varied with the depth; accordingly the effects on the ship and the gill-net were different, but the difference was so small as to be insignificant.

Fig. 2.9. Estimated ocean current chart in the experimental sea region.
● observation point   solid line—summer 1955, broken line—summer 1956

(c) Accuracy of observation values

If the ship's head corresponded to the drifting coefficient and the direction, the scattering around the regression lines was pretty large. Particularly in the drifting coefficient, the scattering was remarkable so that it had to be examined closely. In Fig. 2.4 (a)(b)(c), if the data are thought to be distributed normally around the lines, each standard deviation is calculated as 0.007, 0.011, 0.006. Then these values were converted into distances for a thirty-minute period of time, corresponding to the mean wind velocities, these being 6.0, 4.6, 6.7 m/s for each group. Those were σ=0.06, 0.07, 0.05 mile respectively. Now, it is impossible to analyze the causes, the partial currents, the instabilities of the wind direction and velocity, the duration of the wind, the stabilities of drifting postures, the error of a determined position being thought as elements of causes and appearing in the form of the above-mentioned scatterings.

(d) Fitness of the experimental equations

As the experimental equations of drifting distance and of direction show each mean, it is natural that they will be fit if treated independently. However, as an estimated position is fixed by the combination of both direction and distance, the fitness of an independent item is questionable.

Now, if the continuous drifting is assumed on all the data, the total drifting hours were 76^{h}5 and the drifted position was 29°5 ahead of the direction in the wind blew away and 55.0 miles from the datum point. On the other hand, from the experimental equations, the calculated position was 27°9, 56.7 miles from the datum point. Therefore, it was only admitted that the direction error was 1.6 degrees and the drifting distance error was 1.7 miles. That fact only proves the fitness of the experimental equation, and it suggests that in any drifting one can estimate the position by the same way and accuracy.

For example, the author applied the experimental equations to the drifting positions during the experiments carried out in summer 1972. As a result, the total drifting hours were 43^{h}5, and the sum of the drifted distances and of its estimated distances were 32.6 miles, 31.9 miles respectively; the mean values of drifting direction and estimated direction were 21°2 and 22°2; so they agree pretty well. Or when the distance made good and the course made good are calculated under the assumption of the continuous drifting for 11 days, the position after the drifting is the point in the direction of 154°50′ and 31.1 miles distant from the datum point; on the other hand, the estimated position based on the experimental equations was 154°35′, 30.9 miles from the datum point. Therefore both results were nearly equal.

(e) Example of time constant

The expression formula of time constant $M_S/2\sqrt{KP_0}$ is reduced to $M_SU/2P_0$ by substituting $P_0=KU_S{}^2$. Where $P_0=\rho_a C_a S_a W^2/2=\rho_w C_w S_w U^2/2$ and ρ_a=0.1292 kg·sec^2/m^4, ρ_w=102.55 kg·sec^2/m^4, S_a=365 m^2, S_w=256 m^2, C_a=1.219, C_w=0.903, therefore if one puts M_S, W as 300ton, 10m/s respectively, the time constant is calculated as 26 seconds.

2.2.3 *Analysis of the drift in the Hokusei-Maru*[15]

(1) Purpose of the experiment

When a ship rolls because of the waves, it drifts. The drifting force is connected with a ship's natural rolling period and that of the wave, and it is considered that the force is the greatest when both periods synchronize.[13][16] Suehiro et al.[16] reported from a model experiment that a ship which had no bilgekeels and consequently had a large rolling, drifted more than a ship which had bilgekeels and consequently had a small rolling.

Against their opinion, the author has carried out ship's drifting experiments with real ships since 1964 on oceans, in wind and waves. In the experiments,[5] he could not find a phenomenon with the same wind velocity; when a wind-wave was big, a ship's drifting velocity was greater than that of a small wind-wave, on condition that the wave periods were estimated shorter than the ship's natural rolling periods. In these actual experiments on oceans, the grades of waves were measured by the eye and when the ship got the same wind velocity it was a question whether the ship's conditions (draught, trim) were equal or not. From this standpoint, the author tried to compare the drift of a natural ship's rolling with one reduced by an anti-rolling tank.

Next, if a drift becomes smaller by reduction of the rolling, it will be concluded that an anti-rolling tank is used effectively from the point of watching a fishing gear, in addition to the original purposes that the crew's fatigue is reduced and that the work efficiency is improved. Therefore, in his experiments the author aimed at a valuation on fishery.

(2) Principal dimensions of the ship and its conditions

G.T. 273.3T, length over all 43.43 m, moulded breadth 6.80m, moulded depth 3.40 m, mean draught 2.39 m (max. 2.47 m, min. 2.31 m).

(3) Sea region and periods of experiments

The experiments were carried out in the North Pacific Ocean from June 4 till June 8 and from June 16 till June 21 in 1967. As it took only a few days for both sailings, it was thought that the draught and trim hardly changed, and the depths of water were more than 1000 meters, usually with a fetch of over 100 miles.

(4) Experimental method

A corner reflector (diameter 25 cm) which was connected with a salmon gill-net was used as datum point. The corner reflector on the net (which was about three miles long and about seven meters deep) was not blown by the wind in spite of the ship's movement, because the net works as a sea anchor. Therefore, the driftage by the wind action was calculated from the mutual position relations between the ship and the reflector at the time when observations begin and end. Bearings and distances from the reflector were observed by a radar every 30 minutes as the ship was drifting, and the drifting directions and distances were calculated. Then in order to investigate the difference in drifts caused by a large rolling or a small rolling under the same condition, the anti-rolling tank was in operation or stopped every 30 minutes alternatively. Now by means of that anti-rolling tank

Table 2.2.　*Relation of wind velocity ($W(m/s)$), drifting velocity ($U(m/s)$), ship's head (a (degree)), drifting direction (β (degree)), and angle of cut between wind and swell ($\gamma(degree)$), when anti-rolling tank is in operation and in suspension.*

Date	Anti-rolling tank is in operation						Anti-rolling tank is in suspension					
	No.	W	U	a	β	γ	No.	W	U	a	β	γ
June 4, 5	1	3.5	0.31	97	+ 5	+19	1'	3.4	0.25	103	+ 2	+13
	2	4.0	0.23	109	+ 5	−14	2'	4.5	0.30	95	+ 7	−11
	3	5.0	0.34	95	+21	− 8	3'	4.0	0.16	103	− 9	−13
	4	4.0	0.22	95	+ 1	−20	4'	4.5	0.27	98	+ 6	−15
	M	4.1	0.28	99	+ 8		M'	4.1	0.25	100	+ 2	
5, 6	5	5.5	0.39	94	+17	0	5'	5.0	0.41	97	+11	− 5
	6	5.3	0.36	94	0	− 8	6'	5.3	0.28	94	+14	− 8
	7	5.3	0.31	93	+ 2	− 8	7'	5.3	0.36	93	+ 9	−13
	8	5.3	0.43	95	− 3	−15	8'	5.5	0.42	93	+19	−18
	9	5.0	0.36	93	+11	−18	9'	5.0	0.36	97	− 7	−20
	10	5.5	0.49	96	+10	−13	10'	6.5	0.42	93	+18	− 9
	11	6.5	0.51	94	+19	− 8	11'	6.0	0.53	96	+21	− 8
	M	5.5	0.41	94	+ 8		M'	5.5	0.40	95	+12	
6, 7	12	7.3	0.43	103	+ 6	−25	12'	6.8	0.37	84	+13	−13
	13	7.0	0.40	83	+16	−15	13'	7.3	0.40	90	− 4	−15
	14	5.8	0.40	98	+14	−13	14'	5.4	0.36	93	+27	−13
	15	5.9	0.44	95	+11	−13	15'	6.0	0.40	98	+18	−10
	16	6.0	0.29	95	+43	− 8	16'	6.0	0.25	97	+27	− 8
	M	6.4	0.39	95	+18		M'	6.3	0.36	92	+16	
7, 8	17	9.0	0.63	91	+30	− 4	17'	8.5	0.47	90	+18	− 2
	18	7.5	0.64	88	+17	− 2	18'	7.5	0.66	102	+19	−23
	19	9.0	0.64	93	+22	−23	19'	9.3	0.58	92	+41	−20
	20	10.0	0.69	94	+23	−20	20'	10.3	0.52	89	+17	−10
	M	8.9	0.65	92	+23		M'	8.9	0.56	93	+24	
16, 17	21	4.5	0.38	84	+32	+ 3	21'	4.3	0.34	83	+41	+ 2
	22	4.3	0.35	85	+38	− 9	22'	4.1	0.27	92	+21	−25
	23	4.3	0.27	97	+ 4	var.	23'	4.9	0.29	96	+33	var.
	24	5.3	0.35	105	+12	〃	24'	4.5	0.28	90	+ 5	〃
	25	6.3	0.35	96	+36	〃	25'	6.0	0.37	92	+25	−30
	26	6.3	0.41	90	+14	+15	26'	6.5	0.38	87	+19	+15
	M	5.2	0.35	93	+23		M'	5.1	0.32	90	+24	
17, 18	27	5.5	0.41	82	+57	+23	27'	6.3	0.56	85	+50	+13
	28	6.5	0.54	88	+46	+13	28'	6.8	0.43	87	+44	+18
	29	6.3	0.44	83	+32	+23	29'	5.9	0.57	83	+44	+23
	30	5.7	0.47	83	+43	+24	30'	7.5	0.46	90	+36	+ 8
	31	7.3	0.52	91	+41	+ 3	31'	7.0	0.50	91	+46	+ 2
	M	6.3	0.48	85	+44		M'	6.7	0 50	87	+44	
18, 19	32	4.4	0.29	85	+50	+40	32'	4.7	0.43	81	+58	+38
	33	5.0	0.41	84	+59	+38	33'	5.0	0.40	91	+47	+43
	34	5.1	0.38	88	+64	+45	34'	5.5	0.54	88	+48	+45
	35	5.5	0.50	86	+55	+43	35'	6.0	0.46	84	+48	+43
	36	6.5	0.46	85	+44	+40	36'	6.5	0.45	86	+47	+15
	M	5.3	0.41	86	+54		M'	5.5	0.46	86	+50	
20, 21	37	5.8	0.49	89	+38	+ 5	37'	6.0	0 56	90	+44	+ 5
	38	6.3	0.57	89	+27	+10	38'	7.0	0.60	93	+40	+13
	39	7.8	0.67	93	+29	+12	39'	8.3	0.55	90	+34	+13
	40	8.0	0.56	91	+35	− 7	40'	7.3	0.44	93	+38	− 8
	41	6.5	0.44	94	+30	− 8	41'	6.8	0.45	89	+26	− 5
	42	6.9	0.45	90	+30	− 9	42'	6.5	0.45	94	+18	− 9
	M	6.9	0.53	91	+32		M'	7.0	0.51	92	+33	

(MN type) with which the ship was equipped, the rolling moment caused by the waves and the moment caused by the water of the tank acted in an opposite direction. Therefore, the actual rolling moment of the hull was offset and rolling angle of the hull was also reduced.

(5) Results and discussion

The author converted the drifting distances guided by the above-mentioned experiments into drifting velocities, and compared those drifting conditions when the anti-rolling tank was in operation or stopped, and indicated the data in Table 2.2. In the table, α shows the angle between a ship's head and the wind direction, β shows the difference in angle between the ship's drifting direction and the direction in which the wind blows away. It was thought as a plus when the ship drifted towards the bow away from the direction in which the wind blew, and as a minus when the ship drifted towards the stern. M, M' show the mean values for each day.

The experiments with the anti-rolling tank in operation or stopped were carried out alternatively every 30 minutes and they were practiced for several hours every day. They went on for 11 days in all. When the connection chart for the drifting is drawn by assuming that the experiments were carried out continuously,
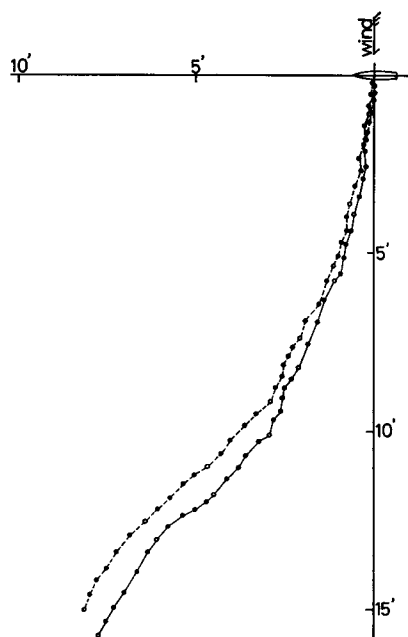
Fig. 2.10. Connected drifting chart.
    solid line—anti-rolling tank in operation
    broken line—anti-rolling tank in suspension
    ● observation point every 30 minutes
    ○ opening observation point or closing point every day
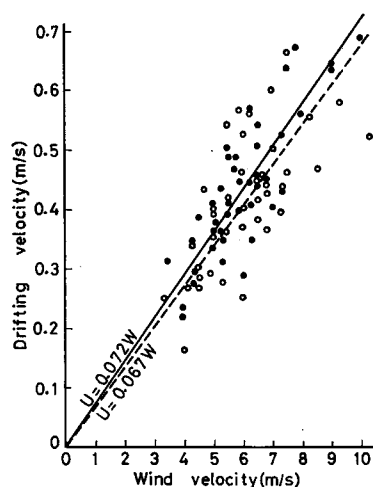
Fig. 2.11. Relation between wind velocity and drifting velocity.
    ● solid line—anti-rolling tank in operation
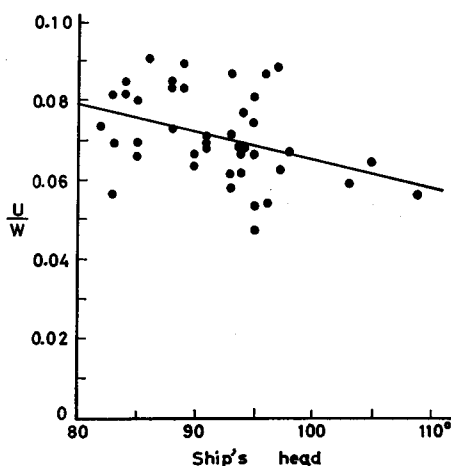   ○ broken line—anti-rolling tank in suspension

Fig. 2.12(a). Relation between ship's head and U/W when an anti-rolling tank is used.
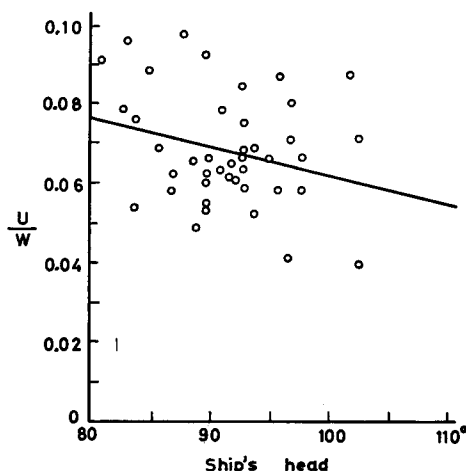
Fig. 2.12(b). Relation between ship's head and U/W when an anti-rolling tank is not used.

it looks like Fig. 2.10. As a whole, it will be found that they drifted mostly toward the same direction and through an equal distance. Therefore, even if one used an anti-rolling tank to reduce the rolling, he could hardly obtain a better efficiency than the drifting distance with natural rolling under the condition of the wind velocity being less than 11m/s. The angle of rolling was $1°0 \sim 6°0$ when the anti-rolling tank was in operation, and $1°3 \sim 8°5$ when the tank was stopped, and the arithmetic mean was $2°2$ and $3°9$ respectively.

(a) Relation between wind velocity and drifting velocity

Based on the above-mentioned results, each measured value is plotted in Fig. 2.11 by describing the drifting velocity (U) in the axis of ordinate and the wind velocity (W) in the axis of abscissa. When the smoothing according to the linear equation is carried out, the experimental equations at the time of the operation and stop of the tank are represented by the least square method as follows.

$$\text{anti-rolling tank in operation} \quad U(m/s) = 0.072 \ W(m/s)$$
$$\text{anti-rolling tank in suspension} \quad U(m/s) = 0.067 \ W(m/s)$$

(b) Relation between the drifting velocity and the ship's head

The relation between the drifting velocity U(m/s) divided by the wind velocity W(m/s) in Table 2.2 and the ship's head (α) is shown in Fig. 2.12 (a)(b), and the relations are smoothed by the equation $U/W = a - b\alpha$, and are expressed as follows:

$$\text{anti-rolling tank in operation} \quad \frac{U}{W} = 0.136 - 0.00069\alpha$$

$$\text{anti-rolling tank in suspension} \quad \frac{U}{W} = 0.134 - 0.00071\alpha$$

The author will compare these relations with the above-mentioned relations (between

wind velocity and drifting velocity). $U=0.072W$, when the anti-rolling tank is in operation, thus corresponds to the value when the ship's head is 91°5; and $U=0.067W$, when the anti-rolling tank is in suspension, thus corresponds to the value when α is 93°5.

(c) Interrelation among the wind velocity, the ship's head and the drifting direction

  Fig. 2.13 describes the angle (α) between a ship's head and the wind direction in the axis of ordinate and it describes the wind velocity in the axis of abscissa. There isn't any relation between both so that it isn't thought that a ship's head is determined by the wind velocity.

  Next, the relation between the wind velocity and the drifting direction is shown in Fig. 2.14, from which it is seen that a drifting direction is not affected by the wind velocity whether strong or weak.
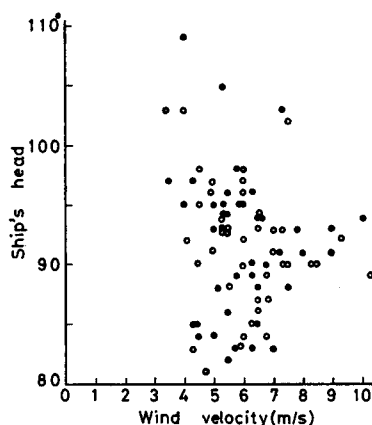
Fig. 2.13. Relation between wind velocity and ship's head.
● — anti-rolling tank in operation
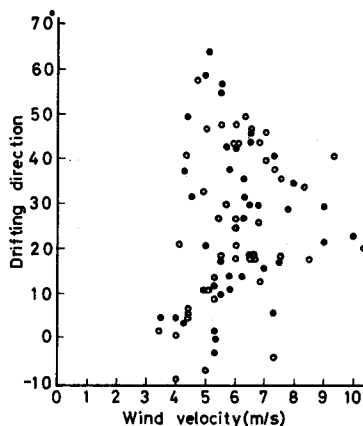○ — anti-rolling tank in suspension

Fig. 2.14. Relation between wind velocity and drifting direction.
● — anti-rolling tank in operation
○ — anti-rolling tank in suspension

(d) Relation between a ship's head and the drifting direction

  The relations between a ship's head (measured in the direction of bow-side based the direction of the wind) and the drifting direction (measured in plus when it drifts bow-side based on the direction in which the wind blows away) are shown in Fig. 2.15, and it is obvious that a correlation between them can be found. If this relation is expressed by this linear equation $\beta=a-b\alpha$, we get:

   anti-rolling tank in operation $\beta = 204°1 - 1.943\alpha$
   anti-rolling tank in suspension $\beta = 213°3 - 2.046\alpha$

Both of them indicate almost the same tendency, and the difference between them within $110°\geqq\alpha\geqq80°$ is 0°9 in mean error. Now the scattering of β around the regression lines is 13°5 (s.d.) in the case of the anti-rolling tank in operation and 13°4 (s.d.) in the case of its suspension. Therefore the scatterings in both cases

are almost the same.

On the balance, it is thought that a ship will drift in a definite direction in the most settled posture against the wind, but in the phenomenon a remarkable tendency appears. The relation between the ship's head and the drifting direction within several hours, when the ship's draught and trim do not change is shown in Fig. 2.16 (a)(b). Fig. 2.16 (a)(b) are homologous figures with Table 2.2. (each point shows the average value of each 30-minute observation) Both figures indicate max., min., mean of amplitude (difference between maximum and minimum every 30 minutes) of a ship's head and of the drifting directions as follows:

anti-rolling tank in operation

ship's head   21°, 3°, 10°
drifting direction   37°, 11°, 23°

anti-rolling tank in suspension

ship's head   14°, 4°, 9°
drifting direction   36°, 11°, 23°

A ship's head observed every 30 minutes rolled pretty much from side to side, and the amplitudes (difference between maximum and minimum) were max. 38°, min. 8°, mean 18°.
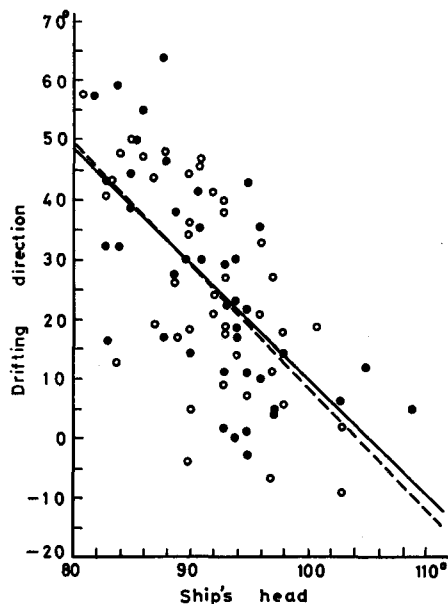

Fig. 2.15.   Relation between ship's head and drifting direction.
●, solid line—anti-rolling tank is used
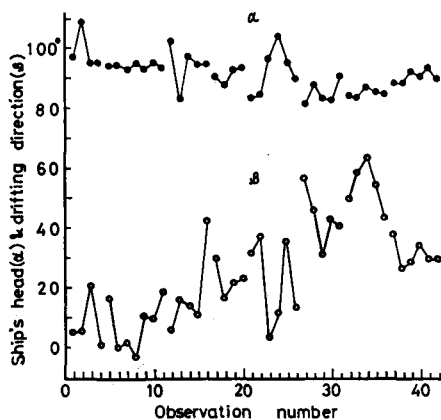○, broken line—anti-rolling tank is not used

Fig. 2.16(a). Ship's head and drifting direction when anti-rolling tank is used.
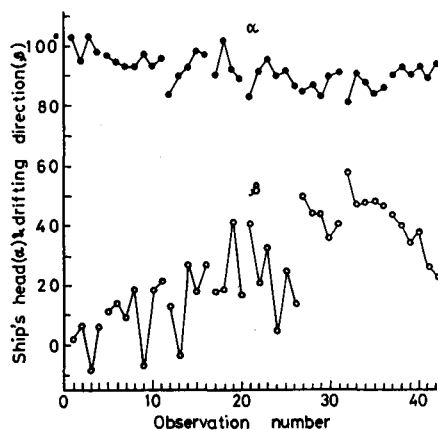● — ship's head, ○ — drifting direction

Fig. 2.16 (b).   Ship's head and drifting direction when anti-rolling tank is not used.
● — ship's head, ○ — drifting direction

— 25 —

(e) Transition condition of drift

The above-mentioned experiments (the case of the Oshoro-Maru expressed in 2.2.2 is the same) were carried out in a stationary state. However any fishing boat opens a drift immediately after casting the fishing gear, accordingly the problem concerning the effect of the initial condition upon the drift remains to be solved.

To examine the subject, the following experiments were carried out in the Okhotsk Sea in July, 1975. The ship's engine was stopped; at that moment the ship's head turned in the direction in which the wind blew. Then the ship's head fell gradually toward the lee and reached a stationary state. While this was happening, the transition state was measured every 30 seconds and the result is shown in Fig. 2.17 in relation to the time elapsed. According to the figure, the ship's head reached a stationary state after several minutes. Accordingly, when a ship opens a drift, if the ship's head turns to the direction in which the wind blows, it is considered that the drift reaches a stationary state within several minutes. Therefore the effect of the initial condition on the drift may be ignored.

(f) Drift of datum point by the action of the wind

To measure the degree of fixation of the reflector connected to the gill-net against the water, a buoy, as shown in Fig. 2.18, is manufactured. And it is thrown down near the reflector (within 0.5 mile), and the distance which the reflector drifts toward the lee is calculated by the change of both positions. The above water portion of the buoy is constituted by the pole (height: 250 cm, diameter: head 1.0 cm, bottom 2.7 cm) and the reflector (height: 10 cm, diameter: 20 cm, wrapped in vesicatory (happosuchiroru in Japanese)) which is connected to
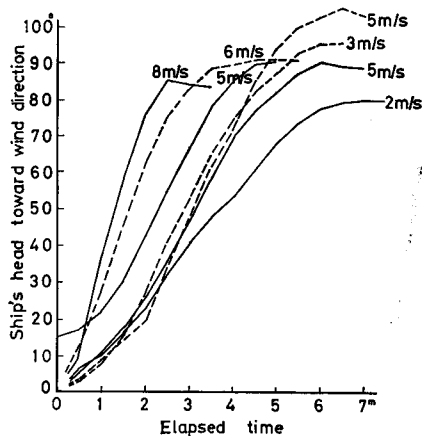

Fig. 2.17.   Time required to reach the stationary state.
solid line—gets the wind from starboard
broken line—gets the wind from port
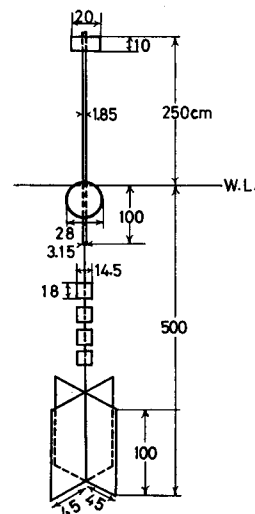figures show wind velocity

Fig. 2.18. Dimensions of the buoy.

the top of the pole. The under water portion is constituted by the pole (length: 100 cm, diameter: head (bottom of float) 2.9 cm, bottom: 3.4 cm) which extends from above water, spherical float (diameter: 28 cm), three cylindrical floats (each of them: diameter=14.5 cm, height=18 cm) and four resistance plates (each of them: height=100 cm, width=45 cm) which are enclosed in an iron pipe and spread watertight canvas.   And the plates are fixed mulually at a right angle.

The relation between the drifting velocity (U) of the buoy and the wind velocity (W) is expressed as $U=0.0068W$.   Here, the ratios of resistance coefficients are treated as follows: sphere is 1, cylinder is 2, plate is 5.

The experiments were carried out at 7 points in the Okhotsk Sea in July, 1975. The reflector which was connected to the gill-net was drifted toward the lee side 0.02 mile per 30 minutes at the maximum and 0.005 mile on the average, as shown in Fig. 2.19.   These distances are considered to be negligible in comparison with the ship's drift.

(g)   Ocean current in the sea region

The ocean current in the experimental sea region was estimated as less than 0.05 knot as shown in Fig. 2.20[14], and the distance between the ship and the reflector was less than four miles, therefore the ship and the reflector are considered to be affected almost similarly by the movement of the sea water.
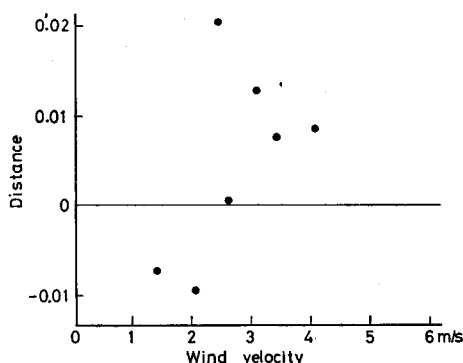

Fig. 2.19.   Distance of the datum point drifting toward the lee side by wind action per 30 minutes.
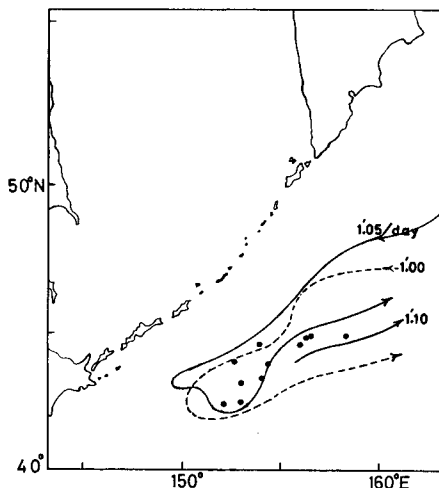

Fig. 2.20.   Estimated ocean current chart in the experimental sea region.
● — observation point
solid line — summer 1956
broken line — summer 1955

2.2.4 *Wind tunnel experiments about the drift by the action of the wind on the Oshoro-Maru*[17]

(1)   Aim of this item

About the actual experiments on the ocean, an analysis of phenomena must be

done by a statistical method because we can't fix its outer conditions. After all, while drifting, a ship's head yaws because of a change in direction of the wind, its velocity, and the compulsory gyrations by the motion of the waves.

A wind tunnel experiment is the fundamental method to calculate the stability of the ship's head, the drifting direction and the drifting distance in the case of a ship drifting by a regular wind direction and wind velocity. As to the object of the experiment, the Oshoro-Maru was selected in order to compare guided results with those of actual experiments.

(2) Wind tunnel experiment

(a) Wind tunnel and balance
As for the wind tunnel and balance, the 0.5 m Göttingen type of wind tunnel and the balance of four component forces of the Faculty of Fisheries, Hokkaido University were used.

(b) Model
The dimensions of the image model was decided as 1/200 of the actual ship, taking into consideration the fact that the diameter of the measuring portion of the wind tunnel is 0.5 m, and the model was varnished. The principal dimensions of the actual ship corresponding to the model were as follows.

    length over all 66.7 m,   length between perpendiculars 60.5 m,
    length over all under water portion 63.6 m, moulded breadth 11.00 m,
    draught F. 3.65 m, A. 4.97 m, center of gravity ⊗ aft 2.39 m,
    longitudinal projected area above the water-line (B) 365.0 m²,
    longitudinal projected area under the water-line (B') 256.0 m².
However, the fittings on the deck were simplified.

(c) Methods of experiment
The model was fixed to the installation stick with four piano wires by using tight fittings. Since the installation stick could rotate, the wind directions for the ship's fore and aft lines could change easily. The angle of attack varied every ten degrees; furthermore, as to the bending portion of the lift coefficient, it varied every five degrees. Whenever the wind velocity was measured, it was 20.5~22.7 m/s and Reynolds' number corresponding to the length between perpendiculars was $4.21 \times 10^5 \sim 4.66 \times 10^5$ (here: 760 mm, 15°C).

(3) Results

(a) Above water portion
The lift coefficient C_L, the drag coefficient C_D, the resultant force coefficient C_R', the direction angle for the resultant force from the right aft θ are expressed in the following equations.

$$C_L = \frac{L}{\frac{1}{2}\rho V^2 B}, \quad C_D = \frac{D}{\frac{1}{2}\rho V^2 B}, \quad C_R' = \frac{R}{\frac{1}{2}\rho V^2 B}, \quad \theta = a + \tan^{-1}\frac{C_L}{C_D}$$

where V: relative wind velocity (m/s), ρ: air density (kg·sec²/m⁴),
      a: relative wind angle measured from the bow (degree),
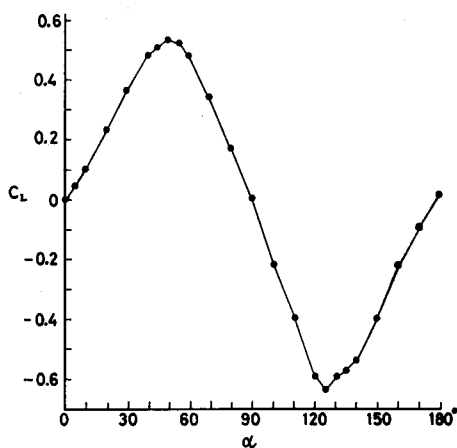
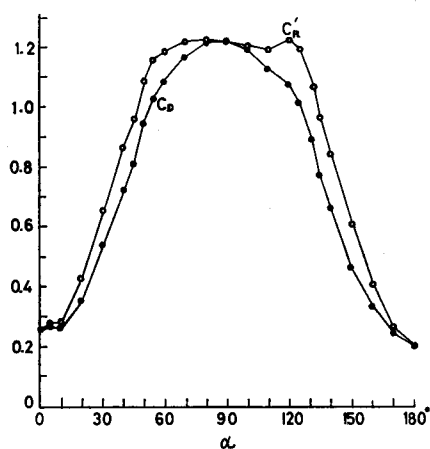Fig. 2.21. Lift coefficient C_L of the above water portion of the ship.

Fig. 2.22. Drag and resultant force coefficients C_D, C_R' of the above water portion of the ship.
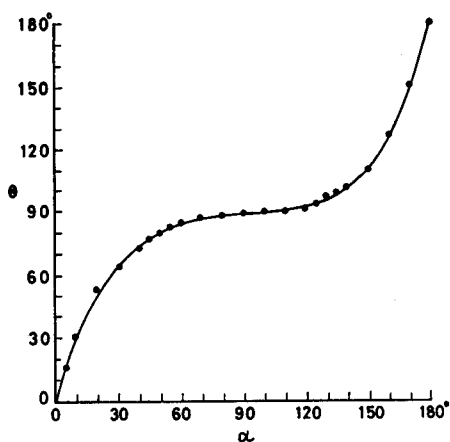

Fig. 2.23. Direction angle of the resultant force from the right aft θ of the above water portion of the ship.
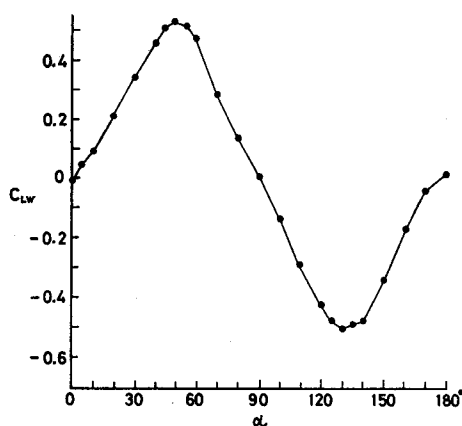

Fig. 2.24. Lift coefficient C_{LW} of the under water portion of the ship.

L: lift acted upon the above water portion (kg),

D: drag acted upon the above water portion (kg),

R: resultant force acted upon the above water portion (kg).

The results of the experiments are shown in Fig. 2.21, 22, 23.

(b) Under water portion

Each coefficient is guided the same way as that of the above water portion. The hydrodynamic peculiarity of the under water portion is expressed as follows by adding suffix $_W$.
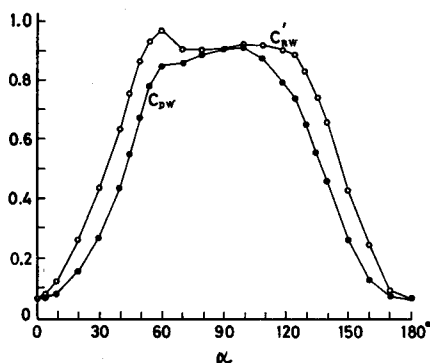
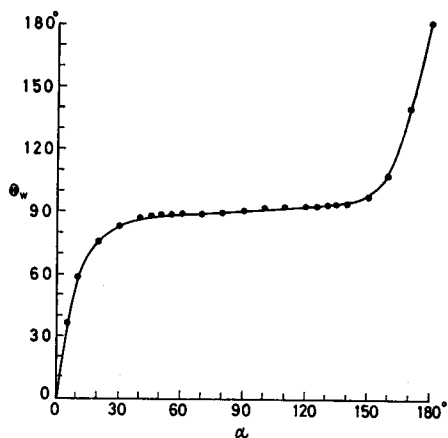Fig. 2.25. Drag and resultant force coefficients C_{DW}, C'_{RW} of the under water portion of the ship.

Fig. 2.26. Direction angle of the resultant force from the right aft Θ_W of the under water portion of the ship.
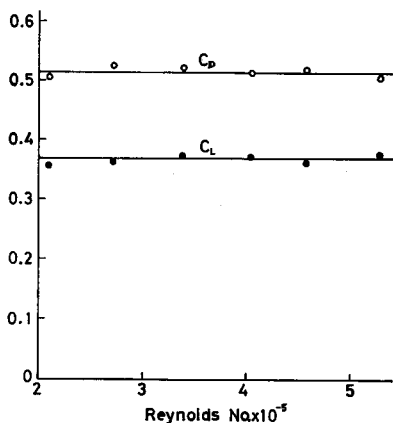

Fig. 2.27(a). Relation between the coefficient C_L, C_D and Reynolds number. (above water portion)
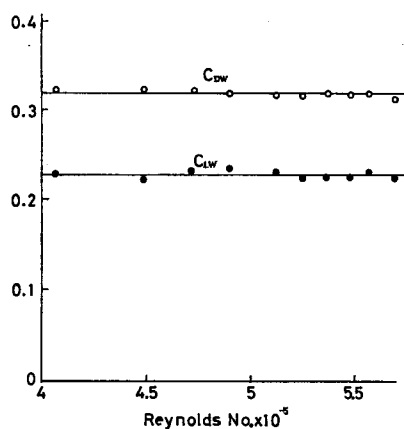
Fig. 2.27(b). Relation between the coefficient C_{LW}, C_{DW} and Reynolds number. (under water portion)

$$C_{LW} = \frac{L_W}{\frac{1}{2}\rho V^2 B'}, \quad C_{DW} = \frac{D_W}{\frac{1}{2}\rho V^2 B'}, \quad C'_{RW} = \frac{R_W}{\frac{1}{2}\rho V^2 B'}, \quad \Theta_W = \alpha + \tan^{-1}\frac{C_{LW}}{C_{DW}}$$

and the results are shown in Fig. 2.24, 25, 26.

Still more, the above-mentioned values were obtained from the experiments in which the wind velocity in the tunnel was from 20.5m/s to 22.7m/s. To confirm the variation of the above-mentioned coefficients with a change in the wind velocity, the next experiments were carried out.

Fig. 2.28.   Length between the stem and
the center of pressure.
●, solid line—above water portion
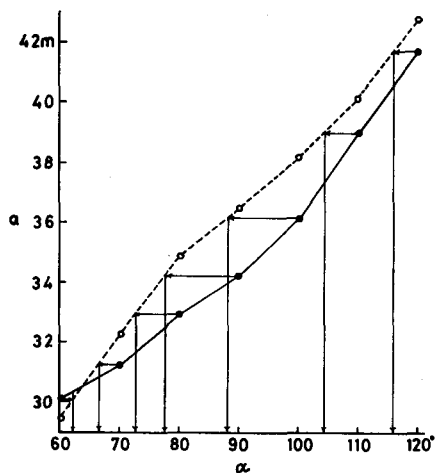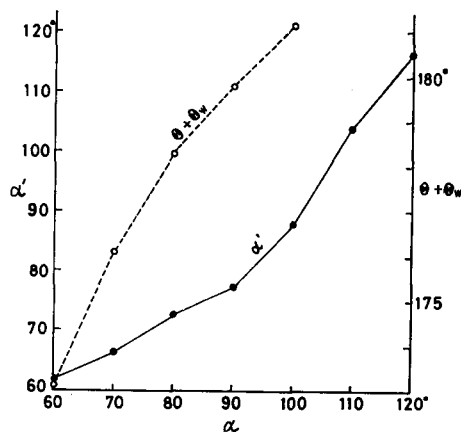○, broken line–under water portion

Fig. 2.29.   Relation between angle of attack
a (above water portion) and a′ (under
water portion) when both centers of
pressure are at the same position, and
a sum of θ and θ_W.

As to the image models of the above water and under water portions, changes
in lift and drag corresponding to Reynolds' various numbers were observed by
fixing an attack angle at 30° and by changing the wind velocities.   The results
are shown in Fig. 2.27 (a)(b) and the coefficients are thought to be definite.

(c)   Drifting posture, direction and distance

The conditions to determine the drifting posture and the direction by the
action of the wind are the next three.   One condition is that an acting line of
pressure working on the above water and on the under water portion be in accord;
the second is that the difference between both directions of the resultant forces be
180°, and the last is that both resultant forces be equal.   Fig. 2.28 shows the
lengths between the stem and the center of pressure working on the above water
and the under water portions.   When both centers of pressure have the same
position, the relations between the angle of attack a (above water portion) and $a′$
(under water portion) are shown in Fig. 2.29.   If a, $a′$ are guided, the direction of
the resultant force corresponding to a, $a′$ will be as in Fig. 2.23 and Fig. 2.26, so
that the total of both directions is shown in Fig. 2.29; a to satisfy $\theta+\theta_W=180°$ is
91°8.   Therefore, $a′$ corresponding to $a=91°8$ is 78°7 from Fig. 2.29.   And in
order to have the resultant forces acting on the above and under water portions
equal, the following equation must be used, $\rho_a C_a S_a W^2/2 = \rho_w C_w S_w U^2/2$.   Where, ρ_a,
ρ_w equal 0.1292 kg·sec²/m⁴, 102.55 kg·sec²/m⁴ (760 mm, 5°C, 32‰) respectively, and
$C_a=1.219$ (from Fig. 2.22), $C_w=0.904$ (from Fig. 2.25), therefore $U=0.041\sqrt{S_a/S_w}\,W$
is obtained.

(4)   Discussion

If the Oshoro-Maru suffers a swell from the same direction as that of a wind,

on the condition that the mean draught be 3.75 m and the trim be 1.10~1.65 m, it is obvious that the ship's head leans to 95° toward the wind direction statistically (refer 2.4). Therefore, in the next equations

$$U = \{0.058 + 24.2\,e^{-5.14t} - (0.00005 + 0.022\,e^{-3.14t})a\}\sqrt{\frac{S_a}{S_w}}\,W,$$

$$\beta = (293.4 - 62.6\,t) - (3.117 - 0.886\,t)\,a,$$

by employing $t=1.32$, $a=95$, U(m/s)$=0.050\sqrt{S_a/S_w}\,W$ (m/s), $\beta=26°$ are calculated.

On the other hand, according to the wind tunnel experiment, $a=92°$, $U=0.041\sqrt{S_a/S_w}\,W$, $\beta=10°$ were gotten. When we compare the actual ship with the model, it is natural that, while the ships are drifting both postures appear to be almost the same. Next, as to the drifting velocity, that of the actual ship is slightly larger than that of the model. The reason is considered as follows.

The drag coefficient of a round plate put perpendicularly to an air current is constant till the state of the Reynolds' number is large. If a column is put against it in a similar fashion, it shrinks in proportion to the increase of the Reynolds' number. When one compares the above water portion and the under water portion, the latter shows a configuration that is almost like a column. Accordingly, when a Reynolds' number is large (provided a wind of 10m/s affects the Oshoro-Maru, the Reynolds' number is 4.11×10^7), the resistance of the above water portion becomes relatively large, therefore, it is considered that the drifting velocity increases. Furthermore as to the model, since the fittings on the deck are not considered except for the main articles (bridge, funnel, mast), the area which is affected by the action of the wind decreases a little; accordingly the drifting velocity decreases. Moreover, it is considered that the actual ship drifts with a roll, therefore its effect adds.

Next, the difference in drifting directions between the actual ship and the model is considered as follows. In Fig. 2.30, if a force (f) acts on the hull toward a direction β, the direction β' of the movement is expressed as follows

$$\beta' = \cot^{-1}\left(\frac{m+m_x}{m+m_y}\cot\beta\right)$$

where m : mass of a ship, m_x: additional mass on the fore and aft direction, m_y: additional mass on the beam direction of a ship.

For the Oshoro-Maru, the breadth is 11.00 m and the over all length of the under water portion is 63.6m; accordingly, m_x, m_y are estimated as 0.05, 0.9 respectively. And if one adopts 10°, which is the balanced angle in the wind tunnel experiment, as β, β' is calculated as 18°.

Fig. 2.30. Direction of force and the direction of motion.

About the model, fittings on the deck are not considered except for the main articles, accordingly, a strict comparison between a real ship and a model cannot be made. However, it is explained that both the model and the actual ship turn toward their heads rather than the lee-side. Moreover, the difference between the drifting direction of the actual ship indicated in Table 2.1 (a)(b) and the calculated direction by the experimental equation, that is $\beta = (293.4 - 62.6\,t) - (3.117 - 0.886\,t)a$, was 11.7 degrees indicated by the standard deviation. If one compares the result of the wind tunnel experiment with that of the actual ship, he will find that both agree within the limits of the standard deviation.

2.3 Experiment concerning the accuracy of an estimated drifting position[18]

2.3.1 *Aim of experiment and its method*

The above-mentioned equations referring to a drifting velocity and drifting direction give an average for each experiment. If the equations are used to estimate the drifting positions at the time of the experiment, we will find it easy to estimate positions close to actual drifting positions. In fact, it was so (refer 2.2.2). However, in the case of real problems, it is important that the equations be easily applied at any time to keep an indispensable accuracy. About the two ships mentioned above, the Oshoro-Maru can register the draught and trim at any time by an electric draught meter, and the condition of the wind easily by a windvane and an anemometer. Therefore, since the experimental equations to estimate a drifting position include a whole set of factors concerning direction and distance, an estimated position can also be expected to be quite accurate. On the other hand, when a ship does not have such equipment, we are compelled to estimate the drifting positions by the experimental equations corresponding to conditions classified into several groups.

For this purpose, the Hokusei-Maru was selected to investigate the accuracy of estimated positions. The methods of investigation consisted in estimating the drifting positions in operation in June and July, 1968, in taking the results of a drifting experiment in June 1967, and in investigating and discussing the gaps between the drifting positions and the estimated positions. From the experiment carried out in 1967, the drifting direction was expressed as follows in relation to the direction of the ship's head.

$$\text{anti-rolling tank in operation} \quad \beta = 204°1 - 1.943a$$
$$\text{anti-rolling tank in suspension} \quad \beta = 213°3 - 2.046a$$

And the relation between the drifting velocity and the wind velocity was also indicated as follows.

$$\text{anti-rolling tank in operation} \quad U(\text{m/s}) = 0.072W(\text{m/s})$$
$$\text{anti-rolling tank in suspension} \quad U(\text{m/s}) = 0.067W(\text{m/s})$$

These relations are expressed in detail by looking upon a ship's head and a wind velocity as parameters.

Each of them is $U = (0.136 - 0.00069a)W$, $U = (0.134 - 0.00071a)W$.

However, if the accuracy of an estimated position satisfies the required

Table 2.3. *Relation of wind velocity ($W(m/s)$), ship's head (a(degree)), angle of cut between wind and swell (γ(degree)), drifting distance ($U(n.m.)$) and drifting direction (β (degree)).*

No. of sta.	No. of obs.	U	β	α	γ	W	Tank	No. of sta.	No. of obs.	U	β	α	γ	W	Tank
1	1	0.17	93	68	var.	2.8	op.	5	51	0.42	−15	101	−28	5.5	susp.
	2	0.12	31	88	"	2.8	"		52	0.49	−20	101	− 8	6.0	"
	3	0.26	42	81	"	3.3	"		53	0.41	− 4	106	−18	5.8	"
	4	0.34	13	91	"	3.8	"		54	0.37	− 9	102	−18	5.3	"
	5	0.26	27	76	"	3.3	"		55	0.42	9	105	−13	6.0	"
	6	0.34	35	82	+10	3.5	"		56	0.52	10	98	−13	7.4	"
	7	0.30	41	71	+30	3.5	"		57	0.57	6	95	−13	7.4	"
	8	0.28	52	68	+25	3.5	"		58	0.60	−12	92	−15	6.4	"
	9	0.32	52	71	+20	3.8	"		59	0.46	26	92	− 3	6.8	op.
	10	0.30	74	74	+14	3.6	"		60	0.50	37	91	− 3	6.0	"
2	11	0.22	67	55	var.	2.1	susp.		61	0.44	46	88	− 3	5.5	"
	12	0.23	57	68	+38	2.9	"		62	0.45	30	89	− 3	5.5	"
	13	0.33	59	74	+28	3.3	"	6	63	0.50	44	92	− 3	5.3	"
	14	0.33	42	81	+ 7	3.8	"		64	0.53	40	88	− 3	5.0	"
	15	0.33	54	80	− 5	3.9	"		65	0.35	22	98	−10	5.0	susp.
	16	0.35	63	64	var.	4.2	"		66	0.32	23	93	−10	5.0	"
	17	0.34	76	70	+ 8	3.9	"		67	0.35	39	91	− 8	5.0	"
	18	0.30	80	67	var.	3.1	"		68	0.45	40	95	−10	5.3	"
	19	0.22	63	68	"	3.3	"		69	0.54	42	92	+10	6.8	op.
	20	0.19	66	65	"	2.9	"		70	0.66	33	93	+10	6.8	"
3	21	0.39	42	87	−13	4.8	susp.		71	0.65	25	89	+13	7.0	"
	22	0.41	39	85	−10	4.5	"		72	0.63	50	90	+13	7.3	"
	23	0.46	44	81	− 5	5.0	"	7	73	0.53	39	88	+15	6.8	"
	24	0.44	50	76	0	5.0	"		74	0.55	44	87	+20	7.0	"
	25	0.42	50	74	0	5.3	"		75	0.67	47	84	+23	7.0	susp.
	26	0.39	25	84	−10	5.3	"		76	0.62	47	84	+23	6.8	"
	27	0.42	39	87	−13	5.3	"		77	0.56	39	84	+23	7.0	"
	28	0.42	41	83	−10	5.5	"		78	0.50	46	85	+23	7.0	"
	29	0.49	30	86	−15	5.8	"		79	0.41	47	80	+10	5.0	op.
	30	0.40	46	89	+ 5	5.5	"		80	0.42	42	81	+50	5.0	"
	31	0.42	46	81	+13	5.3	"		81	0.45	65	88	+53	4.3	"
	32	0.41	47	81	+13	5.0	"	8	82	0.34	59	85	+55	3.5	"
4	33	0.31	46	91	−23	2.9	op.		83	0.36	59	83	+58	3.3	"
	34	0.32	40	93	−25	3.0	"		84	0.33	53	85	+55	3.5	"
	35	0.27	30	77	−18	3.5	"		85	0.32	75	65	var.	3.0	susp.
	36	0.25	47	82	−15	3.8	"		86	0.30	90	51	"	3.3	"
	37	0.26	26	87	−23	4.3	"		87	0.33	−11	101	−33	3.5	op.
	38	0.30	17	91	−28	4.8	"		88	0.35	−16	99	−40	3.5	"
	39	0.31	21	93	−28	5.0	"		89	0.28	−12	100	−45	3.0	"
	40	0.34	28	87	−20	4.3	"		90	0.28	− 3	99	−50	3.0	"
	41	0.36	23	80	−10	3.8	"		91	0.24	−16	109	−75	2.8	"
	42	0.35	44	82	− 3	4.5	"		92	0.19	1	111	−70	3.0	"
	43	0.35	46	80	0	5.0	"	9	93	0.20	−10	104	−18	3.0	susp.
	44	0.47	23	85	−15	5.8	"		94	0.17	13	102	−23	2.8	"
	45	0.46	21	82	−18	6.0	"		95	0.15	16	92	−23	2.8	"
	46	0.45	25	88	−23	5.5	"		96	0.21	13	102	−20	3.5	"
	47	0.27	9	102	−20	4.0	susp.		97	0.24	36	94	−23	3.8	"
	48	0.31	−15	110	−28	4.5	"		98	0.21	0	89	−23	3.3	"
	49	0.33	0	107	−30	4.8	"		99	0.24	30	91	−30	3.3	"
5	50	0.34	−16	106	−30	5.0	"		100	0.20	23	90	−33	3.3	"

Table 2.3. (continued)

No. of sta.	No. of obs.	U	β	α	γ	W	Tank	No. of sta.	No. of obs.	U	β	α	γ	W	Tank
	101	0.23	58	70	+25	2.5	op.		109	0.57	33	81	+15	6.3	op.
	102	0.20	61	75	+28	2.3	〃		110	0.51	38	83	+10	6.0	〃
	103	0.29	43	81	+15	3.5	susp.		111	0.58	30	88	+ 5	6.0	〃
10	104	0.40	54	76	+20	3.5	〃		112	0.50	31	89	+ 5	6.3	〃
	105	0.35	50	80	+20	3.0	〃		113	0.47	41	88	+ 8	5.3	〃
	106	0.31	48	79	+18	3.3	〃	11	114	0.49	40	87	+13	4.5	〃
	107	0.33	55	74	+25	3.8	〃		115	0.49	42	85	var.	4.0	〃
	108	0.31	57	76	+25	3.8	〃		116	0.36	27	85	+13	4.5	susp.
									117	0.32	37	74	+18	4.5	〃
									118	0.30	47	78	+13	4.5	〃
									119	0.22	34	84	+13	4.5	〃

accuracy it is more convenient to use the simple method. The effect which different draughts have on the action of the wind is in proportion to the root of the ratio of the projected area of the above water portion to that of the under water portion. Therefore, an estimator must fully consider the changes in a ship's condition in connection with a required accuracy and the quality of given data. In the case of this experiment, the mean draught at the time of sailing and of set sailing in each voyage has a maximum of 2.51 m, a minimum of 2.35 m and an average of 2.45 m. Compared with the conditions in 1967, the difference were a few centimeters only, so that they were not considered particularly. The experiments were carried out in the North Pacific Ocean from June 4 till June 9, and from June 15 till June 20 and from July 2 till July 12 in 1968 in the Okhotsk Sea.

2.3.2　Results and discussion

As to the direction of drifting between the starting point and the ending point for each day, and the distance between both points, when the estimated drift (drifting distance calculated by the ship's head and the wind velocity) and the simply estimated drift (distance calculated by the wind velocity only) are compared with the actual drift, the mean errors about directions and distances were 8°, 0.4 mile in the estimated case and 7°, 0.6 mile in the case of the simply estimated drift. When the author integrated the whole data shown in Table 2.3, assuming that the ship drifted continuously, to the whole drifting time of 59.5 hours, the drifting distance was 41.0 miles, the direction was 34°.6. By contrast, the estimated distance was 37.4 miles, and the direction was 37°.9. Furthermore, the simply estimated distance was 35.3 miles, and the direction was 35°.8. Considering the simply estimated method, it is natural that the estimated distance isn't so accurate as the others but, in watching a fishing gear, a relatively accurate result can be attained because a ship drifts only a few hours.

From this point of view, the author studied the relation between the accuracy of the simply estimated position and the drifting time. The drifting positions and estimated positions every 30 minutes each day are shown in Fig. 2.31. From this figure, it is obvious that the difference in every day's direction and distance,
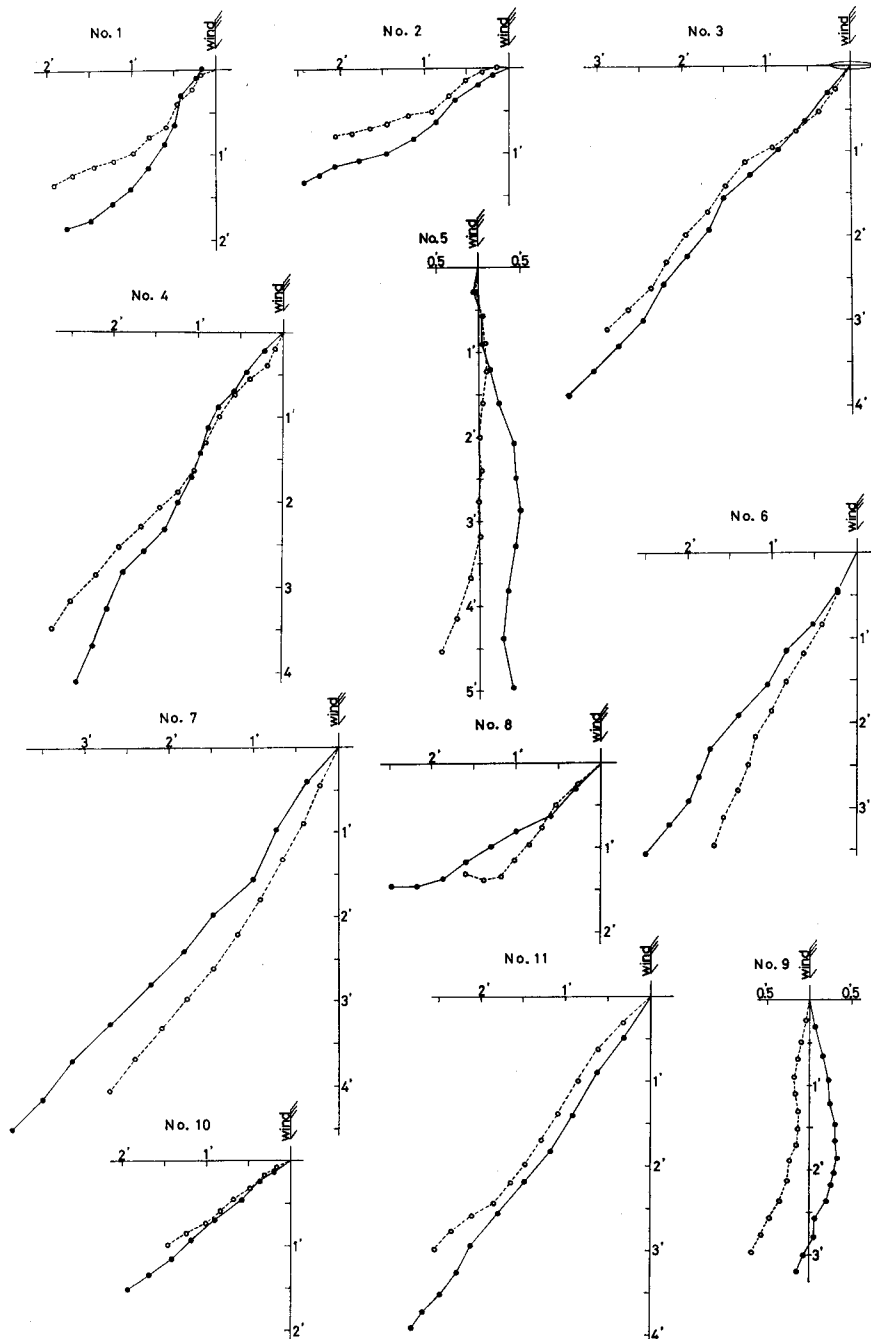
Fig. 2.31. Daily drifting and estimated drifting charts.
●, solid line—determined position and direction every 30 minutes
○, broken line—estimated position and direction every 30 minutes

between starting and ending points, is within 10°, 1 mile from each other.   To show the gap between a determined position and an estimated position, the length of each axis in rectangular co-ordinates, or the polar angle and the radius vector in the polar co-ordinates are always used.   One may see that from Fig. 2.31.   Now, the most direct and indicative method to watch a fishing gear is to consider the direction error from a datum point (fishing gear) and the length between the drifting position and the estimated position.   And so we get the so-called "direction error" and "distance error" to be discussed hereafter.

(1)   Distance error

The distances between the drifting positions and the estimated positions for each day are shown in Fig. 2.32, in relation to the number of drifting hours. As these distances are determined by the scatterings of estimated errors of the drifting distance and drifting direction every 30 minutes, it is difficult to find any regular relations.   However, because the author calculated the standard deviations of errors every 30 minutes, they are shown in Fig. 2.33.   Here is the relation between distance errors and drifting time;

$$\sigma^{(')} = \sqrt{0.08576\, t + 0.003573\, t^2} \doteqdot \sqrt{0.1\, t} \text{ (unit of } t \text{ is hour)}$$

It is difficult to evaluate the longest drifting hours from the moment when a fishing gear is cast to when it is hauled back on a fishing boat.   If it takes eight hours, the length gap between an estimated position and a drifted position is only within one mile in standard deviation.
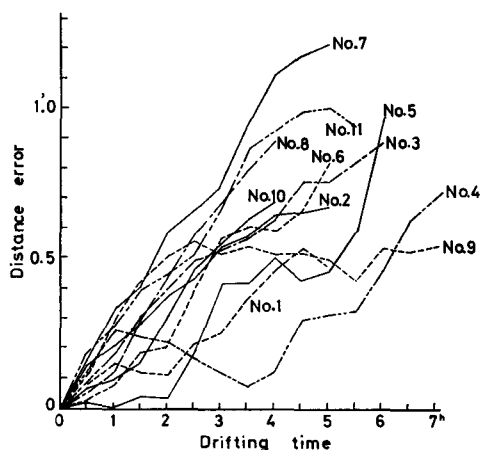

Fig. 2.32. Relation between a distance error (length from drifted position to estimated position) and the drifting time.
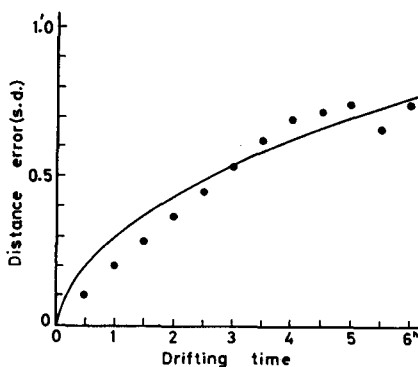
Fig. 2.33. Relation between a distance error (s.d.) and the drifting time.

(2)   Direction error

[Estimated direction − drifting direction] is shown in Fig. 2.34 in relation to the drifting hours every observation day.   After a few hours, the direction errors
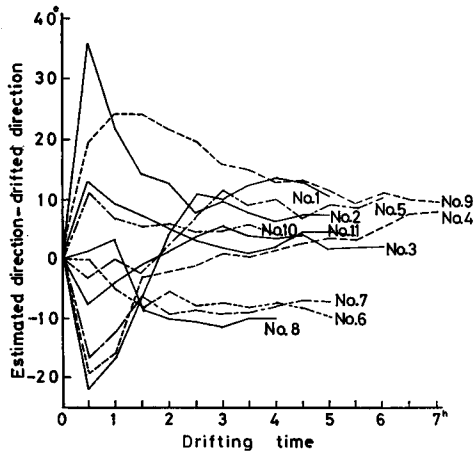
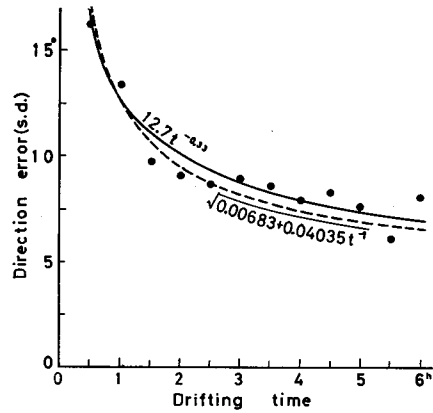Fig. 2.34. Relation between a direction error and the drifting time.

Fig. 2.35. Relation between a direction error (s.d.) and the drifting time.

gradually come to be stable. At the beginning of a drift, there are many scatterings in the data because even just a few estimated errors vibrate sensitively at a given angle. Each standard deviation is also shown in Fig. 2.35 and the direction errors decrease continuously as time passes on. The reason is that the accuracy increases by averaging random errors. However, it is not easy to show the ratio of reduction because the relation in Fig. 2.34 includes the distance error in addition to the pure direction error.

Now, if [estimated drifting distance made good]×[sine of error of drifting direction made good] is $U\sqrt{ct+dt^2}$ (U: drifting velocity, c, d: coefficient) and the error of the estimated direction is $\varDelta\theta$, fundamentally the result will be $Ut\sin\varDelta\theta = U\sqrt{ct+dt^2}$. Therefore $\sin\varDelta\theta$ is expressed as $\sqrt{ct^{-1}+d}$; and by smoothing each point in Fig. 2.35 in that equation

$$\sin\varDelta\theta = \sqrt{0.00683 + \frac{0.04035}{t}}$$

is obtained. Moreover, by imagining a form of at^n and smoothing it for convenience,

$$\sigma = 12°\!.66\, t^{-0.33} \fallingdotseq \frac{13°}{\sqrt[3]{t}}$$

is gotten. If t is eight hours, the direction error is about six degrees in the standard deviation.

(3) Summary

When we discuss a position error synthesizing a distance error and a direction error, the gap is about one mile in usual drifting when a ship drifts for 6~8 hours and the gap of the direction is about six degrees. On the other hand, within a few hours the estimated direction isn't so accurate. However, there is a little gap

between positions themselves so that we can watch a fishing gear without any
trouble. The accuracy of the estimated ship's position required in watching a
fishing gear can't be defined because it differs according to weather conditions, sea
conditions, time, and equipment.

First of all, it is necessary to have some conditions that can decide the course
when the drift closes and the ship begins to move toward the datum point. Next,
when one approaches the object close enough to see it, it is natural that he tries to
find it. At the same time, it is important to foresee the opening time of the watch
and the direction to care for. According to the simply estimated method mentioned
above, it is not difficult to find the object at the time when it comes in sight because
the standard deviation of the drifting direction in a usual drifting time is about six
degrees. (Of course the sphere to watch that one cares for differs from the
distance between the closing point of drift and the beginning point to watch.)
Moreover, it is also easy to obtain information as to the time required to arrive
at the object because the distance between the drifted position and the estimated
position is about one mile (standard deviation).

After all, the method is useful when watching the fishing gear directly. Even
if the usual method is taken while watching, the above-mentioned method is taken
as an auxiliary one or as a preliminary one which can do as well in case the apparatus
is defective. In general, it is practically effective so that the strain of watching is
reduced and easiness obtained since direct and indirect watching can be done.
From those points, the author recommends anyone to investigate and study the
drift of his own ship and use the watching method based on the drifting specific
character of each ship to watch his own fishing gear.

2.4 Method to predict a drifting position

2.4.1 *Aim of study*

On a fishing boat, if someone analyzes the drifting characteristics of his own
ship in detail, his work and operation efficiency become rather easy because it is
possible to watch a fishing gear indirectly, and his efforts are reduced because
repeated sailing and watching can be avoided, when referring to the method of
analysis given previously. Yet, let's think more deeply. A drifting distance is
determined by an external force, the ship's condition, and the drifting time.
Therefore, if those factors are the same, the drifting distance will be the same
whatever the beginning points of drift might be. After all, if one can foresee a
drifting direction and a drifting distance, he will be able to select a beginning
point for his drifting where it is easy to watch a fishing gear.

From this point of view, the author studied a method by the analysis of
phenomena in order to select an opening point of drift by the weather conditions,
the sea conditions, the ship's condition and a prearranged drifting time and to
forecast a closing point of drift, after casting a fishing gear.

2.4.2 *Relation between ship's head and swell*

It is clear that a drifting direction and a drifting distance can be changed

by a ship's head for a wind direction in drifting. In the next part, the author studied what factors make the ship's head settle. A swell is considered to be the factor, and its direction is indicated every 22°5 by eye-measurement. The aim of the study is to forecast the ship's head so that even if the answer is an approximation it is necessary that the method be easy.

For this purpose, the data of the Oshoro-Maru (Table 2.1 (a)(b)) are classified into two groups. One group is that the trim is 1.10~1.65 m, and the other group is that the trim is 1.88~2.07 m. As to the Hokusei-Maru, the data for the purpose of analyzing a drifting phenomenon in 1967 (Table 2.2) were added to the data for estimating a drifting position in 1968 (Table 2.3). They are also classified into two groups. One group is that the trim is 1.87~1.94 m, the other group is that the trim is 2.19~2.21 m. By taking the wind direction as datum line, the swell is minus when it acts upon the bow side and is plus when it rises on the stern side. The ship's head (a) corresponding to the angle (γ) between wind direction and swell direction are shown in Fig. 2.36 (a)(b)(c)(d). In these figures, for a better classification, the data in each group were divided almost in half as to wind velocity, and classified by grades of swells also. However, the data in which the grades of swell were larger than 2 were few and their directions against the wind were limited within a certain narrow region. Therefore the relation between the ship's head and the direction of swell were not derived accurately.

However, the relation being assumed as linear, is represented as follows. From Fig. 2.36 (a) $a=94°6 - 0.479\gamma$, from Fig. 2.36 (b) $a=99°4 - 0.416\gamma$. In those figures, the solid lines show the relations. Now, if γ is within $50°{\sim}{-}50°$, the difference between the calculated values guided by both equations is 4°8 on the average, so if both are treated as belonging to a same population, the relation will be indicated as follows.

$$a = 97°0 - 0.449\gamma$$

As to Fig. 2.36 (c)(d), they are expressed as $a=88°0 - 0.280\gamma$, $a=90°2 - 0.160\gamma$. If γ is also within $50°{\sim}{-}50°$, the difference between both equations is 3°4 on the

Fig. 2.36(a). Relation between a direction of swell and the ship's head. Oshoro-Maru trim 1.10~1.65 m
●, - - - - $W\leqq4.9$ m/s, swell 1
▲, — - — $W\geqq5.0$ m/s, swell 1
△, — — — $W\geqq5.0$ m/s, swell 2

Fig. 2.36(b). Relation between a direction of swell and the ship's head. Oshoro-Maru trim 1.88~2.07 m
●, - - - - $W\leqq6.2$ m/s, swell 1
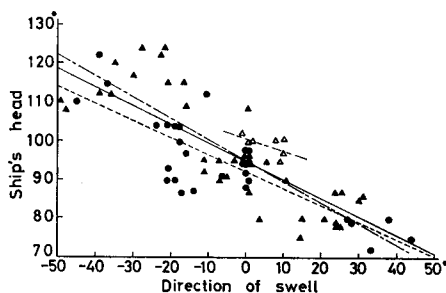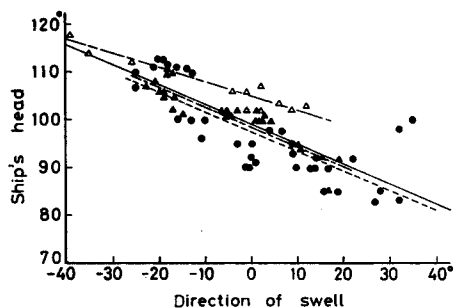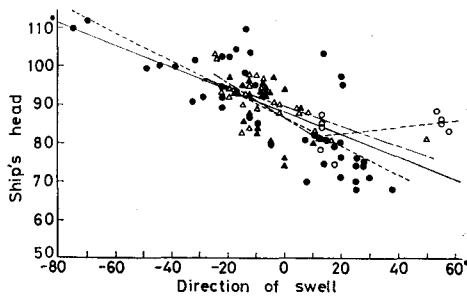▲, — — — $W\geqq6.3$ m/s, swell 1
△, — — — $W\geqq6.3$ m/s, swell 2

Fig. 2.36(c). Relation between a direction
of swell and the ship's head.
Hokusei-Maru trim 1.87~1.94 m
●, ---------- $W \leq 4.9$ m/s, swell 1
○, ————— $W \leq 4.9$ m/s, swell 2
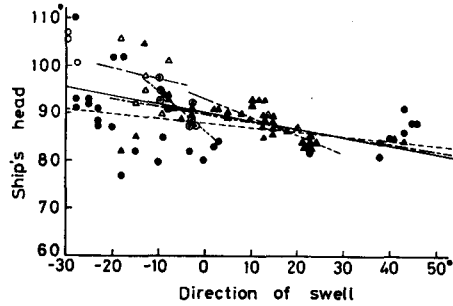▲, ——-—— $W \geq 5.0$ m/s, swell 1
△, ——-—— $W \geq 5.0$ m/s, swell 2

Fig. 2.36(d). Relation between a direction
of swell and the ship's head.
Hokusei-Maru trim 2.19~2.21 m
●, ---------- $W \leq 5.5$ m/s, swell 1
○, ——-—— $W \leq 5.5$ m/s, swell 2
◉, -------- $W \leq 5.5$ m/s, swell 3
▲, ——--—— $W \geq 5.6$ m/s, swell 1
△, ——-—— $W \geq 5.6$ m/s, swell 2
△, ——--——— $W \geq 5.6$ m/s, swell 3

average.   Therefore, when the two equations are unified,

$$a = 89°2 - 0.240\gamma$$

is taken as the equation to forecast a ship's head by the swell in a drift.   The
differences between calculated values by the simplified equations to forecast ship's
heads and each of the data are as follows; in Fig. 2.36 (a) standard deviation is 8°,
in Fig. 2.36 (b) it's 5°, in Fig. 2.36 (c) it's 8° and in Fig. 2.36 (d) it's 6°.   Thus,
even if a swell is weak such as this one, it acts remarkably upon the ship's posture
in drifting.   The reason is considered as follows.

The moment of the wind working on the above water portion of a ship and the
moment of water pressure on the under water portion are expressed respectively
as follows.

$$\frac{1}{2} C_{ma}(a) \rho_a W^2 L_a S_a , \qquad \frac{1}{2} C_{mw}(a') \rho_w U^2 L_w S_w$$

where C_{ma} :   moment coefficient of above water portion,
           C_{mw} :   moment coefficient of under water portion.

If one substitutes the moment coefficient founded on the results of the wind
tunnel experiment, the dimensions of the actual ship, the wind velocity and the
drifting velocity corresponding to the wind in the above mentioned equations,
each moment can be calculated.   For example, the moment coefficients of the
Oshoro-Maru at the time of the wind tunnel experiments are shown in Fig. 2.37 (a),
and the moments when the ship suffers from a wind velocity of 10 meters per second
are shown in Fig. 2.37 (b).

As for the yawing moment due to waves, in case of the cylinder the water line
of which describes a parabola, it is expressed as follows.[19]
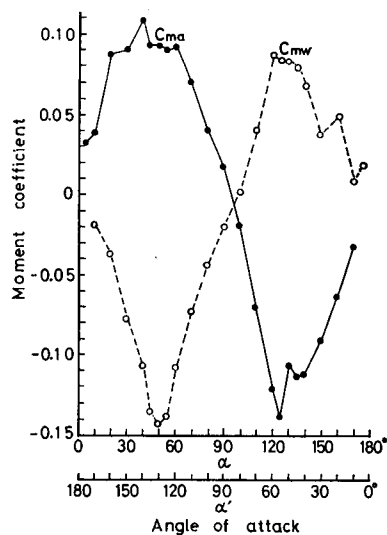
Fig. 2.37(a). Moment coefficient of Oshoro-Maru.
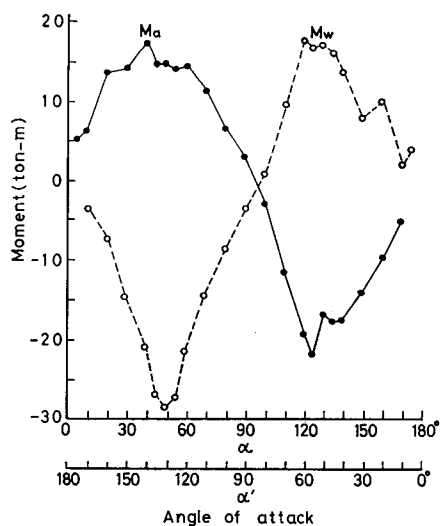
Fig. 2.37(b). Moment when Oshoro-Maru gets a wind of 10 m/s.

$$C_m(\chi)\vartheta\rho g\nabla L_w$$

where C_m: yawing moment coefficient, χ: heading angle, ϑ: wave slope,

∇ : volume of displacement.

On the assumption that the same thing can be said about the ship, the yawing moment coefficients when [wave length / ship's length] are 0.8, 1.0 and 1.25 are shown in Fig. 2.38 (a). As an example of the moment due to swelling, the
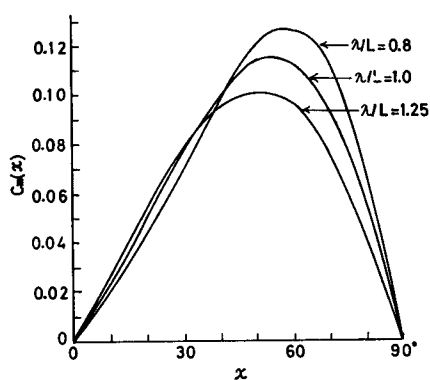
Fig. 2.38(a). Yawing moment coefficient of parabolic cylinder.
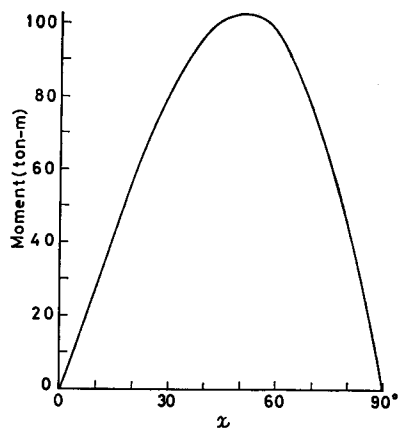
Fig 2.38(b). Example of calculated value of $C_m(\chi)\vartheta\rho g\nabla L_w$.
λ=83.4 m, H=0.83 m, L_w=66.7 m, ∇=1500 m³, ρg=1025

calculated values when L_w=66.7 m, ϑ=0.01 (wave length: 83.4 m, wave height: 0.83 m), ∇=1500m³ and ρg=1025 are shown in Fig. 2.38(b).

Now, if one considers the case when there is no swell, a ship is at a right angle with regard to the wind, and moments by the action of the wind, the water pressure and the wind wave are near zero. Then if a swell is added, the moment which turns a ship to a right angle against its course acts; therefore the attack angles α, α' against the wind direction corresponding to the above and under portion of a ship vary. And the ship is considered to keep its equilibrium by the fact that the composition of the moment vectors of the above and under portion of the ship balances with the moment vector of the swell. In such a case, the balanced state is determined by a combination of the magnitude of the wind velocity and the height and length of the swell. For example, in the case when the grades of swell are less than 3, the moment is largest when the grade is 3, and are 1, 2 in order. As the moment by wind action is proportional to the square of the wind velocity, the deflection of the ship's head ought to be largest when the wind velocity is small and the grade of the swell is 3; it is smallest when the wind velocity is great and the grade of the swell is 2. This tendency is shown in Fig. 2.36.

2.4.3 *Prediction equation of the drift*

(1) Prediction of the drifting velocity

(a) In the case of the Oshoro-Maru

If we look upon the drifting velocity as U(m/s), the wind velocity as W(m/s), the trim as t(m), the ship's head as α (degree), the longitudinal projected area above water line as S_a, under water line as S_w, the next equation is obtained.

$$U = \{0.058 + 24.2\, e^{-5.14t} - (0.00005 + 0.022\, e^{-3.14t})\alpha\} \sqrt{\frac{S_a}{S_w}}\, W$$

Therefore, when we substitute α=97°−0.45γ into the equation, U will be forecasted.

(b) In the case of the Hokusei-Maru

In the case of the Oshoro-Maru, $\sqrt{S_a/S_w}$ and trim in the experiments could be corresponded to the drifting velocity because the draught was always measured by an electric draught meter. However, in the case of general fishing boats, one cannot know the draught and trim at any time so that the draught and trim will correspond to some groups whose conditions are classified in operation. In the case of the Hokusei-Maru, there was only a little difference in draught between the time of departure and that of arrival due to the character of ship. Therefore, it was thought that the draught belonged to the same group and that the trim was classified into two groups as already mentioned.

Next, the drifting velocities are shown in Fig. 2.39(a)(b) in relation to the ship's head (α). Hereupon, since the difference of effect by a magnitude of swell is small they are treated as the same, and if these relations are smoothed by the equation $U/W = a - b\alpha$, they can be expressed as follows:
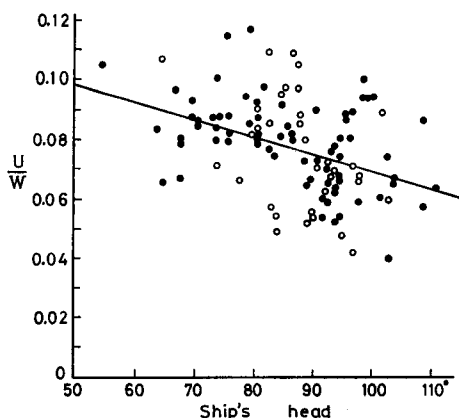
Fig. 2.39(a).   Relation between ship's head
and U/W. (trim 1.87~1.94 m)
● — swell 1,   ○ — swell 2
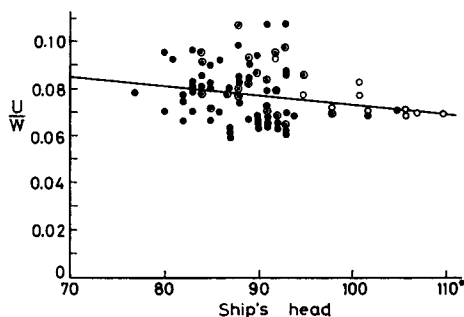
Fig. 2.39(b).   Relation between ship's head
and U/W. (trim 2.19~2.21 m)
● — swell 1,   ○ — swell 2,   ◉ — swell 3

$$\text{group whose trim is } 1.87 \sim 1.94 \text{ m} \qquad \frac{U}{W} = 0.129 - 0.00059a$$

$$\text{group whose trim is } 2.19 \sim 2.21 \text{ m} \qquad \frac{U}{W} = 0.113 - 0.00039a$$

It is the same in the case of the Oshoro-Maru; the greater the trim is, the smaller
a, b are. Moreover, the mean draught of the former group is 2.46 m and that of
the latter group is 2.40 m. The ratio of both $\sqrt{S_a/S_w}$ is less than 1.02 so that it
isn't necessary for us to consider the ratio. Next, as seen in Fig. 2.39 (a)(b), the
relation between the ship's head and U/W is not so remarkable. Then, if each of
the data is thought of as being distributed normally around the regression lines,
each standard deviation will be 0.015 and 0.011. And if they are expressed by
length every 30 minutes, which is the time unit of observation corresponding to the
mean wind velocity for which we get 4.8 and 5.8m/s in each group, then 0.07 and
0.06 mile are gotten as standard deviations.

The factors of scattering were mentioned above, but when one estimates or
forecasts a drifting position, it isn't necessary to be accurate. Particularly in
the case of forecasting, the aim is to select an opening point of drift, because the
sea and weather conditions change after the drifting begins. Therefore, it isn't
necessary for a forecasted position to be accurate anymore. From this point of view,
if two equations indicating the drifting velocity are combined into one, that is,
U/W=0.125–0.00054a, the effect for U/W will be less than 0.0045 when a is within
50°~110°. Therefore, we can easily forecast a distance because it is almost
accurate.

After all, by substituting the relation a=89°–0.24γ,

$$U = (0.077 + 0.00013\gamma)\,W$$

is obtained.

(annotation) There are some differences among coefficients compared with the equation shown in 2.2.3, but the average difference of U/W is 0.003 when a is between 50° and 110°. If we substitute the value in length corresponding to 30 minutes in drifting time and wind velocity 5m/s, it is 0.016 mile. However, concerning the actual experiment on the ocean, it is not much to say that it is impossible to keep the values obtained by adding errors based on unequal conditions with regard to the error of a determined position less than 0.01 mile.

(2) Prediction of the drifting direction

(a) In the case of the Oshoro-Maru

As shown in Fig. 2.3, if we consider a drifting direction as β and the ship's head as a, the following experimental equation is obtained.

$$\beta = (293.4 - 62.6\,t) - (3.117 - 0.886\,t)a$$

Therefore we forecast β by substituting $a = 97° - 0.45\gamma$ into this equation. Then a calculation can be done easily as in the case of the drifting velocity, from a figure or table made in advance.

(b) In the case of the Hokusei-Maru

The relation between the ship's head and the drifting directions are shown in Fig. 2.40 (a)(b) and each is expressed as follows.

$$\beta = 224°1 - 1.978a, \qquad \beta = 213°8 - 2.027a$$
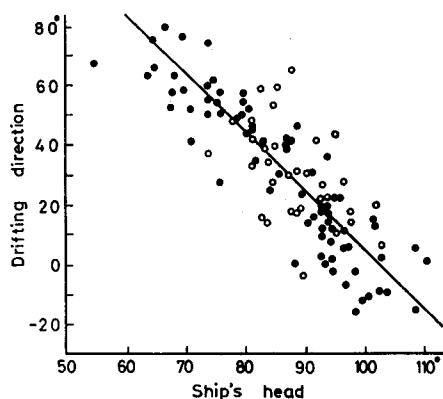
Fig. 2.40(a). Relation between ship's head and drifting direction. (trim 1.87~1.94 m)
● — swell 1,   ○ — swell 2
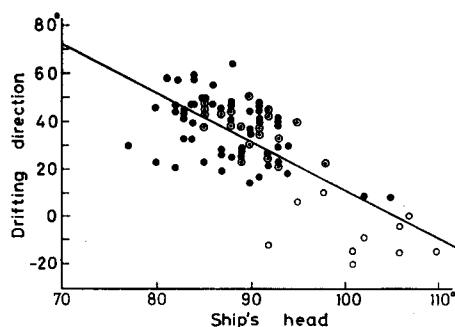
Fig. 2.40(b). Relation between ship's head and drifting direction. (trim 2.19~2.21 m)
● — swell 1,   ○ — swell 2,   ◉ — swell 3

The different calculation value between the two equations is 5° in average when a is within 50°~110°. Therefore, from the standpoint of predicting a drifting direction, if we combine both equations into one, the result is $\beta = 214°7 - 2.080a$, and by substituting $a = 89° - 0.24\gamma$ into the former equation

$$\beta = 29° + 0.50\gamma$$

セ

is obtained.

In general, a drifting direction is considered to be forecast by the direction of the wind and the swell at the beginning of a drift.

(3) Conclusion

The author described a method to forecast the direction and the distance of a drifting ship under certain weather and sea conditions before the opening of a drift, to select the beginning point of the drift, and to estimate a closing point or time. Unless a big change appears in the weather and sea conditions, a ship will drift as expected. However, after a ship begins to drift, it is possible to estimate the ship's position by the ship's head, the wind direction and the velocity recorded on a course recorder and anemograph.

Therefore, when a ship closes a drift and is going to return toward the datum point, if one can determine a ship's relative position with regard to the fishing gear it will take a course based on the relative position. If it is impossible for the ship to do so, it should take a course based on the estimated position. A forecast of driftage is a forecast done in the last analysis, so that we must not overvalue it. However the forecast is significant in making a drift plan.

Concerning the unsolved problems, the author will pursue further studies.

3. Method to determine a fishing boat's position

3.1 Indication of the accuracy of a ship's position

The position lines are broadly divisible into, observing the bearing or distance of a terrestrial object, observing the altitude or included angle of a celestial or terrestrial object, measuring the difference in distance between the observer and each of the two stations, and combining two more position lines at will a position is determined. Then, a systematic error, a random error and blunder are within the bounds of possibility to be included in the observation. However, a blunder can be avoided by attention and skill, and a systematic error can be expected by theory. Therefore, the subject to study is limited to random errors.

Generally, a random error is treated as obeying the Gaussian law, although to check up the matter, the author examined reliabilities of fitness by the χ^2-test for a few examples.

Fig. 3.1(a) shows the histogram of the observation values of the angle included between the observatory on Mt. Hakodate and the chimney of the Faculty of Fisheries of Hokkaido University, the experiment was repeated one hundred times. This distribution fulfills the conditions of a normal distribution in which the mean value is $43°27'.3$ and the standard deviation is $0'.90$. ($\chi^2=2.966$, $\chi^2_{0.75}=3.455$, $\chi^2_{0.90}=2.204$)

Fig. 3.1(b) shows the histogram of the observation values, every 30 minutes, of the Omega A-D pair which were measured from April 16 till April 30, 1974 at the Faculty, and they fit the normal distribution pretty well. (number of data: 720, $\chi^2=28.21$, $\chi^2_{0.50}=29.34$, $\chi^2_{0.75}=24.48$)

Fig. 3.1(c) shows the histogram of the same pair as the former from February 1, 1974 till January 31, 1975. (number of data: 16844) This figure seems to be a
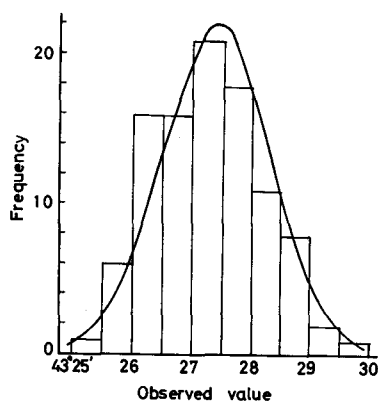
Fig. 3.1(a). Distribution of observed in-
cluded angle by sextant.
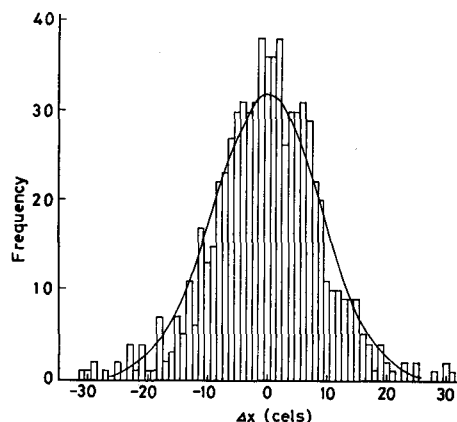
Fig. 3.1(b).   Histogram of Δx (measured
value - mean value) of Omega A-D pair
from April 16, 1974 till April 30.
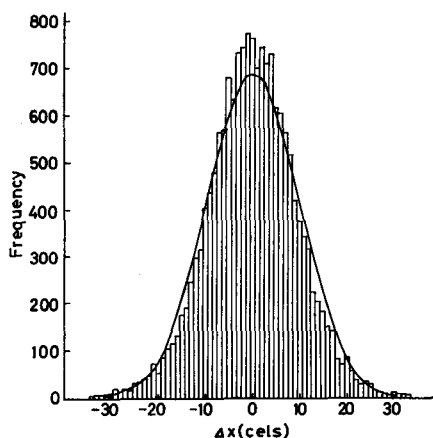
Fig. 3.1(c).   Histogram of Δx of Omega
A-D pair from February 1,1974 till
January 31, 1975.
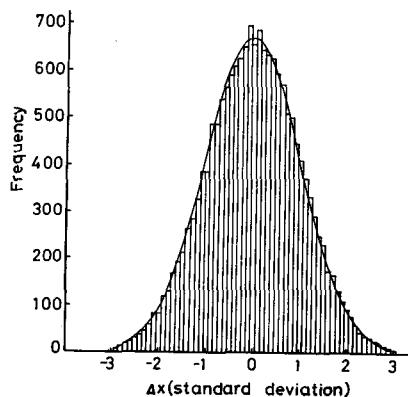
Fig. 3.1(d).   Normalized histogram of Δx
and normal curve.
A-D pair from February 1, 1974 till
January 31, 1975.

normal distribution but its reliability of fitness by the χ^2-test is less than 1%; there-
fore, this distribution does not form a normal curve.   However, as those data are
consecutive figures, it is transformed into a normal model.   Namely, Fig. 3.1(c)
turns into the shape of Fig. 3.1(d), and the fitness by the χ^2-test is larger than 99%.
Therefore, the theory of errors on the Gaussian law is developed.

3.1.1   Position fixed by two position lines

We think the errors of two position lines X and Y whose angle of cut is φ are
distributed normally.   If we put those standard deviations as σ_1 and σ_2, as to any
point $A(X, Y)$, the probability of the axis of abscissas to show the true position
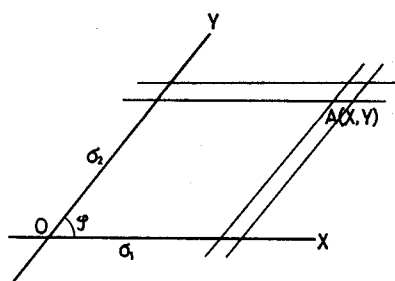
Fig. 3.2. Co-ordinate system.

being between X and $X+\mathrm{d}X$ is

$$\frac{1}{\sqrt{2\pi}\,\sigma_2}\exp\left(-\frac{X^2\sin^2\varphi}{2\sigma_2{}^2}\right)\mathrm{d}X\sin\varphi,$$

and the probability of the axis of ordinates being between Y and $Y+\mathrm{d}Y$ is

$$\frac{1}{\sqrt{2\pi}\sigma_1}\exp\left(-\frac{Y^2\sin^2\varphi}{2\sigma_1{}^2}\right)\mathrm{d}Y\sin\varphi.$$

Therefore, the probability of a ship's position being within the parallelogram overlapped by two fine bands is expressed as follows by the product of both

$$\frac{\sin\varphi}{2\pi\sigma_1\sigma_2}\exp\left\{-\sin^2\varphi\left(\frac{Y^2}{2\sigma_1{}^2}+\frac{X^2}{2\sigma_2{}^2}\right)\right\}\mathrm{d}X\mathrm{d}Y\sin\varphi.$$

In the probability, as $\mathrm{d}X\mathrm{d}Y\sin\varphi$ is the area of this very small parallelogram, the coefficient $\dfrac{\sin\varphi}{2\pi\sigma_1\sigma_2}\exp\left\{-\sin^2\varphi\left(\dfrac{Y^2}{2\sigma_1{}^2}+\dfrac{X^2}{2\sigma_2{}^2}\right)\right\}$ is a probability density function in simultaneous distributions.   Therefore, the locus of a point where the value of the function comes to be equal, in other words, a contour of probability density is expressed by $\sin^2\varphi\left(\dfrac{Y^2}{2\sigma_1{}^2}+\dfrac{X^2}{2\sigma_2{}^2}\right)=K(\text{const.})$, and it constructs ellipses whose origin is the central point.   And the probability density (g) of the intersecting point (O) is guided as follows, by applying $X=Y=0$ to the above-mentioned simultaneous probability density function.

$$g=\frac{\sin\varphi}{2\pi\sigma_1\sigma_2} \tag{3.1}$$

3.1.2 Position fixed by three position lines

(1) Most probable position

We look upon a cocked hat which is constructed with three position lines as ABC and P as any point in the triangle. (Fig. 3.3(a)).   Now, a rectangular coordinates, where A is the origin and AB is x-axis, is described, and we look upon P as x, y.   If we look upon the perpendiculars dropped down from P toward the three sides of the triangle as t_1, t_2, t_3, and the standard deviation of each position line as σ_1, σ_2, σ_3; then a probability that P is in the position whose distance from BC is t_1 is expressed as $k\exp(-t_1{}^2/2\sigma_1{}^2)$.   For the other sides, the same relations are also found.   Therefore, the probability that P is in the position whose distances from three sides are t_1, t_2, t_3 is shown as $k'\exp\left(-\dfrac{t_1{}^2}{2\sigma_1{}^2}-\dfrac{t_2{}^2}{2\sigma_2{}^2}-\dfrac{t_3{}^2}{2\sigma_3{}^2}\right).$

Now, if we look upon the lengths of the sides opposite to A, B, C as a, b, c, and let $\angle A$, $\angle B$, $\angle C$ as θ_1, θ_2, θ_3, the relations between t_1, t_2, t_3 and x, y, c, θ_1, θ_2 are the following $t_1=(c-x)\sin\theta_2-y\cos\theta_2$, $t_2=x\sin\theta_1-y\cos\theta_1$, $t_3=y$.

A most probable position is guided as the point where the probability is the largest.   In order to be guided that way, $\dfrac{y^2}{2\sigma_3{}^2}+\dfrac{\{(c-x)\sin\theta_2-y\cos\theta_2\}^2}{2\sigma_1{}^2}$
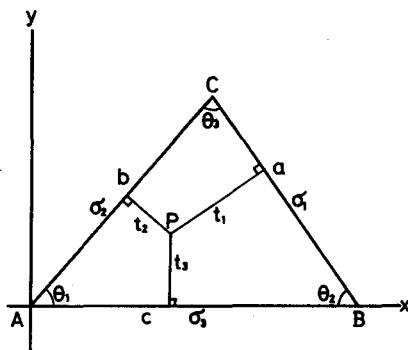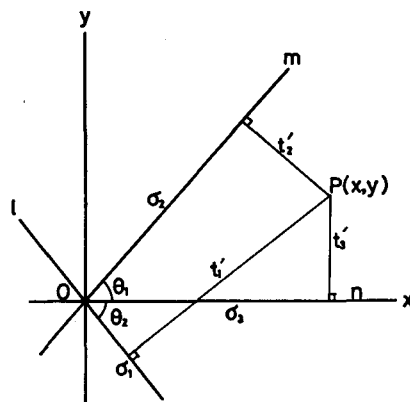
Fig. 3.3(a).   Co-ordinate system.

Fig. 3.3(b).   Relation between any point
and the most proable position lines.

$$+ \frac{(x \sin \theta_1 - y \cos \theta_1)^2}{2\sigma_2^2}$$ must be the smallest.   Now, if we consider this equation

as f, in order to take the extreme value $\partial f/\partial x = 0$, $\partial f/\partial y = 0$ ought to be satisfied.
From them

$$x = \frac{c(\sigma_2^2 \sin^2 \theta_2 + \sigma_3^2 \sin \theta_2 \sin \theta_3 \cos \theta_1)}{\sigma_1^2 \sin^2 \theta_1 + \sigma_2^2 \sin^2 \theta_2 + \sigma_3^2 \sin^2 \theta_3} \ , \ y = \frac{c\sigma_3^2 \sin \theta_1 \sin \theta_2 \sin \theta_3}{\sigma_1^2 \sin^2 \theta_1 + \sigma_2^2 \sin^2 \theta_2 + \sigma_3^2 \sin^2 \theta_3}$$

are guided.   When we substitute these relations into the above-mentioned t_1, t_2, t_3,

$$t_1 = \frac{c\sigma_1^2 \sin^2 \theta_1 \sin \theta_2}{\sigma_1^2 \sin^2 \theta_1 + \sigma_2^2 \sin^2 \theta_2 + \sigma_3^2 \sin^2 \theta_3} \ , \ t_2 = \frac{c\sigma_2^2 \sin \theta_1 \sin^2 \theta_2}{\sigma_1^2 \sin^2 \theta_1 + \sigma_2^2 \sin^2 \theta_2 + \sigma_3^2 \sin^2 \theta_3} \ ,$$

$$t_3 = \frac{c\sigma_3^2 \sin \theta_1 \sin \theta_2 \sin \theta_3}{\sigma_1^2 \sin^2 \theta_1 + \sigma_2^2 \sin^2 \theta_2 + \sigma_3^2 \sin^2 \theta_3} \ ,$$

after all, $t_1 : t_2 : t_3 = \sigma_1^2 \sin \theta_1 : \sigma_2^2 \sin \theta_2 : \sigma_3^2 \sin \theta_3$.   Moreover, there is also a relation
$a/\sin \theta_1 = b/\sin \theta_2 = c/\sin \theta_3$ so that a point which satisfies the following equation;
$t_1 : t_2 : t_3 = \sigma_1^2 a : \sigma_2^2 b : \sigma_3^2 c$ is the most probable position.

(2)   Probability density of the most probable position

The straight lines l, m, n, which are parallel to the former three position lines,
going through the most probable position O, are the most probable position lines.
Now, if we look upon the perpendiculars dropped down from any point P toward
l, m, n as t_1', t_2', t_3', the probability that P, being a point t_1' from the straight line l
is expressed as $k' \exp(-t_1'^2/2\sigma_1^2)$.   As the same relations exist in m and n, the
probability that P, being a point $t_1' \ t_2'$ and t_3' from l, m and n is expressed as follows,
$g \exp(-t_1'^2/2\sigma_1^2 - t_2'^2/2\sigma_2^2 - t_3'^2/2\sigma_3^2)$.   The probability density of P is expressed by the
equation, and the constant g is determined from the fact that the value integrated

over the whole plane is 1. From this, the locus of points whose probability densities are equal satisfy the next equation. $(t_1'^2/2\sigma_1^2 + t_2'^2/2\sigma_2^2 + t_3'^2/2\sigma_3^2) = K$ (K: const.)

Then, there are the following relations; $t_1' = y\cos\theta_2 + x\sin\theta_2$, $t_2' = x\sin\theta_1 - y\cos\theta_1$, $t_3' = y$; if we substitute them into the former equation

$$\left(\frac{\sin^2\theta_2}{2\sigma_1^2} + \frac{\sin^2\theta_1}{2\sigma_2^2}\right)x^2 - 2\left(\frac{\sin\theta_1\cos\theta_1}{2\sigma_2^2} - \frac{\sin\theta_2\cos\theta_2}{2\sigma_1^2}\right)xy$$

$$+ \left(\frac{\cos^2\theta_2}{2\sigma_1^2} + \frac{\cos^2\theta_1}{2\sigma_2^2} + \frac{1}{2\sigma_3^2}\right)y^2 = K \qquad (3.2)$$

Now we define

$$\frac{\sin^2\theta_2}{2\sigma_1^2} + \frac{\sin^2\theta_1}{2\sigma_2^2} = A , \quad \frac{\cos^2\theta_2}{2\sigma_1^2} + \frac{\cos^2\theta_1}{2\sigma_2^2} + \frac{1}{2\sigma_3^2} = B ,$$

$$\frac{\sin\theta_1\cos\theta_1}{2\sigma_2^2} - \frac{\sin\theta_2\cos\theta_2}{2\sigma_1^2} = H ,$$

equation (3.2) is expressed in the form of $Ax^2 - 2Hxy + By^2 = K$, and

$$AB - H^2 = \left(\frac{\sin^2\theta_2}{2\sigma_1^2} + \frac{\sin^2\theta_1}{2\sigma_2^2}\right)\left(\frac{\cos^2\theta_2}{2\sigma_1^2} + \frac{\cos^2\theta_1}{2\sigma_2^2} + \frac{1}{2\sigma_3^2}\right)$$

$$- \left(\frac{\sin\theta_1\cos\theta_1}{2\sigma_2^2} - \frac{\sin\theta_2\cos\theta_2}{2\sigma_1^2}\right)^2 = \frac{\sin^2\theta_3}{4\sigma_1^2\sigma_2^2} + \frac{\sin^2\theta_2}{4\sigma_1^2\sigma_3^2} + \frac{\sin^2\theta_1}{4\sigma_2^2\sigma_3^2} > 0$$

therefore, equation (3.2) takes the shape of an ellipse.

The area (S) of a probability ellipse is expressed as follows;

$$S = \frac{\pi K}{\sqrt{AB - H^2}} = \frac{2\pi\sigma_1\sigma_2\sigma_3 K}{\sqrt{\sigma_1^2\sin^2\theta_1 + \sigma_2^2\sin^2\theta_2 + \sigma_3^2\sin\theta_3}}$$

Next, the probability of a ship's position lying in a belt between an ellipse and an adjacent ellipse is expressed by

$$ge^{-K}dS = \frac{2\pi\sigma_1\sigma_2\sigma_3 g}{\sqrt{\sigma_1^2\sin^2\theta_1 + \sigma_2^2\sin^2\theta_2 + \sigma_3^2\sin^2\theta_3}}\, e^{-K}dK$$

Therefore, the probability of a ship's position being inside of an ellipse is guided as follows by integrating the former equation

$$P = \frac{2\pi\sigma_1\sigma_2\sigma_3 g}{\sqrt{\sigma_1^2\sin^2\theta_1 + \sigma_2^2\sin^2\theta_2 + \sigma_3^2\sin^2\theta_3}} \int_0^K e^{-K}dK$$

$$= \frac{2\pi\sigma_1\sigma_2\sigma_3 g}{\sqrt{\sigma_1^2\sin^2\theta_1 + \sigma_2^2\sin^2\theta_2 + \sigma_3^2\sin^2\theta_3}}\, (1 - e^{-K})$$

Then, if K is treated as an infinity, P is equal to 1. Therefore g is determined as the next equation, that is

$$g = \frac{\sqrt{\sigma_1^2 \sin^2 \theta_1 + \sigma_2^2 \sin^2 \theta_2 + \sigma_3^2 \sin^2 \theta_3}}{2\pi \sigma_1 \sigma_2 \sigma_3} \qquad (3.3)$$

It is obvious that this g expresses the probability density of the most probable position.

3.2 Method to select the position of a datum point (buoy) when a ship anchors it

3.2.1 Characteristics on determining a fishing boat's position

The methods of determining the position of fishing boats were divided into the cases when the origin of observation was fixed and when it was not fixed, however, the former case is the method, by which each measuring point is determined as the position relative to the datum point when repeated operations are carried out in a limited sea area, and the method is useful and appropriate because it is simple and the position of high accuracy can be expected. The latter is the case when a buoy cannot be anchored or when it is unnecessary because of moving to other fishing grounds.

The position measurement in case of the ship at sea is carried out by selecting any object arbitrarily at a fixed point. At that time, it does not matter if the position can be determined with high accuracy, but it cannot be helped if only the position of low accuracy can be obtained.

In the case of a fishing boat near the coast, it is possible for him to anchor a datum point during observations for the purpose of getting a very accurate position. If one determines the position of a datum point accurately and determines each observation point as a relative position for the datum point, he can naturally expect a very accurate position.

In other words, when a ship is out at sea, an officer on duty selects several objects to determine the ship's position at the fixed point. On the other hand, when a fishing boat is near the coast, he selects the most suitable point to determine a ship's position by fixed objects.

Another difference is that the anchored datum point is also determined by shooting the sun at intervals. When a ship sails in contact with the coast or when a ship anchors (anchored datum point comes under this case), the determination of a ship's position is usually done by the observations of objects on land, but when we can't find suitable objects, in other words, when the shore is a flat desert, we can't but depend on astronomical position lines or Loran position lines and so forth. When we depend on them, the method itself is the same as the one described in the next item. It differs however in the fact that the anchored position of a buoy is determined by observations made at intervals.

Fundamentally, in order to determine a position more than two position lines are required and the methods to obtain them were previously stated. When a ship is sailing on the ocean, it frequently depends on observations of the sun at intervals

in order to determine its position during daytime. In such a case, there is only one object to observe in order to get a position line and that is the sun. After a ship sails for several hours, one observes the sun again, and he determines a ship's position by combining both position lines. A weak point that might be fatal in this method is that we can't know the direction and the distance made by the ship moving towards the ground between the first and the second sight. Therefore, we can't but estimate the direction and the distance of sea-water movement from past statistics so that it is natural that the determined position isn't so accurate. In order to correct this lack, the only method is to fix an observation point.

The position of a buoy set up in a fishing ground satisfies that condition as an observation station on land. In other words, at the datum point or at any other point within we can obtain a position in relation to it, if we observe the sun more than twice at intervals, we can determine the observation point. Moreover, it is also possible for us to determine the position by combining the observation of the sun and that of a star at twilight.

3.2.2 *Accuracy contour of a ship's position fixed by the cross bearing method*[20)21)]

We determine a ship's position by observing bearings of terrestrial objects with a compass and by combining more than two guided position lines. As a method, it includes cases of employing radar bearings or wireless bearings. Judging from the accuracy of the position lines, we determine a ship's position with a compass as far as we can see the objects. In order to determine a position, we need only two position lines, however, in order to set up a datum point we must occupy the most suitable place in the case of determining a position with three objects.

The first reason is as follows. If we consider the distances between an observation point and two objects A,B as d_1, d_2, an intersecting angle of two bearings for θ_3, an error included in a bearing as $\Delta\theta$ (standard deviation), the probability density (g_1) of a determined position by two objects A, B is expressed as $\sin\theta_3/2\pi d_1 d_2 (\Delta\theta)^2$. Moreover, when we determine a position by selecting any object C added to two objects A,B, if we consider the distance between the observation point and C as d_3, the intersecting angle of two bearings by A, C for θ_1 and that by B, C as θ_2, the probability density (g_2) of the position fixed by three objects A, B, C is expressed as $(d_1{}^2\sin^2\theta_1+d_2{}^2\sin^2\theta_2+d_3{}^2\sin^2\theta_3)^{1/2}/2\pi d_1 d_2 d_3 (\Delta\theta)^2$. Therefore, if we compare both probabilities, the next relation is obtained.

$$\frac{g_2}{g_1} = \frac{\sqrt{d_1{}^2\sin^2\theta_1+d_2{}^2\sin^2\theta_2+d_3{}^2\sin^2\theta_3}}{d_3\sin\theta_3} = \sqrt{\left(\frac{d_1\sin\theta_1}{d_3\sin\theta_3}\right)^2+\left(\frac{d_2\sin\theta_2}{d_3\sin\theta_3}\right)^2+1}$$

In this relation $(d_1\sin\theta_1/d_3\sin\theta_3)^2+(d_2\sin\theta_2/d_3\sin\theta_3)^2$ is usually larger than zero, so that $g_2>g_1$. In other words, when we determine a ship's position by the bearings of two objects, if a third object is observed, we can always make a determined position more accurate by adding the last position line to the other two, in spite of a distance and a direction, and this simple theory forms a fundamental conception on determining a position.

The second reason is as follows. If one takes three position lines he can find

a blunder or a systematic error.   In other words, systematic errors, random errors and faults can be made when evaluating an observation.   A fault can be avoided by attention and skill.   Systematic errors can also be excluded by theory so that the object of study is limited to random errors and theory of position probability has been worked out.   If random errors follow a normal distribution, we can hardly expect that big errors will appear.   Moreover, systematic errors are corrected in the outline, but we can't foresee when and how a blunder may appear at all. Therefore, it is desirable that an observer adopt a method of determining position that will permit him to find a bluder or an unusual systematic error in advance. In the case of cross bearing by three position lines, we can find unusual value if it is included because three position lines make a large cocked hat.

Because of those reasons, the author studied the most suitable conditions when a position is determined by the bearings of three objects.   In Fig. 3.4, if we consider distances of B, A, C from the observation point P as d_1, d_2, d_3 and the intersecting anglus as $\theta_1, \theta_2, \theta_3$ shown in the figure, a probability density of the determined position P is expressed as $g = \dfrac{\sqrt{d_1^2 \sin^2 \theta_1 + d_2^2 \sin^2 \theta_2 + d_3^2 \sin^2 \theta_3}}{2\pi d_1 d_2 d_3 (\varDelta\theta)^2}$.   These various elements are guided by offering AB, AC, α, β, θ in Fig. 3.4.   If we consider the length of AB as a unit, an accuracy contour is determined by AC/AB and θ. In this case, two methods are possible. One is to examine the change of the accuracy by fixing AC/AB and by changing θ successively.   The other is to examine the change of the accuracy guided by changing AC/AB and fixing θ.   If one understands the changes of the accuracy contours from the movement of intersecting angles formed by the base lines, it will be easy for him to analogize the accuracy contours corresponding to the change of distance.   From such a viewpoint, the author studied this problem. Now, though there are innumerous combinations of AB and AC he thinks $AC/AB=1$ and 2 as models.

Fig. 3.4.   Relation between observation point and three objects.

First of all, if AC equals AB, then each element is expressed as follows:
$d_1 = \sin \beta \operatorname{cosec} (\alpha + \beta)$, $d_2 = \sin \alpha \operatorname{cosec} (\alpha + \beta)$, $d_3 = \sqrt{1 + d_2^2 + 2d_2 \cos (\beta + \theta)}$,
$\sin \theta_1 = \dfrac{\sin (\beta + \theta)}{d_3}$, $\sin \theta_3 = \sin (\alpha + \beta)$.

These relations are effective however when an observation point lies inside section I of Fig. 3.4.   If P is in section II,

$$d_3 = \sqrt{1 + d_2^2 + 2d_2 \cos (\beta - \theta)} , \ \sin \theta_1 = \frac{\sin (\beta - \theta)}{d_3} .$$
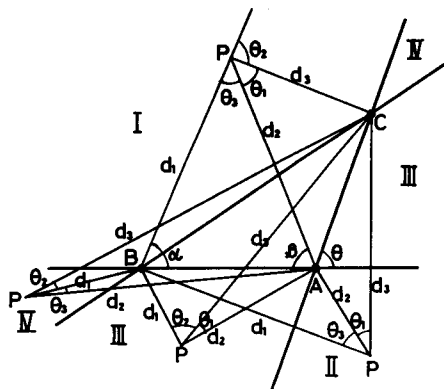
(a) $\theta = 0°$

(b) $\theta = 30°$

(c) $\theta = 60°$

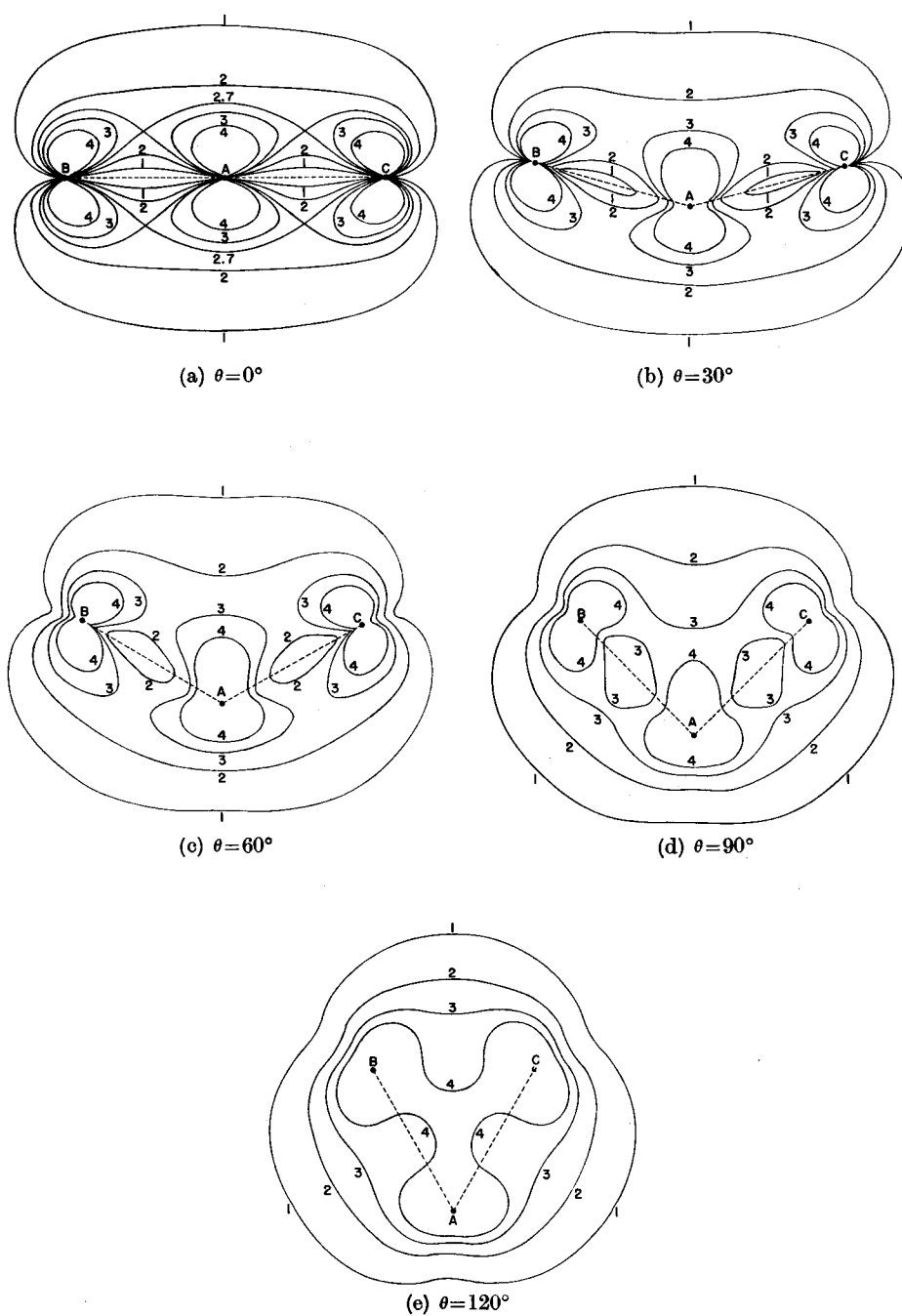(d) $\theta = 90°$

(e) $\theta = 120°$

Fig. 3.5. Accuracy contours for compass bearings $(AB = AC)$.

Furthermore if P is in section III and IV the relations are

$$d_3 = \sqrt{1 + d_2{}^2 + 2d_2 \cos{(\theta - \beta)}}, \quad \sin{\theta_1} = \frac{\sin{(\theta - \beta)}}{d_3}.$$

In any case, the probability density (g) at any point is calculated by these elements. Now, if we think $2\pi(\varDelta\theta)^2 g = g'$ and combine the contours of g' in cases of $\theta = 0°$, 30°, 60°, 90°, 120°, they are shown in Fig. 3.5 (a)(b)(c)(d)(e).

Compare these accuracy contours in relation with one another.

a) When g' is larger than 1 or 2, there is little difference between those area if θ changes. Very accurate portions such as 3, 4 grow as θ increases, however.

b) Very accurate parts are isolated around three objects when $\theta = 0°$, but as θ increases they extend towards the inside.

c) When one locates himself near the baseline, if $\theta = 0°$ part which isn't so accurate is wide, and as θ increases the part decreases gradually. In other words if $\theta = 60°$, part of 1 disappears; 2 vanishes if $\theta = 90°$; and 3 is gone if $\theta = 120°$.

d) When θ is small, there is a marked fluctuation of accuracy as the observation point changes (particularly near the objects), but as θ increases it becomes weak so that a settled position can be obtained easily.

Secondly, if $AB = 1$, $AC = 2$, then each element is expressed as follows: if an observation point is inside section I of Fig. 3.4,

$$d_1 = \sin{\beta} \, \mathrm{cosec}\,(\alpha + \beta), \quad d_2 = \sin{\alpha} \, \mathrm{cosec}\,(\alpha + \beta), \quad d_3 = \sqrt{d_2{}^2 + 4 + 4d_2 \cos{(\beta + \theta)}},$$

$$\sin{\theta_3} = \sin{(\alpha + \beta)}, \quad \sin{\theta_1} = \frac{2 \sin{(\beta + \theta)}}{d_3}.$$

And if P is in section II,

$$d_3 = \sqrt{d_2{}^2 + 4 + 4d_2 \cos{(\beta - \theta)}}, \quad \sin{\theta_1} = \frac{2 \sin{(\beta - \theta)}}{d_3}.$$

Furthermore if the points are in section III and IV,

$$d_3 = \sqrt{d_2{}^2 + 4 + 4d_2 \cos{(\theta - \beta)}}, \quad \sin{\theta_1} = \frac{2 \sin{(\theta - \beta)}}{d_3}.$$

In any case, the probability density at any point is calculated by these elements, and if the contours of g' are combined, they are shown in Fig. 3.6 (a)(b)(c)(d)(e).

From these accuracy contours

a) If one is situated near any object among the three, it is easy to get a very accurate position.

b) If one is situated near either A or B, the baseline of which is short, the region which gives an accurate position is wider than the neighborhood of C.

c) When one is situated near a baseline, it is difficult to get a very accurate position; above all, it is strikingly near the longer baseline AC.

d) Even if one is situated near the baseline AC, the smaller θ is, the wider and less accurate the region is. If θ is 0°, the lower portion under 0.5 exists pretty well, and according to the increase of θ, the inaccurate parts diminish gradually;

(a) $\theta = 0°$

(b) $\theta = 30°$

(c) $\theta = 60°$

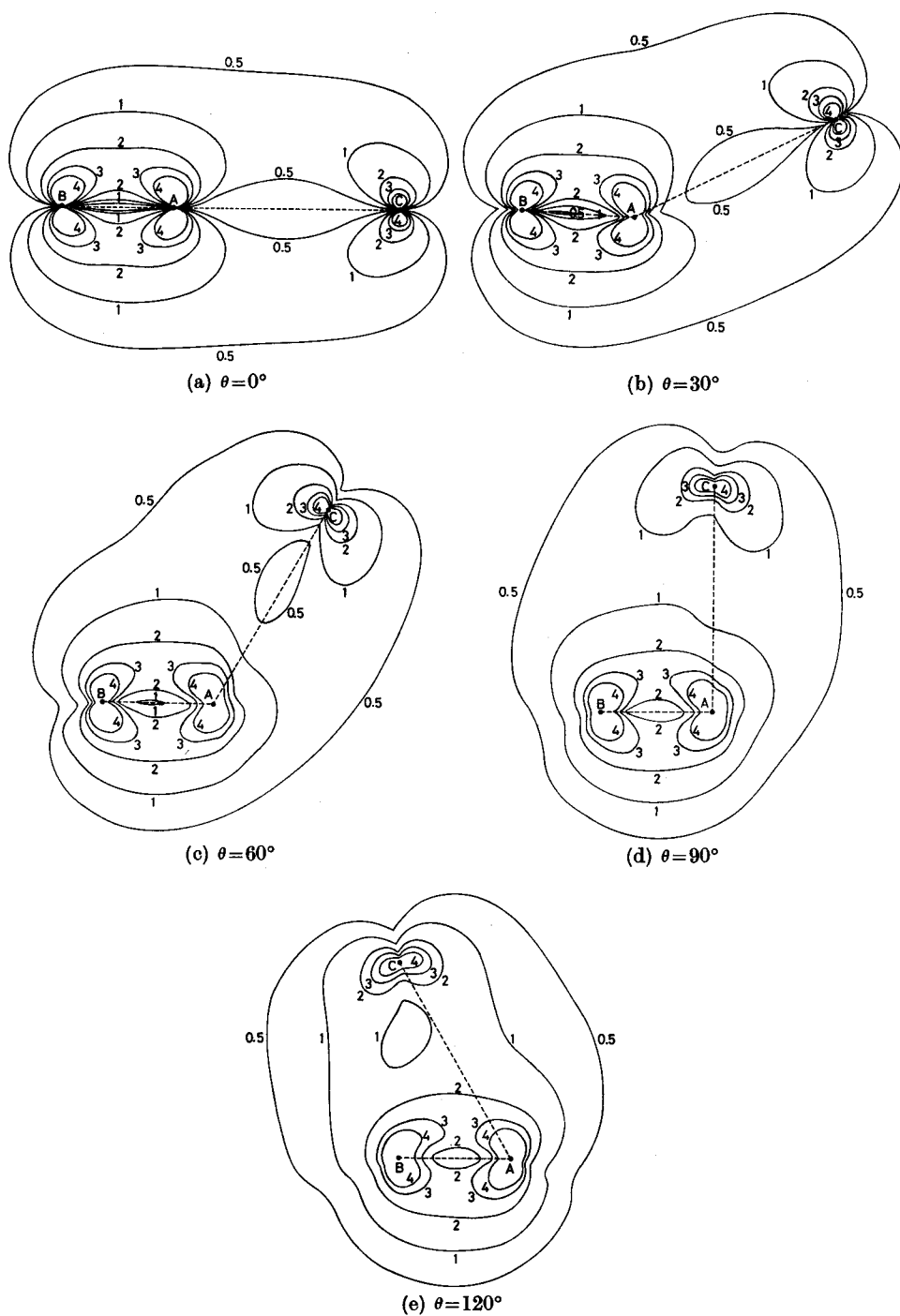(d) $\theta = 90°$

(e) $\theta = 120°$

Fig. 3.6.   Accuracy contours for compass bearings ($AC = 2AB$).

however, distinguished changes are not found on the score of accuracy.

e)   In general, assuming that $g'=0.5$ is a necessary accuracy, the area to satisfy the condition differs merely less than five percent with Fig. 3.6 (a)~(e).   On the other hand, if g' is expected to be more than 1 or 2 or 3 or again 4, the region increases gradually in due order of Fig. 3.6 (a)(b)(c)(d)(e).

Secondly, when one compares Fig. 3.5 with Fig. 3.6, the less accurate regions are not much related to the magnitude of θ; however the larger θ is, the wider and more accurate the region is.   Moreover, even if one is situated near the baselines, the larger θ is, the smaller and less accurate the region is.   These are common features.

In the above sentences, the author mentioned the characteristics concerning the relation between the observation points and the disposition of the objects. When one sets up a datum point, one must select a point where very accurate positions can be obtained easily.   In Fig. 3.5 and Fig. 3.6 it is desirable that the number of regions be more than 4, but actually the most suitable datum point is selected under the control of the fishing ground and the depth of water at a pre-arranged point.

The above-mentioned results are expected when AB and AC equal 1 (Fig. 3.5) and $AB=1$, $AC=2$ (Fig. 3.6), and when AB and AC vary 'n' times respectively, the accuracy of the determined position increases or decreases in inverse proportion n^2; and when either of the two varies 'n' times, the accuracy varies in proportion to the relation between Fig. 3.5 and Fig. 3.6.

Therefore in the case of selecting a position to set up a datum point, one should base his choice on the accuracy contours around the three fixed objects as seen in Fig. 3.5, Fig. 3.6 and on a sense of proportion.

3.2.3   *Accuracy contours of a ship's position fixed by the horizontal sextant angles*[20][21]

The above-mentioned method itself to determine a ship's position by compass bearings is always accepted in general navigation because a navigator can practice the method easily.   But sometimes the datum point cannot be provided at an appropriate place by approaching coast because of the relations between the existence of dangerous matters, water depth, etc. and the operating sea area. Whether the position is suitable or not must be judged by the observer in relation to the required accuracy and that of a determined position.   Then if he cannot satisfy the required accuracy by the cross bearing method, he must use the horizontal sextant angles method.

The method is as follows; the observer selects three clear objects, and measures each horizontal angle between the central object and the one on the right and on the left with a sextant and he applies each guided angle to the angle between the central fixed arm and the right and left arms on a station pointer and he operates the apparatus so that the three arms can touch three objects on a chart, and he determines a ship's position as the intersection of two circular arcs including the angles.   That method has been chiffy accepted in determining positions during a hydrographical survey, but it is impossible for him to try to determine a position on a fishing boat as exactly as it is done on a surveying ship.

Because in the case of a survey, the observer selects the datum points used to determine a ship's position easily and sets up land marks or stations at suitable points according to a plan prepared before the departure, whereas for ordinary ships the determination of a ship's position must be done by natural objects. Therefore he can't attain the aim unless he thinks about the problems of operation and considers a counterplot.

Furthermore, as to this method, similar vague explanations have been described in many special works. The reason of such vagueness is due to the fact that the angles of cut and the distances are treated separately. Therefore, first of all, it is important to clarify the relation between each function and to try to analyze this problem making sure whether it is the standpoint of occupying a position or that of determining a position.
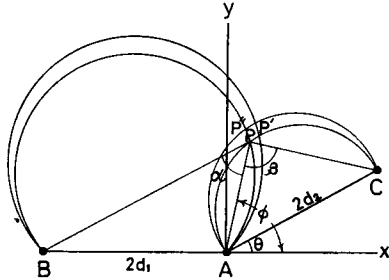
In Fig. 3.7, if we consider three objects as A, B, C, the origin as A, the co-ordinates as such a figure, a circular arc including AB in α as $\widehat{APB}$, a circular arc including AC in β as $\widehat{APC}$, the lengths of AB, AC as $2d_1$, $2d_2$, and $\angle BAC$ as $180°-\theta$, the equations of the two circles are expressed as follows in relation with one another.

Fig. 3.7. Co-ordinate system.

$$\begin{cases} x^2 + 2d_1x + y^2 - 2d_1y \cot \alpha = 0 & (3.4) \\ x^2 - 2d_2(\cos \theta - \cot \beta \sin \theta)x + y^2 - 2d_2(\sin \theta + \cot \beta \cos \theta)y = 0 & (3.5) \end{cases}$$

If we consider the intersecting point of the two circles as $P(x_1, y_1)$, and $\angle PAX$ as ϕ, from (3.4)–(3.5)

$$2(d_1 + d_2 \cos \theta - d_2 \cot \beta \sin \theta)x_1 = 2(d_1 \cot \alpha - d_2 \sin \theta - d_2 \cot \beta \cos \theta)y_1$$

$$\therefore \quad \cot \phi = \frac{d_1 \cot \alpha - d_2 \sin \theta - d_2 \cot \beta \cos \theta}{d_1 + d_2 \cos \theta - d_2 \cot \beta \sin \theta} \tag{3.6}$$

If β is a constant and α, ϕ are variables

$$\Delta\phi = \frac{d_1 \sin^2 \phi \Delta\alpha}{(d_1 + d_2 \cos \theta - d_2 \cot \beta \sin \theta) \sin^2 \alpha}$$

When an observed angle α includes an error $\Delta\alpha$, if we consider an intersection of two circular arcs as P'

$$\widehat{PP'} = 2d_2 \operatorname{cosec} \beta \Delta\phi = \frac{2d_1 d_2 \sin^2 \phi \Delta\alpha}{(d_1 + d_2 \cos \theta - d_2 \cot \beta \sin \theta) \sin^2 \alpha \sin \beta} \tag{3.7}$$

Next, if α is a constant and β, ϕ are variables, from (3.6)

$$\Delta\phi = \frac{d_2 \sin \phi \sin (\theta - \phi) \Delta\beta}{(d_1 + d_2 \cos \theta - d_2 \cot \beta \sin \theta) \sin^2 \beta}$$

is guided. When β includes an error $\Delta\beta$, if we consider an intersection of two circular arcs as P''

$$\widehat{PP''} = \frac{2d_1d_2 \sin\phi \sin(\phi-\theta)\Delta\beta}{(d_1+d_2\cos\theta-d_2\sin\theta\cot\beta)\sin\alpha\sin^2\beta} \tag{3.8}$$

And if we consider an angle formed by the tangents of each circle at point P as ε, the probability density (g) of intersection (P) is indicated as $g=1/2\pi\widehat{PP'}\,\widehat{PP''}\sin\varepsilon$ substituting $\sigma_1=\widehat{PP'}\sin\varepsilon$, $\sigma_2=\widehat{PP''}\sin\varepsilon$ into $g=\sin\varepsilon/2\pi\sigma_1\sigma_2$. Moreover, if we consider an angle formed by each radius at intersection (P) of the circles as η,

$$\cos\eta = \frac{2d_1d_2\cot\alpha(\sin\theta+\cot\beta\cos\theta)-2d_1d_2(\cos\theta-\cot\beta\sin\theta)}{2\sqrt{d_1{}^2+d_1{}^2\cot^2\alpha}\,\sqrt{d_2{}^2(\cos\theta-\cot\beta\sin\theta)^2+d_2{}^2(\sin\theta+\cot\beta\cos\theta)^2}}$$

$$= \cos(\alpha+\beta-\theta)$$

Therefore, an intersecting angle (ε) of each circular arc is expressed as $180°-(\alpha+\beta-\theta)$. If we substitute the relations between $\widehat{PP'}$, $\widehat{PP''}$, ε and α, β, θ, ϕ, d_1, d_2 into the equation of g

$$g = \frac{(d_1+d_2\cos\theta-d_2\cot\beta\sin\theta)^2\sin^3\alpha\sin^3\beta}{8\pi d_1{}^2d_2{}^2\sin^3\phi\sin(\phi-\theta)\sin(\alpha+\beta-\theta)\Delta\alpha\Delta\beta}$$

is guided, from equation (3.6)

$$\sin^2\phi = \frac{(d_1+d_2\cos\theta-d_2\cot\beta\sin\theta)^2}{(d_1\cot\alpha-d_2\sin\theta-d_2\cot\beta\cos\theta)^2+(d_1+d_2\cos\theta-d_2\cot\beta\sin\theta)^2}$$

$$\cos^2\phi = \frac{(d_1\cot\alpha-d_2\sin\theta-d_2\cot\beta\cos\theta)^2}{(d_1\cot\alpha-d_2\sin\theta-d_2\cot\beta\cos\theta)^2+(d_1+d_2\cos\theta-d_2\cot\beta\sin\theta)^2}$$

therefore

$$g = \frac{\{(d_1+d_2\cos\theta-d_2\cot\beta\sin\theta)^2+(d_1\cot\alpha-d_2\sin\theta-d_2\cot\beta\cos\theta)^2\}^2\sin^3\alpha\sin^3\beta}{8\pi d_1{}^2d_2{}^2\sin(\alpha+\beta-\theta)(d_1+d_2\cos\theta-d_2\cot\beta\sin\theta)(d_1\cos\theta+d_2-d_1\cot\alpha\sin\theta)\Delta\alpha\Delta\beta} \tag{3.9}$$

is guided and by affording α, β, θ, d_1, d_2 in it, the numerical value of g is calculated. As the accuracy contours are determined by d_1/d_2 and θ, we look at the cases when $AC=AB$ and $AC=2AB$, $\theta=0°$, $30°$, $60°$, $90°$, $120°$ as models.

First of all, we put $AC=AB=1$; on the distribution of the situation in Fig. 3.4, if A is considered as the central object in section I and II, and B or C is considered as the central object in section III or IV, $g'(=2\pi g\Delta\alpha\Delta\beta)$ in each section is expressed as follows.

section I

$$g' = \frac{\{2+\cot^2\alpha+\cot^2\beta-2(\cot\alpha+\cot\beta)\sin\theta+2(1-\cot\alpha\cot\beta)\cos\theta\}^2\sin^3\alpha\sin^3\beta}{(1+\cos\theta-\cot\alpha\sin\theta)(1+\cos\theta-\cot\beta\sin\theta)\sin(\alpha+\beta-\theta)}$$

section II

$$g' = \frac{\{2+\cot^2\alpha+\cot^2\beta+2(\cot\alpha+\cot\beta)\sin\theta+2(1-\cot\alpha\cot\beta)\cos\theta\}^2\sin^3\alpha\sin^3\beta}{(1+\cos\theta+\cot\alpha\sin\theta)(1+\cos\theta+\cot\beta\sin\theta)\sin(\alpha+\beta+\theta)}$$

section III

$$g' = \frac{\left\{\left(\cos\frac{\theta}{2}-\cot\beta\sin\frac{\theta}{2}\right)^2+\left(2\cos\frac{\theta}{2}\cot\alpha-\sin\frac{\theta}{2}+\cot\beta\cos\frac{\theta}{2}\right)^2\right\}^2\sin^3\alpha\sin^3\beta}{4\left(\cot\beta\sin\frac{\theta}{2}-\cos\frac{\theta}{2}\right)\left((\cos\theta+\cot\alpha\sin\theta)\cos^2\frac{\theta}{2}\sin\left(\alpha+\beta+\frac{\theta}{2}\right)\right)}$$

section IV

$$g' = \frac{\left\{\left(\cos\frac{\theta}{2}+\cot\beta\sin\frac{\theta}{2}\right)^2+\left(2\cos\frac{\theta}{2}\cot\alpha+\sin\frac{\theta}{2}+\cot\beta\cos\frac{\theta}{2}\right)^2\right\}^2\sin^3\alpha\sin^3\beta}{4\left(\cot\beta\sin\frac{\theta}{2}+\cos\frac{\theta}{2}\right)(\sin\theta\cot\alpha-\cos\theta)\cos^2\frac{\theta}{2}\sin\left(\frac{\theta}{2}-\alpha-\beta\right)}$$

Then α in these equations is measured as an angle APB in section I and II, and as an angle BPC in section III and IV.

In this way, the condition of g' being a constant are described by repeating calculations as α gradually changes, because we calculate β which satisfies the condition if α and θ are given elements of each equation. The results are shown in Fig. 3.8 (a)(b)(c)(d)(e). From these figures the following matters are derived.

a) Near the base lines, if θ is small, a portion which isn't so accurate occupies a wide range, and the portion decreases as θ increases. The tendency is particularly conspicuous for the inner part limited by three objects (section I).
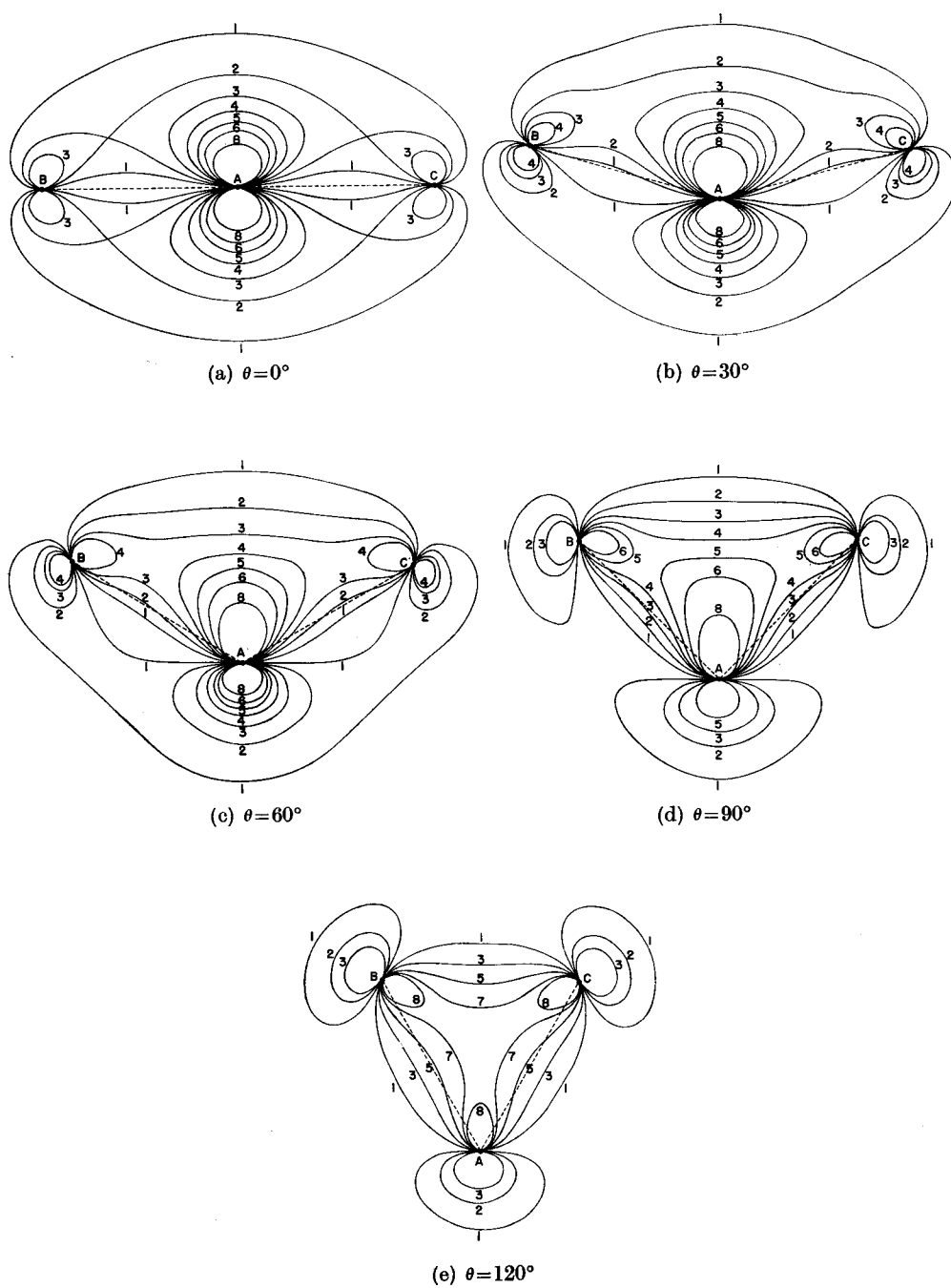
b) When we compare each section, in section I the very accurate portion occupies a wide range, while in section II, III, IV it occupies only a narrow range. This fact becomes conspicuous as θ increases. As to the part where g' is less than 1, this fact can't be applied. In other words, the accuracy decreases rapidly toward the zero line (circumscribed circle of triangle ABC) in section I, but in the other sections the degree of decrease is moderate.

c) The conditions to get a very accurate position are that we situate ourselves in section I and yet near object A.

Furthermore, in the inner part of a triangle formed by three objects, it is possible for us to select B or C as a central object, but we can't change the accuracy of a determined position. When A is selected as the central object and when C is selected as the central object, if we consider g' as g_A', g_c', they are expressed as follows:

$$g_A' = \frac{(1+\cos\theta-\cot\beta\sin\theta)^2\sin^3\alpha\sin^3\beta}{\sin^3(\theta+\angle PAC)\sin\angle PAC\sin(\alpha+\beta-\theta)}$$

$$g_c' = \frac{(1+\cos\theta-\cot\beta\sin\theta)^2\sin^3(\alpha+\beta)\sin^3\beta}{8\cos^3\frac{\theta}{2}\sin^3\left(\frac{\theta}{2}+\beta+\angle PAC\right)\sin(\beta+\angle PAC)\{\sin\alpha+\sin(\alpha-\theta)\}}$$

(a) $\theta=0°$

(b) $\theta=30°$

(c) $\theta=60°$

(d) $\theta=90°$

(e) $\theta=120°$

Fig. 3.8.   Accuracy contours for horizontal sextant angles $(AB=AC)$.

Therefore, the ratio is expressed as

$$\frac{g_{c}{}'}{g_{A}{}'} = \frac{(\sin \beta \cot \angle PAC + \cos \beta) \{\sin \alpha + \sin (\alpha - \theta)\}}{\sin (\alpha + \beta - \theta)}$$

and the relation between $\angle PAC$ and α, β, θ is the following;

$$\cot (\angle PAC + \theta) = \frac{\cot \alpha - \sin \theta - \cot \beta \cos \theta}{1 + \cos \theta - \cot \beta \sin \theta}$$

therefore

$$\cot \angle PAC = \frac{\cot \alpha \cos \theta - \cot \beta + \sin \theta}{1 + \cos \theta - \cot \alpha \sin \theta}$$

and if we substitute this relation into the numerator of the proportional equation written above

$$\frac{(\sin\alpha \sin \beta \sin\theta + \sin\beta \cos \alpha \cos\theta - \cos\alpha\sin\theta\cos\beta + \sin \alpha \cos\beta\cos\theta)(\sin\alpha + \sin\alpha \cos\theta - \cos\alpha\sin\theta)}{(1 + \cos \theta - \cot \alpha \sin \theta) \sin \alpha}$$

$= \sin(\alpha + \beta - \theta)$, therefore $g_{c}/g_{A} = 1$ is guided. The fact g_{A} is equal to g_{c} is proved. Moreover in the case when B is selected as the central object it is the same.

Secondly, if we put $AB = 1$, $AC = 2$, g' in each section is indicated as follows.

section I

$$g' = \frac{\{(1 + 2 \cos \theta - 2 \cot \beta \sin \theta)^2 + (\cot \alpha - 2 \sin \theta - 2 \cot \beta \cos \theta)^2\}^2 \sin^3 \alpha \sin^3 \beta}{4(1 + 2 \cos \theta - 2 \cot \beta \sin \theta)(2 + \cos \theta - \cot \alpha \sin \theta) \sin (\alpha + \beta - \theta)}$$

section II

$$g' = \frac{\{(1 + 2 \cos \theta + 2 \cot \beta \sin \theta)^2 + (\cot \alpha + 2 \sin \theta - 2 \cot \beta \cos \theta)^2\}^2 \sin^3 \alpha \sin^3 \beta}{4(1 + 2 \cos \theta + 2 \cot \beta \sin \theta)(2 + \cos \theta + \cot \alpha \sin \theta) \sin](\alpha + \beta + \theta)}$$

And in section III, g' is calculated by replacing AB, AC, θ in section I with BC, AC, $180° - \angle ACB$ or AB, BC, $180° - \angle ABC$. In section IV, g' is gotten by the process just mentioned, but this time following section II. Hereupon, the relations between $180° - \angle ACB$, $180° - \angle ABC$ and θ, $AB(=1)$, $AC(=2)$ are as follows.

$$\sin \angle ACB = \frac{\sin \theta}{\sqrt{5 + 4 \cos \theta}}, \ \sin \angle ABC = \frac{2 \sin \theta}{\sqrt{5 + 4 \cos \theta}}, \ BC = \sqrt{5 + 4 \cos \theta}$$

The condition of g' as a constant is obtained by repeating the calculations as α gradually changes, because we can calculate β which satisfies the condition if α and θ are given elements of each equation. And the results are shown in Fig. 3.9 (a)(b)(c)(d)(e). From these figures the following matters are derived.

(a) $\theta=0°$

(b) $\theta=30°$

(c) $\theta=60°$

(d) $\theta=90°$

(e) $\theta=120°$
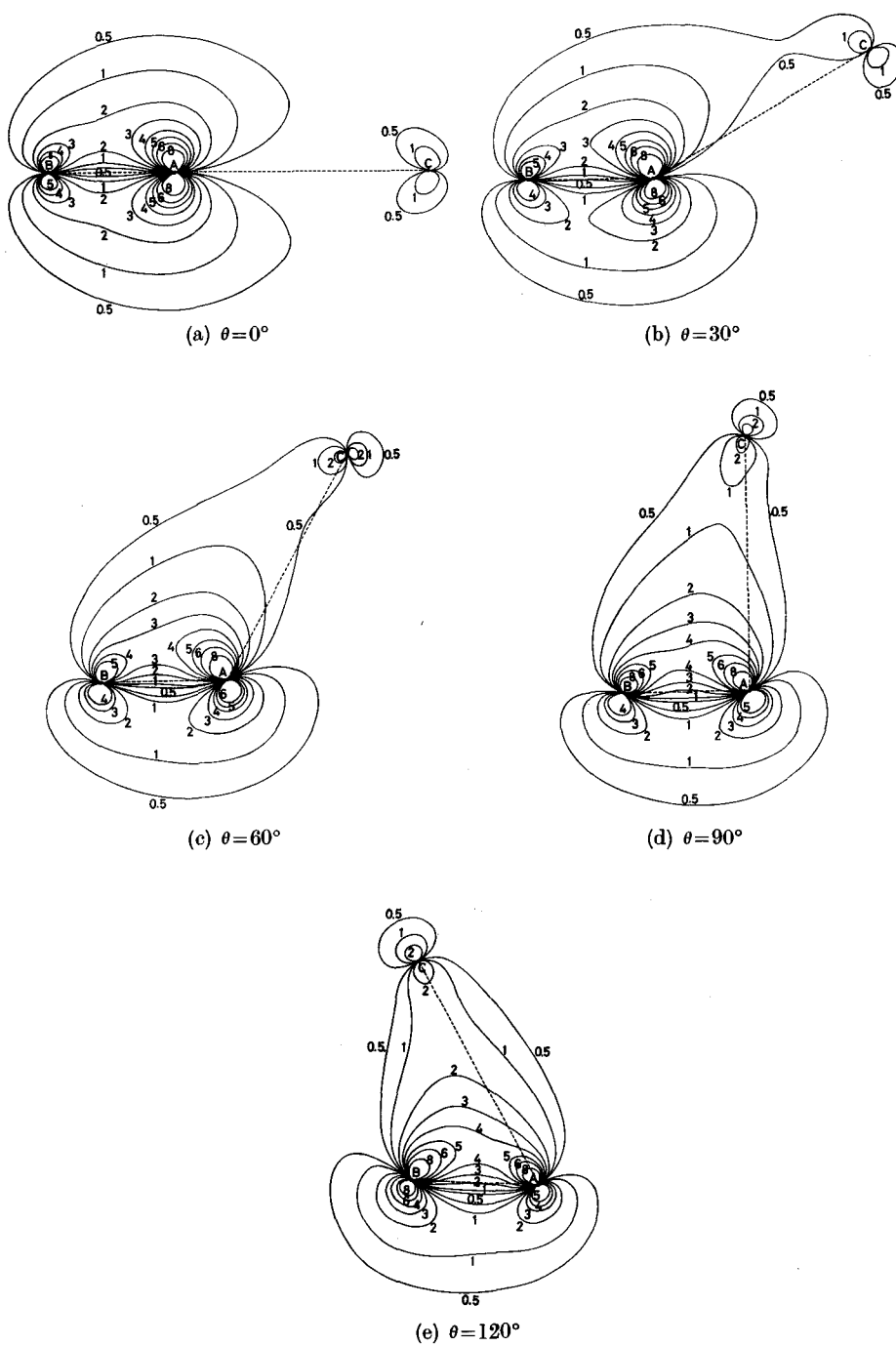
Fig. 3.9.   Accuracy contours for horizontal sextant angles $(AC=2AB)$.

a) The worst condition is when an observation point is situated on the circumference which passes through the three objects.

b) To get a very accurate position an observer must be in section I and near the intersection of the shorter two among the three base lines (AB, AC, BC). That is to say, when θ is smaller than $104°29'$ when situated near the object A, but larger than $104°29'$ when situated near the object B inside the triangle ABC, then an accurate position is easy to derive. On the other hand, an inaccurate position is obtained only in the neighborhood of the intersection between the longer two base lines.

c) In the neighborhood of the base line, inaccurate regions are wide if θ is small. Above all, it is strikingly in the vicinity of the longer ones.

d) The region where a very accurate position is derived increases gradually in due order of Fig. 3.9 (a)(b)(c)(d)(e).

3.2.4 *Systematic errors in the horizontal sextant angles*[22]

When the observer compares the accuracy contours shown in Fig. 3.5 and Fig. 3.8 or Fig. 3.6 and Fig. 3.9, he must think of the values of g' and the squares of angular error which are accepted as a constant.

Errors in measuring a horizontal angle and in plotting it cannot be determined regularly since they vary with the shape of the object and the distance between the object and the observation point on a chart. If they are half as large as that of the bearings plotted on a chart, he multiplies the value shown in Fig. 3.8 and Fig. 3.9 by four and must compare its value with Fig. 3.5 and Fig. 3.6. In general, it is obvious that Fig. 3.8 and Fig. 3.9 are several times more accurate than Fig. 3.5 and Fig. 3.6, but as it may happen that the horizontal sextant angles include systematic errors, he must care for those errors and remove them. Unless the errors are well understood and eliminated, sometimes the significance of the accurate measurement is lost, and the laborious but fruitless result ensues. Among systematic errors, the one based on a drift of the observation point is most difficult to be removed. In the case of determining a position exactly on a fishing boat in operation, the angles are measured at a datum point, so that this problem doesn't exist.

The next problem is how to treat systematic errors based on the fact that two objects together with the observer are not on one horizontal plane. It is ideal for him to select three objects which are situated on one horizontal plane with the observer and are well arranged and clear, but such favorable objects are not always found. Therefore, first he must select objects which are well arranged and must remove systematic errors caused by the fact that the objects and the observer are not on the same horizontal plane.

In Fig. 3.10, we consider $A'B'$ as a celestial horizon, A, B as objects, Z as the zenith and θ_1, θ_2 as the altitudes of each object. If each vertical circle $A'Z$, $B'Z$ are draw through A, B, an included angle of objects A, B is considered as a and the true horizontal angle is shown as $a+\Delta a$, $\angle Z=A'B'=a+\Delta a$, $AB=a$, $AZ=90°-\theta_1$, $BZ=90°-\theta_2$, therefore

$$\cos a = \sin \theta_1 \sin \theta_2 + \cos \theta_1 \cos \theta_2 \cos (a+\Delta a)$$

$$\therefore \quad \Delta a = \cos^{-1}\left(\cos a \sec \theta_1 \sec \theta_2 - \tan \theta_1 \tan \theta_2\right) - a$$

As this corrected value is small when each object is low in altitude, the effects are unimportant if an amendment isn't done.   On the other hand, when each object is high in altitude, an amendment must be done.   The corrected values are shown in Fig. 3.11.

The reason why the horizontal sextant angles method has been used as a method to determine a ship's position exactly is based on the fact that a position line is very accurate, so that it is far more important to remove systematic errors (especially when they are large) which affect other things in a constant aspect than to consider random errors (errors in measurement and in plotting).
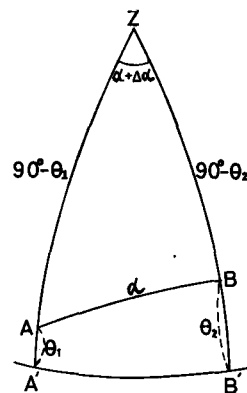
Fig. 3.10.   Relation between observed angle (a) and horizontal angle ($a + \Delta a$).

3.3   Method to determine a ship's position when it does not anchor a datum point

3.3.1   *Characteristics of a fishing boat's position*

As it was mentioned before, a datum point is set up at a suitable position so that the observer can know a ship's position very accurately.   If each observation
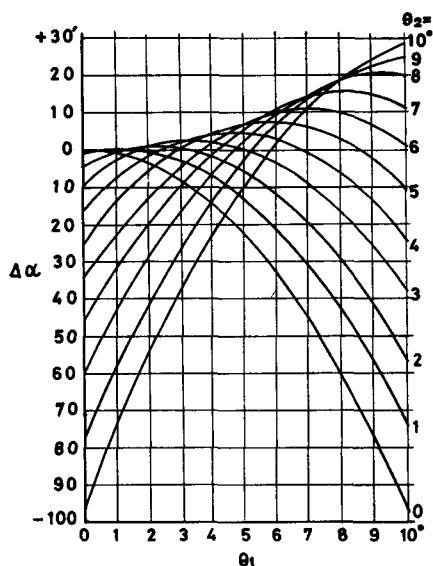
Fig. 3.11(a).   Correction values when two objects, together with observer, are not in one horizontal plane: $a = 30°$.

Fig. 3.11(b).   Correction values when two objects, together with observer, are not in one horizontal plane: $a = 40°$.

Fig. 3.11(c). Correction values when two objects, together with observer, are not in one horizontal plane: $a=50°$.

Fig. 3.11(d). Correction values when two objects, together with observer, are not in one horizontal plane: $a=60°$.

Fig. 3.11(e). Correction values when two objects, together with observer, are not in one horizontal plane: $a=70°$.

Fig. 3.11(f). Correction values when two objects, together with observer, are not in one horizontal plane: $a=80°$.

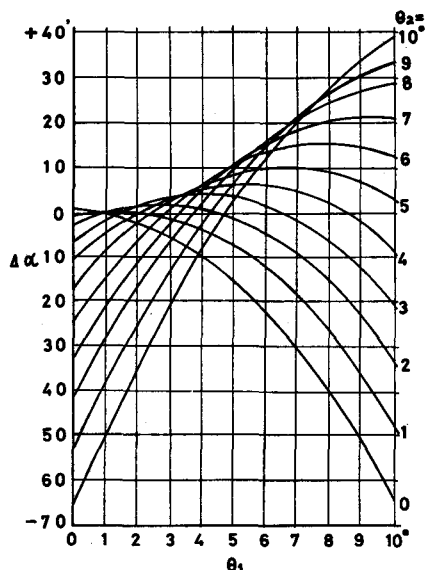Fig. 3.11(g). Correction values when two objects, together with observer, are not in one horizontal plane: $a=90°$.
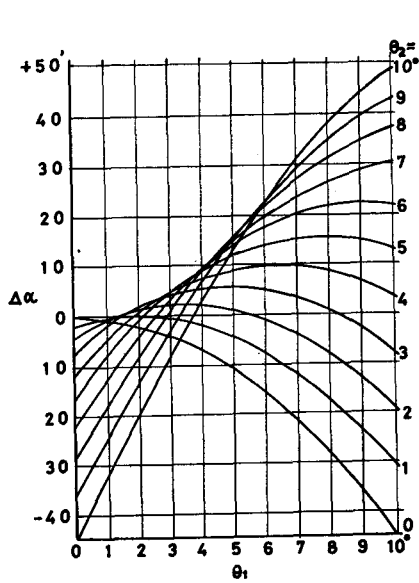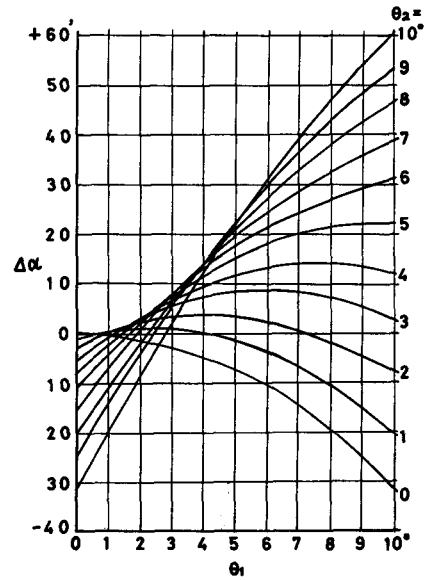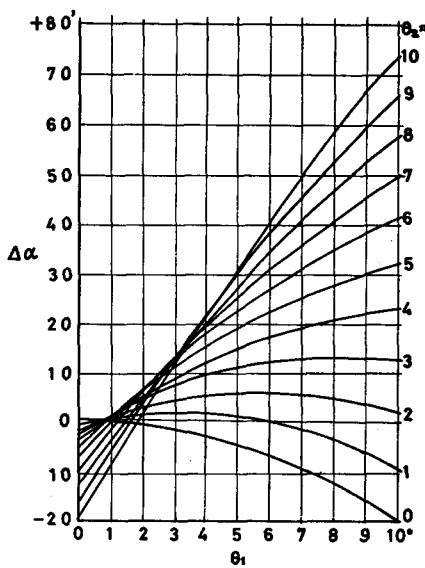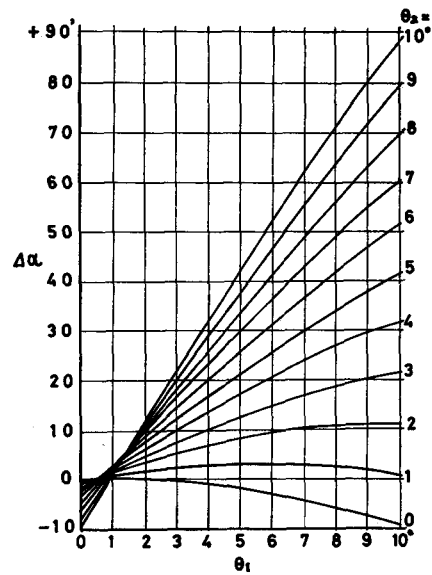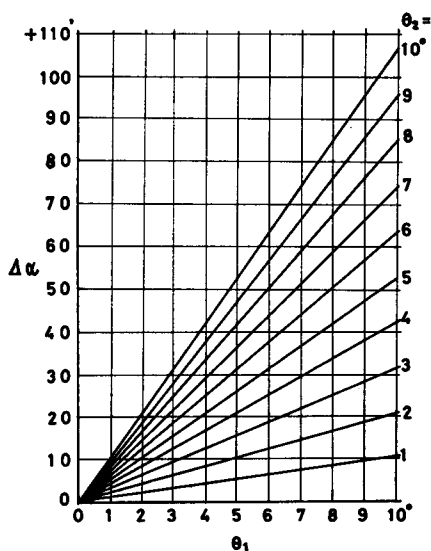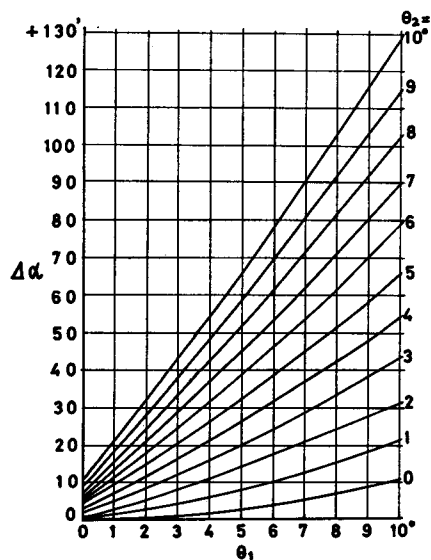

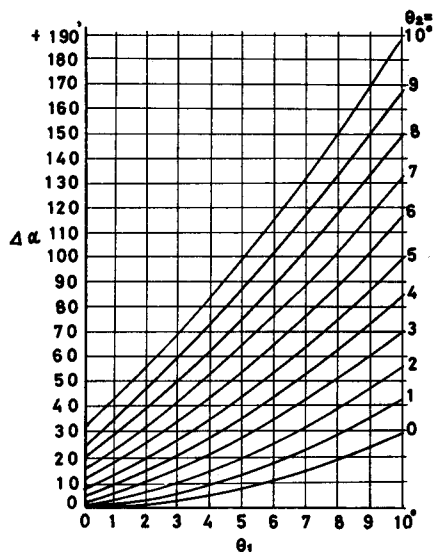Fig. 3.11(h). Correction values when two objects, together with observer, are not in one horizontal plane: $a=100°$.

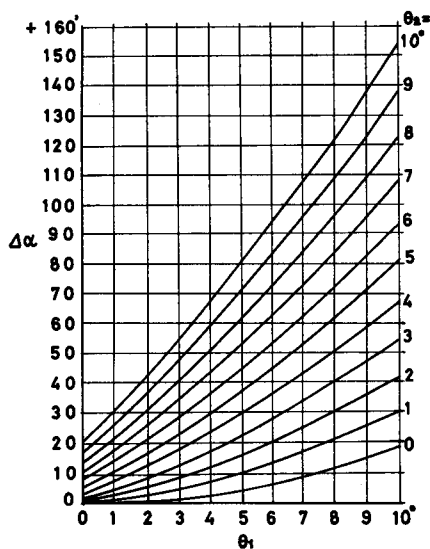Fig. 3.11(i). Correction values when two objects, together with observer, are not in one horizontal plane: $a=110°$.

Fig. 3.11(j). Correction values when two objects, together with observer, are not in one horizontal plane: $a=120°$.

point is taken as a relative position for the datum point, it is also expressed in geographical co-ordinates. This method is simple and convenient, and is excellent because the observation can be carried out regardless of day and night. In deep sea where a datum point is not set up, the determination of a ship's position must be done by a similar method in the case of a sea-going vessel. Then the main aim is to determine a sea-going ship's position in a safety voyage, so that the position is thought widely. On the other hand, on a fishing boat in operation, a more exact valuation as a particle is required because a determined position must be accurate enough to indicate a fishing ground and to analyze observation data. If a determined position cannot satisfy these conditions, then we must find a plan that will satisfy them.

In determining a ship's position in the offing, it is easy to use the cross bearing method as far as we can observe objects on the land, but when the determined position is less accurate than the required values, the horizontal sextant angles method must be used. Moreover, on the ocean, apart far from the land, he must determine his own ship's position by celestial observations or Loran fix etc. In that case, it is necessary to examine whether a guided position is as accurate as the required values or not, to plan the countermeasure.

3.3.2 Determination of a ship's position by the cross bearing method[23]

It is possible to determine a position by two bearings, but the case is less accurate than that of three bearings and in the case of two bearings it is impossible to find a blunder or systematic errors which may be present, so that the author studied the determination of a ship's position by three bearings.

The accuracy contours shown in Fig. 3.5 and Fig. 3.6 are useful when we think of situations to obtain a very accurate position, but from the standpoint of determining a position, it is natural that we treat each point in a different way. In other words, the standpoint to determine a position at any point shows that an observation point is fixed and the objects are selected at will so that it is just the opposite of the standpoint mentioned previously. Moreover, the accuracy of a determined position is in function of the distances and the intersecting angles in substance, so that it must be judged and selected whatever conditions are given.

In this paper the author studied the selection in the case of objects being in a straight line and whose arrangement is thought to be the most typical.

In Fig. 3.12, if we consider the observation point as O, the three objects selected at will on the straight line LL' as A, B, C, and the measure d_1, d_2, d_3, l, θ_1, θ_2, θ_3, α, β, ε in such a figure
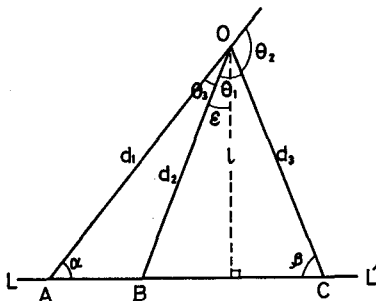
$$d_1 = l \operatorname{cosec} \alpha, \ d_2 = l \sec \varepsilon, \ d_3 = l \operatorname{cosec} \beta,$$

$$\sin \theta_1 = \cos (\beta - \varepsilon), \ \sin \theta_2 = \sin (\alpha + \beta),$$

$$\sin \theta_3 = \cos (\alpha + \varepsilon),$$

Fig. 3.12. Relation between observation point and three objects.

therefore the probability density of the observation point is expressed as follows.

$$g = \frac{\sqrt{\cos^2(\beta-\varepsilon)\cos^2\varepsilon\sin^2\beta + \sin^2\alpha\sin^2\beta\sin^2(\alpha+\beta) + \sin^2\alpha\cos^2\varepsilon\cos^2(\alpha+\varepsilon)}}{2\pi l^2(\Delta\theta)^2}$$

And the next equations must be satisfied together so that g may take the extreme value; $\partial g/\partial\alpha=0$, $\partial g/\partial\beta=0$, $\partial g/\partial\varepsilon=0$, namely

$$\sin^2\beta\sin(\alpha+\beta)\sin(2\alpha+\beta) + \cos^2\varepsilon\cos(\alpha+\varepsilon)\cos(2\alpha+\varepsilon) = 0$$

$$\sin^2\alpha\sin(\alpha+\beta)\sin(\alpha+2\beta) + \cos^2\varepsilon\cos(\beta-\varepsilon)\cos(2\beta-\varepsilon) = 0$$

$$\sin^2\beta\cos(\beta-\varepsilon)\sin(\beta-2\varepsilon) - \sin^2\alpha\cos(\alpha+\varepsilon)\sin(\alpha+2\varepsilon) = 0$$

By solving these simultaneous equations, $\varepsilon=0$, $\alpha=\beta$ are first guided.   Next, if these relations are substituted into the first or second equation,

$$\sin^2\alpha\sin 2\alpha\sin 3\alpha + \cos\alpha\cos 2\alpha = \cos\alpha(-8\sin^6\alpha + 6\sin^4\alpha - 2\sin^2\alpha + 1) = 0$$

is guided.   On $8\sin^6\alpha - 6\sin^4\alpha + 2\sin^2\alpha - 1 = 0$, if $\sin\alpha = x$, $8x^3 - 6x^2 + 2x - 1 = 0$

and if $x = y+h$, $8y^3 + (24h-6)y^2 + (24h^2-12h+2)y + 8h^3 - 6h^2 + 2h - 1 = 0$

is guided and moreover if $h=1/4$,

$$y^3 + \frac{1}{16}y - \frac{3}{32} = 0$$

is guided.   From this, three roots are obtained by Cardan's formula and the real root is adopted as the solution, that is

$$y = \sqrt[3]{\frac{3}{2\times 32} + \sqrt{\left(\frac{3}{2\times 32}\right)^2 - \left(\frac{-1}{3\times 16}\right)^3}} + \sqrt[3]{\frac{3}{2\times 32} - \sqrt{\left(\frac{3}{2\times 32}\right)^2 - \left(\frac{-1}{3\times 16}\right)^3}}$$

$$= 0.4085914$$

Therefore from the relation of $\sin^2\alpha = 0.6585914$, $\alpha = 54°15'$ is obtained.   Then g is equal to $0.91641/2\pi l^2(\Delta\theta)^2$ and the intersecting angles are as follows: $\theta_1=\theta_3=35°45'$, $\theta_2 = 108°30'$.

Next, the probability densities are shown in Fig. 3.13 (a)(b)(c)(d)(e)(f)(g) when the positions are determined at the fixed point O by the bearings of any three objects A, B, C on the straight line. (In the case $g'=2\pi l^2(\Delta\theta)^2g$) If we compare those probability densities with the maximum value (=0.91641) of g', when three objects are selected at will as it was already mentioned, we can find some combinations standing comparison with it if ε is within $30°$.

3.3.3 Determination of a ship's position by the horizontal sextant angles[24]

As the accuracy of a determined position is in function of the intersecting angle, the distances and the angular errors, the best method to select the objects is determined according to the conditions of existence of the objects.   There are many conditions, but the author analyzes one case in particular, that is when the
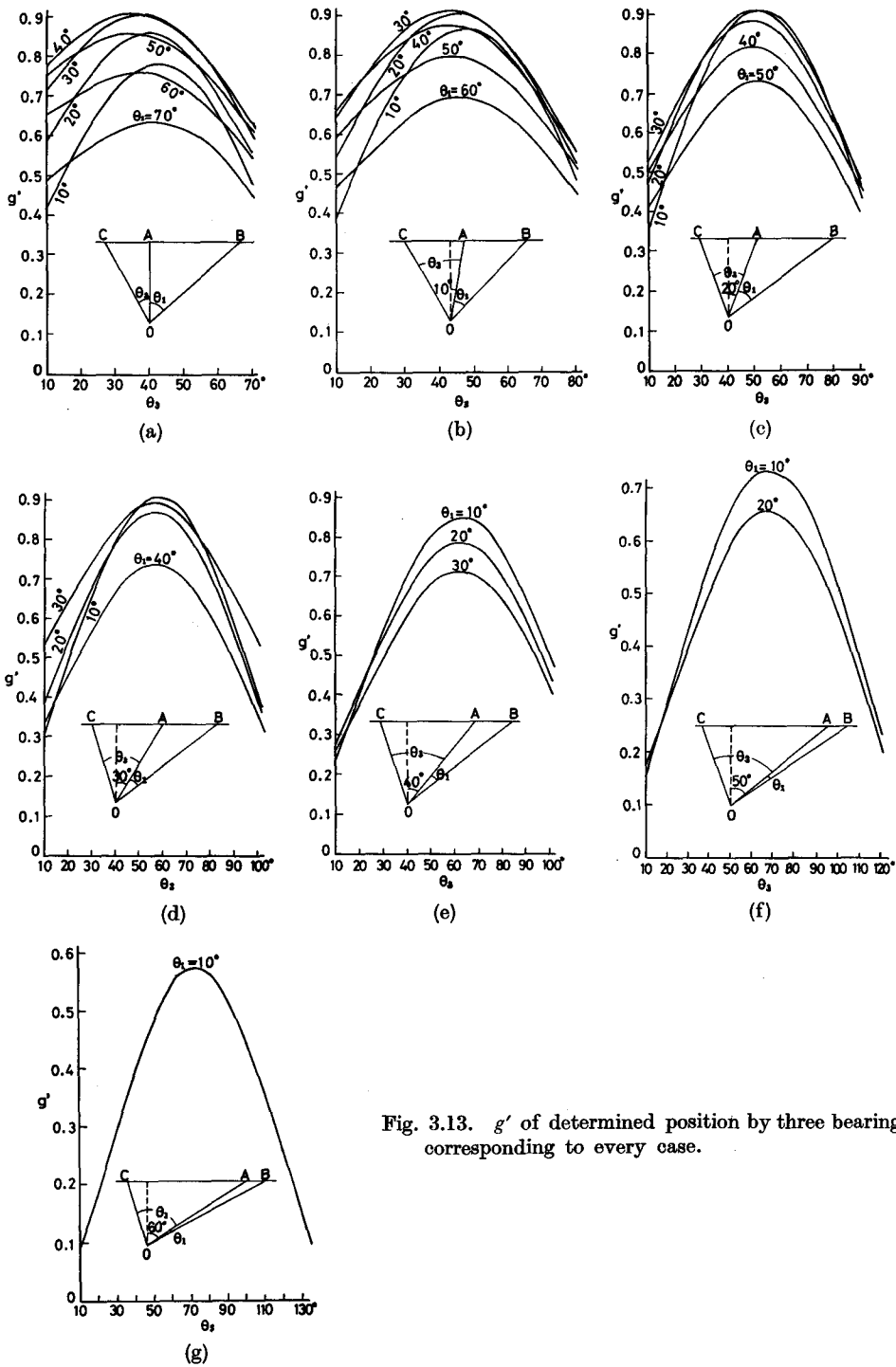
Fig. 3.13. g' of determined position by three bearings
corresponding to every case.

objects lie on a straight line; the other cases are considered in general.

In Fig. 3.14, he considers an observation point as P and supposes that numberless objects lie on the straight line LL'. If he considers a perpendicular distance from LL' to P as l (constant length) and sets three objects A,B,C on the line LL' at will, an observation point is determined as the intersection of two circular arcs by getting two horizontal angles α, β. Now, if he thinks $AC=2d_1$, $AB=2d_2$, $\angle APC=\alpha$, $\angle APB=\beta$, $\angle PAB=\phi$, and considers an intersection of two arcs as P' when β is constant and α includes an error $\Delta\alpha$, from the equation (3.7) $\widehat{PP'}=2d_1 d_2 \sin^2 \phi \Delta\alpha/(d_1+d_2) \sin^2 \alpha \sin \beta$ is guided. If he considers an intersection of two arcs as P'' when α is constant and β includes an error $\Delta\beta$, from the equation (3.8), then $\widehat{PP''}=2d_1 d_2 \sin^2 \phi \Delta\beta/(d_1+d_2) \sin \alpha \sin^2 \beta$ is guided. If he looks upon an angle formed by the tangents of the two circles at point P as ε, the probability density (g) of intersection P is expressed as $g=\sin \varepsilon/2\pi\sigma_1\sigma_2$.

Now, if each observation is done at a fixed observation point, σ_1, σ_2 are $\widehat{PP'}$ $\sin \varepsilon$, $\widehat{PP''} \sin \varepsilon$ respectively and $\sin \varepsilon$ equals $\sin (\alpha+\beta)$. Therefore, g equals $1/2\pi$ $\widehat{PP'}\widehat{PP''} \sin (\alpha+\beta)$. If he substitutes the above-stated $\widehat{PP'}$, $\widehat{PP''}$ into g, $g=(d_1+d_2)^2$ $\sin^3 \alpha \sin^3 \beta/8\pi d_1^2 d_2^2 \sin (\alpha+\beta)\sin^4 \phi \Delta\alpha\Delta\beta$ is guided. The relations between d_1, d_2 and l, α, β, ϕ are expressed as $d_1=l \sin \alpha/2 \sin \phi \sin (\phi-\alpha)$, $d_2=l \sin \beta/2 \sin \phi \sin(\phi+\beta)$, so that

$$g = \frac{\{\sin \alpha \sin (\beta+\phi)+\sin \beta \sin (\phi-\alpha)\}^2 \sin \alpha \sin \beta}{2\pi l^2 \sin (\alpha+\beta) \sin^2 \phi \Delta\alpha\Delta\beta} = \frac{\sin (\alpha+\beta) \sin \alpha \sin \beta}{2\pi l^2 \Delta\alpha\Delta\beta}$$

is formulated. From this equation, it is clear that the probability density of an observation point changes with the angles of circumference α, β and has no connection with ϕ. From $\partial g/\partial\alpha=0$, $\partial g/\partial\beta=0$, α must equal β, and equal 60° so that g may be the maximum for variables α, β. Then, $g'(=2\pi l^2 g\Delta\alpha\Delta\beta)$ equals $3\sqrt{3}/8$. When angle α is a constant, g is the maximum for a variable β when
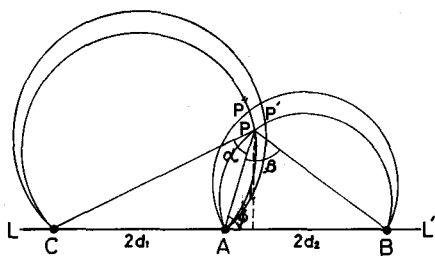

Fig. 3.14. Relation between observation point and three objects.

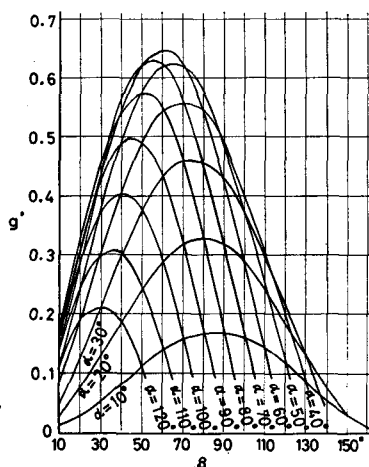Fig. 3.15. Transitions of g' corresponding to any α/ and β.

Table 3.1. *Condition of* $\sin^2 a \sin 2a > 0.64952 \ (l'/l)^2$.

l'/l	0.9	0.8	0.7	0.6	0.5	0.4	0.3	0.2
$a=\beta$	72~47°	77~41°	80~36°	83~31°	85~27°	87~23°	88~19°	89~14°

$\sin\beta\cos(a+\beta)+\sin(a+\beta)\cos\beta=\sin(2a+\beta)=0$. From this equation when $\beta=90°-a/2$, g is the maximum. In that case, g' is expressed as $g'=\sin a \cos^2 (a/2)$. The movement of g' corresponding to the combination of a, β is shown in Fig. 3.15.

Next, the author looks upon a perpendicular distance (l) from P to LL' where objects are as a variable. When the distance between an observation point and straight line LL' is l, the maximum value of g is $0.64952/2\pi l^2 \Delta a \Delta \beta$(where he puts this value as g_1) in the case of $a=\beta=60°$. Now, when he selects objects on a line where a perpendicular distance from the observation point to the line is l' (where $l'<l$), the region where g is larger than g_1 is guided easily by the next relation; $\sin a \sin \beta \sin (a+\beta)>0.64952 \ (l'/l)^2$. Now, if he simplifies this problem and puts $a=\beta$, $\sin^2 a \sin 2a>0.64952 \ (l'/l)^2$ is guided. The results are indicated in Table 3.1. As the l'/l decreases, the region to select from is spread. Therefore, it is better for him to select objects as close as he can, if they are chosen at will.

3.3.4 *Determination of a ship's position by celestial observations*

Concerning the method of determining an observation point by the use of three or two position lines gotten through observing the altitudes of heavenly bodies, the author studies a criterion to select objects from the point of position probability. The probability density of each of the positions determined by the simultaneous observations of two and three celestial bodies is expressed as $\sin \varphi/2\pi\sigma^2$, $(\sin^2 \theta_1+\sin^2 \theta_2+\sin^2 \theta_3)^{1/2}/2\pi\sigma^2$ (where σ: standard deviation of an observation, $\varphi, \theta_1, \theta_2, \theta_3$: angles of cut of position lines) and these are maximums when $\varphi=90°$, $\theta_1=\theta_2=\theta_3=60°$.

Now, in the case of determining a position by three position lines, the accuracy of the most probable position depends on the intersecting angles and σ. As a matter of fact, however, if a large cocked hat is formed, the observer is not sure that the position lines do not include any systematic errors, and if a cocked hat is formed chiefly through systematic errors, he must remove systematic errors in advance rather than random errors.

Therefore in such a case, it is natural that he removes systematic errors by using the bisectors of the position lines and looks upon the intersecting point of three bisectors as a position. In that cases, there are two possibilities. Either the intersection of the bisectors is the center of the inscribed circle of the cocked hat or the centers of the escribed circles are considered. Which case it is in selecting a ship's position must be judged by the azimuths of three heavenly bodies. Random errors and systematic errors being taken into account, the most reasonable method is to select three celestial bodies whose differences of azimuths are all 120°. The method of selecting two bodies whose difference of azimuths is 90° is 0.67 as accurate as that of selecting three bodies whose differences of azimuths are all 60° or 120°.

Moreover, in the two position method there is no consideration of systematic

errors so that the method is not suitable when he tries to find a more accurate position. Moreover, even if three heavenly bodies are selected very carefully, a region whose radius is 1.5 nautical miles must be thought about so that a determined position may keep a probability of 95% (cf. chapter 4). Therefore, if he requires a more accurate position by observing the altitudes of all heavenly bodies successively for n times and by calculating each mean value, he can guide a fairly trustworthy position because the random errors are reduced to $n^{-1/2}$. For example, if he hopes to obtain a ship's position with 95% probability within a circle whose radius is one mile, by selecting the best three heavenly bodies, he will attain his aim by observing each three times and calculating each mean value. As a matter of fact in that case, a total number of nine observations is required of him, so that it is necessary to consider a ship's drift.

3.3.5 Discussion

(1) Comparison between the positions determined by celestial observations and those determined by cross bearings

The standard deviation of a compass bearing drawn on a chart is one degree[25]. If he considers the distance between an object and an observer as d_i the standard deviation of a position line is expressed as $d_i \sin 1° = 0.01745 d_i$. On the other hand, the standard deviation of a celestial observation is $0'.75$ from many reports.[26-29]

Therefore, the probability densities of the positions fixed by three position lines through celestial observations and cross bearings are expressed respectively as;

$$\frac{\sqrt{\sin^2 \theta_1 + \sin^2 \theta_2 + \sin^2 \theta_3}}{2\pi(0'.75)^2} \quad , \quad \frac{\sqrt{d_1^2 \sin^2 \theta_1 + d_2^2 \sin^2 \theta_2 + d_3^2 \sin^2 \theta_3}}{2\pi d_1 d_2 d_3 (0.01745)^2}$$

Now, in order to compare them easily, if he regards $d_1 = d_2 (= d)$, their ratio is $1/(0'.75)^2 : 1/(0.01745d)^2 = 1 : (43/d)^2$. Therefore, if d equals 43 miles, the positions determined by compass bearings are as accurate as those determined by celestial observations. From this relation, for an observation point which is ten miles from the objects and for which the cross bearing method is used mainly, a position fixed by this method is more than ten times as accurate as that fixed by celestial observations.

(2) Comparison between the positions fixed by cross bearings and those fixed by horizontal sextant angles

First of all, at one observation point, if the observer can select the most suitable ones among the objects at will which are on a straight line, the ratio of each probability density, when he selects the most suitable objects by three cross bearings and two horizontal angles is expressed as $0.9164/(\Delta\theta)^2 : 0.6495/(\Delta\theta')^2 = 1.4 : (\Delta\theta/\Delta\theta')^2$, where $\Delta\theta$, $\Delta\theta'$ indicate angular errors on each method. Hereupon an error plotted by the horizontal sextant angles method changes with the distance between an observation point and an object on the chart and also with the shape of the object.[22] Therefore, he can't fix the value of $\Delta\theta/\Delta\theta'$ uniformly but considers it as more than two. Now, if he thinks $\Delta\theta/\Delta\theta'$ is two, a position fixed by the
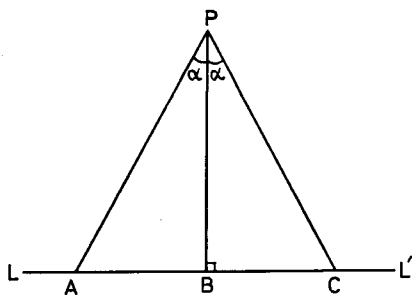
Fig. 3.16.   Relation between observation point and three objects.

horizontal sextant angles method is three times as accurate as that fixed by the cross bearing method.

Next, the author will discuss the case when the same objects on the straight line LL' are chosen on an observation point. Now, in order to simplify this problem, when he looks upon the observation point as P, the objects as A,B,C, $PB \perp LL'$, $PA=PC$ in Fig. 3.16, and if he considers the probability density of a determined position by three bearings as g_1 and that of a determined position by horizontal sextant angles as g_2, $g_1 : g_2$ is expressed as follows.

$$g_1 : g_2 = \frac{\sqrt{\sin^2\alpha\,\cos^2\alpha + \sin^2\alpha\,\cos^2\alpha + \cos^4\alpha\,\sin^2 2\alpha}}{2\pi l^2 (\varDelta\theta)^2} : \frac{\sin^2\alpha\,\sin 2\alpha}{2\pi l^2 (\varDelta\theta')^2}$$

where $\alpha = \angle APB = \angle CPB$. When he tries to find conditions of g_1 equaling g_2, if he looks upon $\varDelta\theta/\varDelta\theta'$ as p, from the relation $\sqrt{2 + 4\cos^4\alpha} = 2p^2 \sin^2\alpha$,

$$4(p^4 - 1)\sin^4\alpha + 8\sin^2\alpha - 6 = 0$$

is lead and $\sin^2\alpha = (-2 \pm \sqrt{6p^4 - 2})/2(p^4 - 1)$ is guided.   Therefore,

$$\sin\alpha = \sqrt{\frac{\sqrt{6p^4 - 2} - 2}{2(p^4 - 1)}}$$

is the solution.   From that equation, if p is 2, α equals $30°26'$, and if p is 2.5, α equals $24°39'$.   Since the value of α changes with p, it is difficult for him to estimate the numerical value itself.   He must notice the fact, however, that there is a α to satisfy the above-mentioned equation if p changes.

As it was mentioned above, if the selected objects are limited, the horizontal sextant angles method can be less accurate than the cross bearing method.   When he observes an oblique angle it is necessary for him to correct it so that it may not include systematic errors.   Moreover, if the observations aren't done at a fixed position, it doesn't play a part as an exact method.   He must recognize that there are many troubles when he uses that method.

(3)   The other method

When an observer determines a ship's position by the Loran position lines, if he is situated near the master station and in a triangle formed by three stations, and if a combination of position lines is accurate enough to satisfy a ship's position, he can use this method effectively. (cf. chapter 4)

Moreover, it was reported,[30] after investigations about NNSS, that this method can give very accurate positions.   It is useful, but there are various problems when one utilizes it on a fishing boat.

4.   Error boundary of a determined position

4.1   Purpose of indicating an error boundary

In the former chapter, the author studied and discussed methods to fix a datum point in order to determine a ship's position, and methods to determine a fishing boat's position at any point.   In this chapter, the author studies a required boundary that may keep a needed probability for a position with regard to a determined position.   A position is determined by several methods and each determined position differs in accuracy according to each method.   Therefore, the preciseness or inaccuracy of the position must be evaluated by some method.   The necessity isn't limited to a fishing boat in operation; however, its quality differs from that of an ocean-going vessel.   In other words, in ordinary navigation, a ship's position and the course are determined for its safety movement so that there is no difficulty in the routine work except for particular cases when a determined position isn't strictly evaluated.   Here the meaning of 'particular' indicates the cases when a ship cannot determine its position for many hours or when it navigates in a dangerous place such as a sea with reefs.

In a fishing-ground, a position, depending on the exact water temperature, the salinity, the topography and geology of the sea-bottom, must be accurate in itself, and the observer can't ignore the evaluation of each determined position.

As to the evaluation of the accuracy, the next two methods are considered. One is to evaluate it by the probability density of a guided position as stated in the former chapter.   The other is to do it by indicating a required boundary in order to keep a needed position probability as to a determined position.   As the former depends on the theory of probability, it is effective and suitable in evaluating a determined position and in comparing each position relatively.   In the latter case, in other words, when he evaluates a position by the probability zone (error boundary), it is suitable in theory to draw an ellipse enclosed by an accuracy contour.   Therefore, it is effective and suitable for him to compare each position by means of an ellipse, but it is very difficult for him to draw each error boundary on the paper when he tries to indicate them concretely.   As a matter of fact, it is important to recognize that there is a theoretical answer, but that, at the same time, he must try to embody the answer.   The author thinks the indication of an error boundary should be done by the ellipse system of probability fundamentally, so that he leads the elements of the ellipse for several combinations of position lines and looks upon them as criterions to judge the effectiveness of the practical solutions to be embodied.   Moreover, the author advocates the circle system of probability as a concrete indication.   The reason he does it is that the theoretical answer isn't practical if it isn't embodied by some method however highly evaluated it may be.

From this point of view, the author aimed at the method which indicates a probability boundary by a single quantity and described only the fundamental items as to the probability ellipse system.

4.2 Probability ellipse system

4.2.1 *Error boundary in the case of two position lines*

From 3.1.1 the probability contours were indicated as $(Y^2/2\sigma_1{}^2+X^2/2\sigma_2{}^2)\sin^2\varphi$ $=K$. If he transforms this equation,

$$\frac{Y^2}{(\sqrt{2K}\sigma_1\cosec\varphi)^2} + \frac{X^2}{(\sqrt{2K}\sigma_2\cosec\varphi)^2} = 1 \qquad (4.1)$$

is guided. Therefore, from equation (4.1) each conjugate semidiameter (a_x, a_Y) is expressed as follows, $a_x=\sqrt{2K}\sigma_2\cosec\varphi$, $a_Y=\sqrt{2K}\sigma_1\cosec\varphi$. Next, the area (S) of the ellipse is expressed as $S=\pi a_x a_Y \sin\varphi=2\pi K\sigma_1\sigma_2\cosec\varphi$ and from this relation $dS=2\pi\sigma_1\sigma_2\cosec\varphi\,dK$ is guided. Therefore, the position probability (P) between a long and narrow portion which is enclosed by the ellipse (4.1) and an adjacent ellipse to it is guided as $P=\int_0^K e^{-K}\,dK = 1-e^{-K}$, so that $K = \log_e(1-P)^{-1}$ is gotten, therefore

$$a_x = \sqrt{2\log_e\!\left(\frac{1}{1-P}\right)}\,\sigma_2\cosec\varphi \qquad (4.2)$$

$$a_Y = \sqrt{2\log_e\!\left(\frac{1}{1-P}\right)}\,\sigma_1\cosec\varphi \qquad (4.3)$$

Then if he considers the semi-major of an ellipse as a, and the semi-minor of it as b, the relations between a, b and a_x, a_Y, are expressed

$$\begin{cases} ab = a_x a_Y \sin\varphi & (4.4) \\ a^2+b^2 = a_x{}^2+a_Y{}^2 & (4.5) \end{cases}$$

When he looks upon the intersecting angles between the conjugate axes and the major axis as α and φ-α, the next relation exists.

$$\tan\alpha\tan(\varphi-\alpha) = \frac{b^2}{a^2} \qquad (4.6)$$

From equation (4.4) (4.5)

$$a = \sqrt{\frac{a_x{}^2+a_Y{}^2+\sqrt{(a_x{}^2+a_Y{}^2)^2-4a_x{}^2a_Y{}^2\sin^2\varphi}}{2}} \qquad (4.7)$$

$$b = \sqrt{\frac{a_x{}^2+a_Y{}^2-\sqrt{(a_x{}^2+a_Y{}^2)^2-4a_x{}^2a_Y{}^2\sin^2\varphi}}{2}} \qquad (4.8)$$

are obtained, and from equation (4.6), $\dfrac{\sin\alpha\sin(\varphi-\alpha)}{\cos\alpha\cos(\varphi-\alpha)} = \dfrac{\cos(\varphi-2\alpha)-\cos\varphi}{\cos(\varphi-2\alpha)+\cos\varphi} = \dfrac{b^2}{a^2}$ is led, and when he arranges the relation in order, $\cos(\varphi\text{-}2\alpha)=\{(a^2+b^2)/(a^2-b^2)\}\cos\varphi$ is gotten, so that an angle of rotation is obtained from the next equation.

$$a = \frac{1}{2}\left\{\varphi - \cos^{-1}\left(\frac{a^2+b^2}{a^2-b^2}\cos\varphi\right)\right\} \tag{4.9}$$

Then as the area (S) of a probability ellipse is $\pi a_x a_Y \sin\varphi$, if he substitutes (4.2) (4.3) into $\pi a_x a_Y \sin\varphi$

$$S = 2\pi \log_e\left(\frac{1}{1-P}\right)\sigma_1\sigma_2 \cosec\varphi \tag{4.10}$$

Now, if P is 0.95, equation (4.2) (4.3) (4.10) are $a_x=2.4477\sigma_2 \cosec\varphi$, $a_Y=2.4477\sigma_1$ $\cosec\varphi$, $S=18.823\sigma_1\sigma_2 \cosec\varphi$. Next, when he adapts these relations to the error boundaries of ships' positions determined by several methods they are as follows.

(1) Error boundary of a position determined by celestial observations

If he looks upon the accuracies of the position lines guided by observing two celestial bodies at the same time $\sigma_1=\sigma_2=0\rlap{.}'75$, $a_x=a_Y=1\rlap{.}'84 \cosec\varphi$.

From equation (4.7)

$$a = \sqrt{\frac{2a_x{}^2 + \sqrt{(2a_x{}^2)^2 - 4a_x{}^4\sin^2\varphi}}{2}} = \sqrt{2}\,a_x\cos\frac{\varphi}{2} = 1\rlap{.}'30\cosec\frac{\varphi}{2},$$

from (4.8)

$$b = \sqrt{\frac{2a_x{}^2 - \sqrt{(2a_x{}^2)^2 - 4a_x{}^4\sin^2\varphi}}{2}} = \sqrt{2}\,a_x\sin\frac{\varphi}{2} = 1\rlap{.}'30\sec\frac{\varphi}{2},$$

from (4.9)

$$a = \frac{1}{2}\left\{\varphi - \cos^{-1}\left(\frac{2a_x{}^2\cos^2\dfrac{\varphi}{2} + 2a_x{}^2\sin^2\dfrac{\varphi}{2}}{2a_x{}^2\cos^2\dfrac{\varphi}{2} - 2a_x{}^2\sin^2\dfrac{\varphi}{2}}\cos\varphi\right)\right\} = \frac{\varphi}{2},$$

and from (4.10) $S=10.59\cosec\varphi$ squre miles.

(2) Error boundary of a position fixed by cross bearings

If the author looks upon distances from an observation point to objects as d_1, d_2, and the standard deviation of observing and plotting error as one degree

$$a_x = 0.0427\,d_2\cosec\varphi, \quad a_Y = 0.0427\,d_1\cosec\varphi$$

$$a = 0.0302\sqrt{d_1{}^2+d_2{}^2+\sqrt{d_1{}^4+d_2{}^4+2d_1{}^2d_2{}^2-4d_1{}^2d_2{}^2\sin^2\varphi}}\;\cosec\varphi$$

$$b = 0.0302\sqrt{d_1{}^2+d_2{}^2-\sqrt{d_1{}^4+d_2{}^4+2d_1{}^2d_2{}^2-4d_1{}^2d_2{}^2\sin^2\varphi}}\;\cosec\varphi$$

$$a = \frac{1}{2}\left\{\varphi-\cos^{-1}\frac{(d_1{}^2+d_2{}^2)\cos\varphi}{\sqrt{d_1{}^4+d_2{}^4+2d_1{}^2d_2{}^2-4d_1{}^2d_2{}^2\sin^2\varphi}}\right\}$$

(3) Error boundary of a position fixed by horizontal sextant angles

As the simplest example, if he thinks three objects (A,B,C) are on a straight line and considers both d_1 and d_2 as 1 in Fig. 4.7 and puts $\Delta\alpha=\Delta\beta$,

$$a_X = \frac{9.79\Delta\alpha}{\{4+(\cot\alpha-\cot\beta)^2\}\sin^2\alpha\sin\beta} \,,\ a_Y = \frac{9.79\Delta\beta}{\{4+(\cot\alpha-\cot\beta)^2\}\sin\alpha\sin^2\beta}$$

$$a = \frac{6.92\Delta\alpha\sqrt{\sin^2\alpha+\sin^2\beta+\sqrt{(\sin^2\alpha+\sin^2\beta)^2-4\sin^2(\alpha+\beta)\sin^2\alpha\sin^2\beta}}}{\{4+(\cot\alpha-\cot\beta)^2\}\sin^2\alpha\sin^2\beta}$$

$$b = \frac{6.92\Delta\beta\sqrt{\sin^2\alpha+\sin^2\beta-\sqrt{(\sin^2\alpha+\sin^2\beta)^2-4\sin^2(\alpha+\beta)\sin^2\alpha\sin^2\beta}}}{\{4+(\cot\alpha-\cot\beta)^2\}\sin^2\alpha\sin^2\beta}$$

$$S = \frac{\pi(9.79)^2\sin(\alpha+\beta)\Delta\alpha\Delta\beta}{\{4+(\cot\alpha-\cot\beta)^2\}^2\sin^3\alpha\sin^3\beta}$$

are led. a is calculated from equation (4.9) after a, b have been guided.

(4) Error boundary of a position determined by Loran position lines

In the case of common chain stations, if he considers each included angle as φ_1, φ_2, the intersecting angle (θ) of the position lines is expressed as $\theta=(\varphi_1+\varphi_2)/2$. If he looks upon σ_0 as a standard deviation on a base line founded on a measurement of time difference, the standard deviation of each position line is expressed as $\sigma_1=\sigma_0\cosec(\varphi_1/2)$, $\sigma_2=\sigma_0\cosec(\varphi_2/2)$. Therefore

$$a_X = 2.4477\sigma_0\cosec\frac{\varphi_1}{2}\cosec\frac{1}{2}(\varphi_1+\varphi_2)\,,\ a_Y = 2.4477\sigma_0\cosec\frac{\varphi_2}{2}\cosec\frac{1}{2}(\varphi_1+\varphi_2)$$

$$S = \pi(2.4477)^2\sigma_0{}^2\cosec\frac{\varphi_1}{2}\cosec\frac{\varphi_2}{2}\cosec\frac{1}{2}(\varphi_1+\varphi_2)$$

$$a = 2.4477\sigma_0\cosec\frac{1}{2}(\varphi_1+\varphi_2)$$

$$\cdot\sqrt{\cosec^2\frac{\varphi_1}{2}+\cosec^2\frac{\varphi_2}{2}+\sqrt{\left(\cosec^2\frac{\varphi_1}{2}+\cosec^2\frac{\varphi_2}{2}\right)^2-4\sin^2\frac{1}{2}(\varphi_1+\varphi_2)\cosec^2\frac{\varphi_1}{2}\cosec^2\frac{\varphi_2}{2}}}$$

$$b = 2.4477\sigma_0\cosec\frac{1}{2}(\varphi_1+\varphi_2)$$

$$\cdot\sqrt{\cosec^2\frac{\varphi_1}{2}+\cosec^2\frac{\varphi_2}{2}-\sqrt{\left(\cosec^2\frac{\varphi_1}{2}+\cosec^2\frac{\varphi_2}{2}\right)^2-4\sin^2\frac{1}{2}(\varphi_1+\varphi_2)\cosec^2\frac{\varphi_1}{2}\cosec^2\frac{\varphi_2}{2}}}$$

and a is calculated from equation (4.9) after a, b have been obtained.

4.2.2 Error boundary in the case of three position lines

An ellipse which is expressed by $Ax^2-2Hxy+By^2=K$ shapes a standard form that $A'x^2+B'y^2=K$ for a new rectangular co-ordinates if axes of co-ordinates are

revolved round an angle δ which satisfies $\tan 2\delta = -2H/(A-B)$. Then the equation of the probability ellipse is expressed as follows.

$$\left(\frac{\sin^2\theta_2}{2\sigma_1^2} + \frac{\sin^2\theta_1}{2\sigma_2^2}\right)x^2 - 2\left(\frac{\sin\theta_1\cos\theta_1}{2\sigma_2^2} - \frac{\sin\theta_2\cos\theta_2}{2\sigma_1^2}\right)xy$$

$$+ \left(\frac{\cos^2\theta_2}{2\sigma_1^2} + \frac{\cos^2\theta_1}{2\sigma_2^2} + \frac{1}{2\sigma_3^2}\right)y^2 = K$$

Therefore

$$\tan 2\delta = \frac{\sigma_1^2\sigma_3^2\sin 2\theta_1 - \sigma_2^2\sigma_3^2\sin 2\theta_2}{\sigma_2^2\sigma_3^2\cos 2\theta_2 + \sigma_1^2\sigma_3^2\cos 2\theta_1 + \sigma_1^2\sigma_2^2} \tag{4.11}$$

is obtained. Moreover

$$A'B' = AB - H^2 = \frac{\sigma_1^2\sin^2\theta_1 + \sigma_2^2\sin^2\theta_2 + \sigma_3^2\sin^2\theta_3}{4\sigma_1^2\sigma_2^2\sigma_3^2},$$

$$A' + B' = A + B = \frac{\sigma_1^2\sigma_2^2 + \sigma_2^2\sigma_3^2 + \sigma_1^2\sigma_3^2}{2\sigma_1^2\sigma_2^2\sigma_3^2}$$

so that

$$A' = \left\{\frac{\sigma_1^2\sigma_2^2 + \sigma_2^2\sigma_3^2 + \sigma_1^2\sigma_3^2}{4\sigma_1^2\sigma_2^2\sigma_3^2}\right.$$

$$\left. - \frac{\sqrt{(\sigma_1^2\sigma_2^2 + \sigma_2^2\sigma_3^2 + \sigma_1^2\sigma_3^2)^2 - 4\sigma_1^2\sigma_2^2\sigma_3^2(\sigma_1^2\sin^2\theta_1 + \sigma_2^2\sin^2\theta_2 + \sigma_3^2\sin^2\theta_3)}}{4\sigma_1^2\sigma_2^2\sigma_3^2}\right\} \tag{4.12}$$

$$B' = \left\{\frac{\sigma_1^2\sigma_2^2 + \sigma_2^2\sigma_3^2 + \sigma_1^2\sigma_3^2}{4\sigma_1^2\sigma_2^2\sigma_3^2}\right.$$

$$\left. + \frac{\sqrt{(\sigma_1^2\sigma_2^2 + \sigma_2^2\sigma_3^2 + \sigma_1^2\sigma_3^2)^2 - 4\sigma_1^2\sigma_2^2\sigma_3^2(\sigma_1^2\sin^2\theta_1 + \sigma_2^2\sin^2\theta_2 + \sigma_3^2\sin^2\theta_3)}}{4\sigma_1^2\sigma_2^2\sigma_3^2}\right\} \tag{4.13}$$

From these equations, a semi-major and a semi-minor are obtained each one as $\sqrt{K/A'}$, $\sqrt{K/B'}$. The probability that a ship's position is in a probability ellipse is expressed as $P = 1 - e^{-K}$ so that the value of K according to $P = 0.95$ is shown as $K = \log_e 20$.

(1) Error boundary of a position determined by celestial observations

If he looks upon intersecting angles by three position lines as θ_1, θ_2, θ_3 and the standard deviation of each position line as $0'.75$,

$$A' = 0'.44444\left\{3 - \sqrt{9 - 4(\sin^2\theta_1 + \sin^2\theta_2 + \sin^2\theta_3)}\right\},$$

$$B' = 0'.44444\left\{3 + \sqrt{9 - 4(\sin^2\theta_1 + \sin^2\theta_2 + \sin^2\theta_3)}\right\}$$

are led from equation (4.12)(4.13). The semi-major and the semi-minor are

expressed as

$$a = \frac{2\rlap{.}'5962}{\sqrt{3-\sqrt{9-4(\sin^2\theta_1+\sin^2\theta_2+\sin^2\theta_3)}}},$$

$$b = \frac{2\rlap{.}'5962}{\sqrt{3+\sqrt{9-4(\sin^2\theta_1+\sin^2\theta_2+\sin^2\theta_3)}}}$$

and as revolved angle is expressed as $\tan 2\delta=(\sin 2\theta_1-\sin 2\theta_2)/(\cos 2\theta_1+\cos 2\theta_2+1)$ from equation (4.11),

$$\delta = \frac{1}{2}\left(\tan^{-1}\frac{\sin 2\theta_1-\sin 2\theta_2}{\cos 2\theta_1+\cos 2\theta_2+1}\right)$$

is obtained.

(2) Error boundary of a position fixed by cross bearings

If he looks upon distances from an observation point to objects as d_1, d_2, d_3, the scatterings of position lines are expressed as $\sigma_1=0.01745d_1$, $\sigma_2=0.01745d_2$, $\sigma_3=0.01745d_3$ respectively. If he substitutes them into equations (4.11) (4.12) (4.13)

$$\delta = \frac{1}{2}\left(\tan^{-1}\frac{d_1^2d_3^2\sin 2\theta_1-d_2^2d_3^2\sin 2\theta_2}{d_1^2d_3^2\cos 2\theta_1+d_2^2d_3^2\cos 2\theta_2+d_1^2d_2^2}\right)$$

$$A' = 1642\left[\frac{d_1^2d_2^2+d_2^2d_3^2+d_1^2d_3^2}{2d_1^2d_2^2d_3^2}\right.$$

$$\left.-\frac{\sqrt{(d_1^2d_2^2+d_2^2d_3^2+d_1^2d_3^2)^2-4d_1^2d_2^2d_3^2(d_1^2\sin^2\theta_1+d_2^2\sin^2\theta_2+d_3^2\sin^2\theta_3)}}{2d_1^2d_2^2d_3^2}\right]$$

$$B' = 1642\left[\frac{d_1^2d_2^2+d_2^2d_3^2+d_1^2d_3^2}{2d_1^2d_2^2d_3^2}\right.$$

$$\left.+\frac{\sqrt{(d_1^2d_2^2+d_2^2d_3^2+d_1^2d_3^2)^2-4d_1^2d_2^2d_3^2(d_1^2\sin^2\theta_1+d_2^2\sin^2\theta_2+d_3^2\sin^2\theta_3)}}{2d_1^2d_2^2d_3^2}\right]$$

are obtained. If he considers the probability that it is in ellipse as 0.95, the semi-major and semi-minor can be calculated from $\sqrt{\log_e 20/A'}$, $\sqrt{\log_e 20/B'}$.

4.3 95% radial error system and its problems

In Fig. 4.1, the correct position lines are drawn as X, Y, and the two lines intersect each other at P. On the other hand, if he considers the observed position lines as X' Y', a ship's position is determined at the intersecting point between them.

Now, when he considers the angle of cut between the position lines as φ, PO as d, lengths of perpendiculars from O to X and Y as l_1 and l_2 respectively and draws rectangular co-ordinates as shown in that figure, $X=l_1\cot\varphi+l_2\operatorname{cosec}\varphi$, $Y=l_1$. In the figure, when scatterings of l_1, l_2 are expressed by σ_1, σ_2 and that of X', Y' by σ_X, σ_Y, $\sigma_X^2=\sigma_1^2\cot^2\varphi+\sigma_2^2\operatorname{cosec}^2\varphi$, $\sigma_Y=\sigma_1$. If he considers a standard deviation of d as σ_d, $\sigma_d^2=\sigma_X^2+\sigma_Y^2=\sigma_1^2(\cot^2\varphi+1)+\sigma_2^2\operatorname{cosec}^2\varphi=(\sigma_1^2+\sigma_2^2)\operatorname{cosec}^2\varphi$, so that

$\sigma_d = \sqrt{\sigma_1{}^2 + \sigma_2{}^2}$ cosec φ is given.

Trow et al. look upon a circle whose radius is $2\sigma_d$ as an error boundary, and this is an indication method called 95 per cent radial error system. This method seems to be simple, but it has fatal faults as follows.

Now, to simplify a general comparison, if the author considers each position line of equal accuracy, the standard deviation as σ, and the intersecting angle of the position lines as φ, then the ratio of the semi-major of 95% probability ellipse $(= 2.4477\sigma$ cosec φ $\sqrt{1 + \cos\varphi})$ with regard to 95% radial error

Fig. 4.1. Co-ordinate system.

$(= 2\sqrt{2}\,\sigma$ cosec $\varphi)$ by two position lines is shown as $1.2239\cos(\varphi/2):1$, therefore, when $\cos(\varphi/2)$ equals 0.81707, in other words when φ takes $70°25'$, both lengths are equal and if φ comes to be more than $70°25'$ the semi-major of the ellipse becomes smaller than the radius of circle.

Next, in the case of three position lines, a semi-major of 95% probability ellipse is expressed as $3.46164\sigma/\sqrt{3 - \sqrt{9 - 4(\sin^2\theta_1 + \sin^2\theta_2 + \sin^2\theta_3)}}$ but it can't be expressed by the 95% radial error system. The system is of little value if it cannot be adapted to three position lines which are always utilized, therefore if the author conducts a radius by the next means (cf. 4.4.2), it can be expressed as follows; $3.46410\sigma/\sqrt{\sin^2\theta_1 + \sin^2\theta_2 + \sin^2\theta_3}$. The case when the two lengths are exactly equal occurs when $\sin^2\theta_1 + \sin^2\theta_2 + \sin^2\theta_3$ equals 1.99714. Therefore, for a combination exceeding this limit, it is more effective to draw an error circle by a semi-major rather than by the radius of circle.

For combinations in which all three intersecting angles are acute angles, he had better draw an error circle by a semi-major than a radius because the combination often occurs in a routine work. This irrationality can be explained by the fact that the probability of an observation point being in a circle whose radius is 95% radial error is 95.5~98.2%. The essential weakness in this method is based on an incomplete fundamental equation; the method tries to support theoritical weak points for practical convenience; therefore, its value as a practical solution cannot be trusted.

4.4 Probability circle system

An ellipse connects each point whose probability density is equal, and an outline on the 95% probability ellipse was described already. It is known theoretically, but hindrances occur when the author applies them in practice. Particularly in the case of cross bearings, horizontal sextant angles and the Loran position lines, even if he can know the existence of theoretical solutions, it is very difficult for him to apply them in practice. Merely in the case of determining a position by celestial observations, he can calculate the numerical values of the major diameter, the minor diameter and the direction of the axes in advance, but he can't avoid
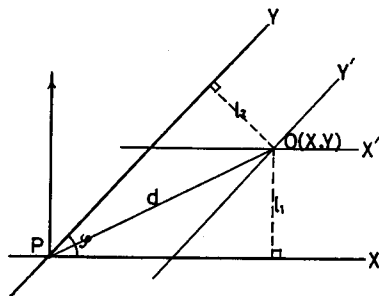
the trouble caused by the revolving axes when he tries to draw them.

The author thinks that the valuation of a determined position must be done by its probability density so that he thinks an error boundary can be expressed reasonably well by the probability ellipse system. In practice, however, both the theory and the utility must be thought in the same dimension. From such a point of view, the author advocates the 95% probability circle as the indication of error boundary which includes both a theory that induces a probability concept and a possibility that embodies it at field.

When he thinks of the 95% probability circle, he calculates the radius corresponding to the condition by which he unifies a probability in a circle as 95%, and tries to consider the radius as a practical solution.

Fortunately, the determination of a ship's position in a fishing ground is carried out under sufficient considerations so that a determined position can exist with a probability required in a boundary, which isn't so inferior as that of a probability ellipse, such as demonstrated in the following case.
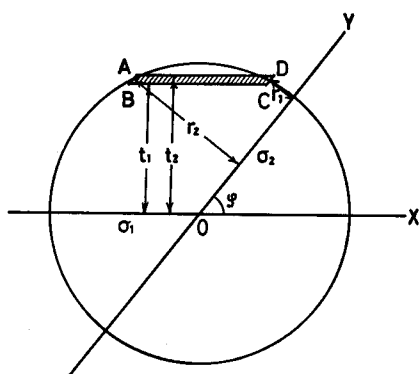

Fig. 4.2. The two-position line case.

4.4.1   95 per cent probability circle[10]

In Fig. 4.2, if he considers two position lines as X, Y, each standard deviation as σ_1, σ_2, the intersecting angle as φ and if he draws a circle with the radius of R by centering the intersection O, a probability that an observation point is included in a thin band formed by two parallel lines whose distances from position line X are t_1 and $t_2(=t_1+\varDelta t)$ is given by

$\dfrac{1}{\sqrt{2\pi}\sigma_1}\displaystyle\int_{t_1}^{t_2}\exp\left(-\dfrac{t^2}{2\sigma_1^2}\right)\mathrm{d}t$ and a probability that a ship's position is within two parallel lines whose distances from the

position line Y are r_1 and r_2 is shown by $\dfrac{1}{\sqrt{2\pi}\sigma_2}\displaystyle\int_{r_1}^{r_2}\exp\left(-\dfrac{r^2}{2\sigma_2^2}\right)\mathrm{d}r$.

Therefore, the probability that the ship's position lies within the parallelogram $(ABCD)$ formed by thin bands whose distances from X are t_1 and t_2 and the parallel lines whose distances from Y are r_1 and r_2 is given by

$$P=\frac{1}{2\pi\sigma_1\sigma_2}\int_{t_1}^{t_2}\mathrm{e}^{-\frac{t^2}{2\sigma_1^2}}\,\mathrm{d}t\int_{r_1}^{r_2}\mathrm{e}^{-\frac{r^2}{2\sigma_2^2}}\,\mathrm{d}r$$

where the following relations exist

$$r_1=t\cos\varphi-\sqrt{R^2-t^2}\sin\varphi,\quad r_2=t\cos\varphi+\sqrt{R^2-t^2}\sin\varphi,\quad t=\frac{1}{2}(t_1+t_2).$$

The probability that the ship's position lies within a cricle of radius R is obtain-

ed by adding the numerous probabilities within the parallelogram. Now, he considers the relation between σ_1 and σ_2 as $\sigma_2 = n\sigma_1$ $(n \geq 1)$, and the above-mentioned calculations were carried out by taking $\Delta t (= t_2 - t_1)$ as $0.05\sigma_1$. Then a probability $P(R)$ within a circle of a given radius R is calculated, and R which satisfies the relation $P(R) = 0.95$ can be obtained by the accumulation of the above-stated calculations.

Thus when the radius R of the 95 per cent probability circle is given, from $R = K\sigma_1\sqrt{1+n^2} \csc \varphi$ the coefficient K corresponding to an arbitrary angle and an accuracy ratio (n) is easily computed. Then the greater n may be, the more easily he can know every detail. To do that, however, extensive calculations are required. Therefore, the author examined the cases of $n = 1, 2, 3, 5, 7.5$ and 10, and as to the other cases he solved them by means which he will describe after.

Coefficient K and radius R given in the above-stated probability integrations are presented in Table 4.1, and the relation between K and the angle of cut for various of $n = \sigma_2/\sigma_1$ is shown in Fig. 4.3, and K is an asymptote to 1.9600 with an increase of σ_2/σ_1. It is also natural that the percentage of error of K which is obtained by the above-mentioned numerical integration becomes smaller as Δt decreases, and in the case of $\Delta t = 0.05\sigma_1$ which the author examined, the percentage was 0.015% under the condition of $\sigma_1 = \sigma_2$ and $\varphi = 90°$. As to the other combinations, it is impossible for him to compare them because no theoritical values can be obtained. They are, however, considered to be smaller in view of the fact that a radius is larger than the radius (in the case of $\sigma_1 = \sigma_2$, $\varphi = 90°$) always, so that the method of calculation satisfies an accuracy which is needed and sufficient.

Then an estimation of K for σ_2/σ_1 except that σ_2/σ_1 is in Table 4.1, is done from Fig. 4.4, and R is of course calculated by the equation $R = K\sqrt{\sigma_1^2 + \sigma_2^2} \csc \varphi$ and the estimated K, but it is easier for him to go directly by the following means.

Table 4.1. *Radius (R) and coefficient(K) of 95 per cent probability circle.*
φ: angle of cut, unit of R: σ_1

| σ_2/σ_1	φ	10°	20°	30°	40°	50°	60°	70°	80°	90°
1	K	1.9550	1.9385	1.9119	1.8762	1.8339	1.7930	1.7576	1.7371	1.7308
	R	15.922	8.015	5.408	4.128	3.386	2.928	2.645	2.495	2.448
2	K	1.9566	1.9462	1.9298	1.9085	1.8848	1.8608	1.8401	1.8257	1.8219
	R	25.195	12.724	8.630	6.639	5.502	4.805	4.379	4.145	4.074
3	K	1.9582	1.9523	1.9434	1.9320	1.9196	1.9076	1.8974	1.8906	1.8882
	R	35.661	18.051	12.291	9.505	7.924	6.965	6.385	6.071	5.971
5	K	1.9590	1.9569	1.9533	1.9488	1.9443	1.9394	1.9356	1.9331	1.9320
	R	57.525	29.175	19.920	15.459	12.942	11.419	10.503	10.009	9.851
7.5	K	1.9596	1.9586	1.9569	1.9549	1.9527	1.9506	1.9489	1.9478	1.9474
	R	85.384	43.329	29.613	23.011	19.287	17.042	15.692	14.965	14.734
10	K	1.9598	1.9592	1.9582	1.9571	1.9558	1.9547	1.9537	1.9531	1.9529
	R	113.42	57.568	39.360	30.599	25.659	22.683	20.895	19.931	19.626
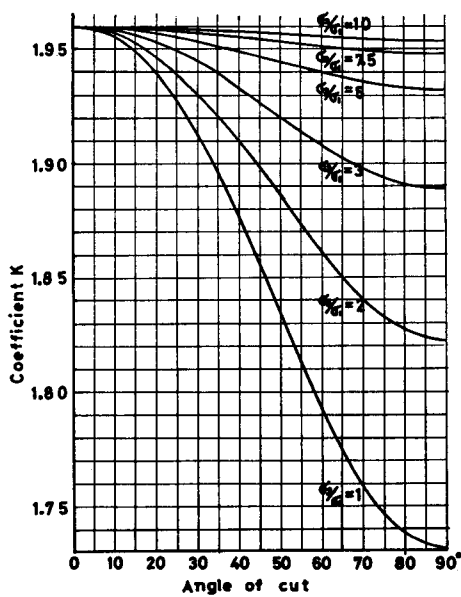
Fig. 4.3.　95 per cent probability circle, K against angel of cut.
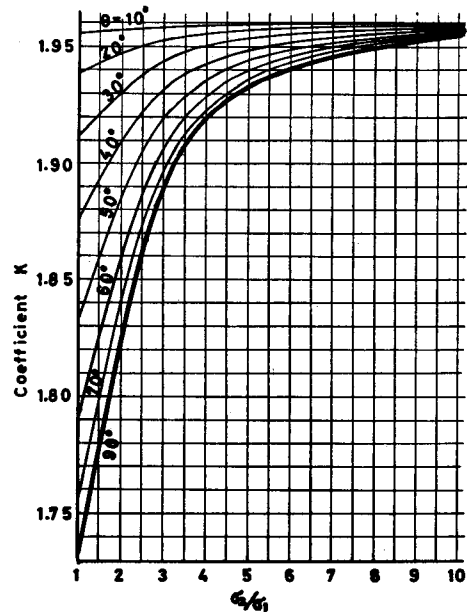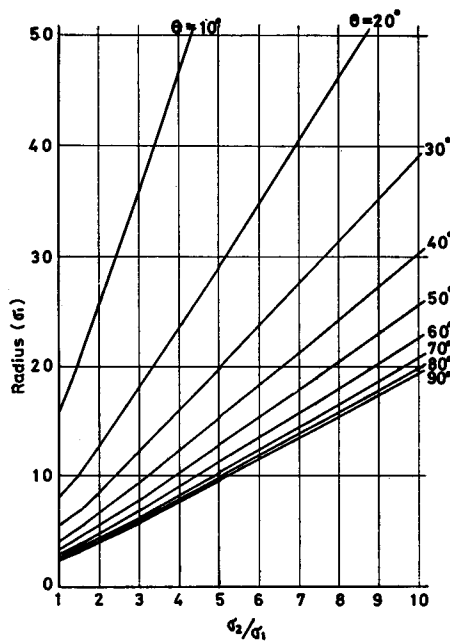

Fig. 4.4.　95 per cent probability circle, K against σ_2/σ_1.

Fig. 4.5.　Radius of the 95 per cent circle against σ_2/σ_1.
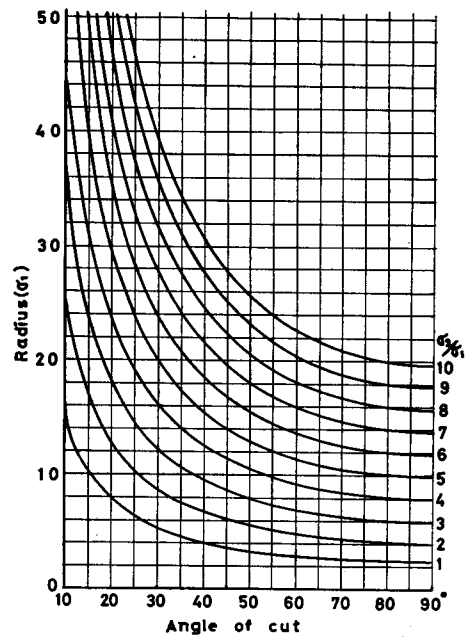

Fig. 4.6.　Radius of the 95 per cent circle against angle of cut.

In other words, if he takes σ_2/σ_1 in the abscissa, R in the ordinate and plot values in Table 4.1, they are almost on straight lines as shown in Fig. 4.5, so that the estimated values corresponding to arbitrary σ_2/σ_1 are given easily. (then R in case of $\sigma_2/\sigma_1=1.5$ is calculated by estimated K in Fig. 4.4) The results are shown in Fig. 4.6 each 1 interval of σ_2/σ_1 being from 1 to 10. As each element of the 95 per cent probability circle is defined by the above-stated means, the author will describe the method to draw an error boundary concretely and the result.

4.4.2 *In the case when position lines are equally accurate[31]*

(1) Error boundary of a ship's position fixed by two position lines

A position gotten by the simultaneous observations of two heavenly bodies or by observations at intervals at a fixed point is within a circle shown in Table 4.2 with the probability of 95 per cent because the standard deviation of each position line is $0'.75$. Moreover, in the case of the cross bearing method, if he considers the distance of an observation point from each object as d, the calculated results are indicated in Table 4.2 as the standard deviation of bearing line is $0.01745d$.

Table 4.2. *Radius of 95 per cent probability circle.*
R_a: *position fixed by two astronomical position lines,*
R_c: *position fixed by two compass bearings, φ: angle of cut*

φ	10°	20°	30°	40°	50°	60°	70°	80°	90°
R_a	$11'.94$	$6'.01$	$4'.06$	$3'.10$	$2'.54$	$2'.20$	$1'.98$	$1'.87$	$1'.84$
R_c	$0.278d$	$0.140d$	$0.094d$	$0.072d$	$0.059d$	$0.051d$	$0.046d$	$0.044d$	$0.043d$

(2) Error boundary of a ship's position fixed by three position lines

In order that the probability ellipse of a ship's position fixed by three position lines coincide with that by two position lines, both major diameters and minor diameters between them must be equal to each other. Now, if he considers the probability that a ship's position is in each error boundary as P, the angle of cut of two position lines as φ, and the intersecting angles in the case of three position lines as θ_1, θ_2, θ_3, the following simultaneous equations are brought forth, that is

$$\sigma'\sqrt{\log\left(\frac{1}{1-P}\right)}\,\operatorname{cosec}\frac{\varphi}{2}=\frac{2\sigma\sqrt{\log\left(\frac{1}{1-P}\right)}}{\sqrt{3-\sqrt{9-4(\sin^2\theta_1+\sin^2\theta_2+\sin^2\theta_3)}}} \qquad (4.14)$$

$$\sigma'\sqrt{\log\left(\frac{1}{1-P}\right)}\,\sec\frac{\varphi}{2}=\frac{2\sigma\sqrt{\log\left(\frac{1}{1-P}\right)}}{\sqrt{3+\sqrt{9-4(\sin^2\theta_1+\sin^2\theta_2+\sin^2\theta_3)}}} \qquad (4.15)$$

if (4.14) is divided by (4.15),

$$\frac{\operatorname{cosec}\dfrac{\varphi}{2}}{\sec\dfrac{\varphi}{2}} = \sqrt{\frac{3+\sqrt{9-4(\sin^2\theta_1+\sin^2\theta_2+\sin^2\theta_3)}}{3-\sqrt{9-4(\sin^2\theta_1+\sin^2\theta_2+\sin^2\theta_3)}}}\,,$$

and if he rearranges this relation

$$\sin\varphi = \frac{2}{3}\sqrt{\sin^2\theta_1+\sin^2\theta_2+\sin^2\theta_3}$$

is obtained, and then if he substitutes the relation into the equation (4.14)

$$\sigma'\operatorname{cosec}\frac{\varphi}{2} = \frac{2\sigma}{\sqrt{3-\sqrt{9-9\sin^2\varphi}}} = \frac{2\sigma}{\sqrt{3-3\cos\varphi}}\ \text{is gotten, and finally}$$

$$\sigma' = \sqrt{\frac{2}{3}}\,\sigma$$

is led. From this matter, the radius (R) of a 95 per cent probability circle of a ship's position fixed by three position lines is expressed as

$$R = \frac{\sqrt{3}\,K'\sigma}{\sqrt{\sin^2\theta_1+\sin^2\theta_2+\sin^2\theta_3}} \qquad (4.16)$$

Where K' is a proporitional constant corresponding to angles $\sin^{-1}\dfrac{2}{3}\sqrt{\sin^2\theta_1+\sin^2\theta_2}$ $+\sin^2\theta_3$ and is obtained from Fig. 4.3 and coefficients K' corresponding to combinations of θ_1, θ_2 and θ_3 are indicated in Table 4.3.

Table 4.3. *Values of coefficient K'.*

θ_2 \ θ_1	10°	20°	30°	40°	50°	60°	70°	80°	90°
10°	1.946	1.927	1.899	1.866	1.829	1.795	1.771	1.756	1.756
20°	1.927	1.904	1.874	1.838	1.804	1.776	1.756	1.749	1.756
30°	1.899	1.874	1.842	1.809	1.780	1.756	1.745	1.742	1.756
40°	1.866	1.838	1.809	1.781	1.756	1.742	1.737	1.742	1.756
50°	1.829	1.804	1.780	1.756	1.740	1.734	1.734	1.740	1.756
60°	1.795	1.776	1.756	1.742	1.734	1.731	1.734	1.742	1.756
70°	1.771	1.756	1.745	1.737	1.734	1.734	1.737	1.745	1.756
80°	1.756	1.749	1.745	1.742	1.740	1.742	1.745	1.749	1.756
90°	1.756	1.756	1.756	1.756	1.756	1.756	1.756	1.756	

(a) Error boundary of a determined position by celestial observations

As the radius of the 95 per cent probability circle of a position determined by simultaneous observations of three heavenly bodies is expressed by $\sqrt{3}K'\sigma/\sqrt{\sin^2\theta_1}$ $+\sin^2\theta_2+\sin^2\theta_3$, the radii of circles corresponding to combinations of θ_1, θ_2 and θ_3 are indicated in Table 4.4 by substituting $\sigma=0'.75$ and the values of Table 4.3 into the equation.

Table 4.4. *Radius of 95 per cent probability circle by three astronomical position lines.* $(\sigma=0\overset{,}{.}75)$

θ_2 \ θ_1	10°	20°	30°	40°	50°	60°	70°	80°	90°
10°	6$\overset{,}{.}$00	3$\overset{,}{.}$97	2$\overset{,}{.}$96	2$\overset{,}{.}$39	2$\overset{,}{.}$03	1$\overset{,}{.}$81	1$\overset{,}{.}$68	1$\overset{,}{.}$61	1$\overset{,}{.}$61
20°	3.97	3.07	2.49	2.11	1.86	1.70	1.61	1.58	1.61
30°	2.96	2.49	2.14	1.89	1.72	1.61	1.56	1.56	1.61
40°	2.39	2.11	1.89	1.73	1.61	1.55	1.53	1.55	1.61
50°	2.03	1.86	1.72	1.61	1.54	1.51	1.51	1.54	1.61
60°	1.81	1.70	1.61	1.55	1.51	1.50	1.51	1.55	1.61
70°	1.68	1.61	1.56	1.53	1.51	1.51	1.53	1.56	1.61
80°	1.61	1.58	1.56	1.55	1.54	1.55	1.56	1.58	1.61
90°	1.61	1.61	1.61	1.61	1.61	1.61	1.61	1.61	

From the view-point of valuing a position, it is desirable that a ship's position lies in the minimum area with a probability required, and this fundamental idea must not be overlooked for convenience of use. Then if he compares the areas of 95 per cent probability circles descrived in this item and the areas of 95 per cent probability ellipses $(=10.588/\sqrt{\sin^2\theta_1+\sin^2\theta_2+\sin^2\theta_3}$ square miles), the results are indicated in Table 4.5. The limit of the area ratio to keep the value as a solution indicating an error boundary is not determined, but in the case of determining a position, the selection of objects is considered to be important to get a highly accurate position, so if three intersecting angles are all acute angles, the area ratios are less than 1.09. Accordingly, the method to indicate error boundaries with circles is considered to be of satisfactory value in practice.

Table 4.5. *Ratio of areas.* (95% *probability circle*/95% *probability ellipse*)

θ_2 \ θ_1	10°	20°	30°	40°	50°	60°	70°	80°	90°
10°	4.50	2.95	2.17	1.72	1.43	1.25	1.14	1.09	1.09
20°	2.95	2.26	1.80	1.50	1.29	1.16	1.09	1.07	1.09
30°	2.17	1.80	1.52	1.32	1.18	1.09	1.05	1.05	1.09
40°	1.72	1.50	1.32	1.18	1.09	1.04	1.02	1.04	1.09
50°	1.43	1.29	1.18	1.09	1.04	1.01	1.01	1.04	1.09
60°	1.25	1.16	1.09	1.04	1.01	1.00	1.01	1.04	1.09
70°	1.14	1.09	1.05	1.02	1.01	1.01	1.02	1.05	1.09
80°	1.09	1.07	1.05	1.04	1.04	1.04	1.05	1.07	1.09
90°	1.09	1.09	1.09	1.09	1.09	1.09	1.09	1.09	

(b) Error boundary of a ship's position fixed by cross bearings

If he puts the distance of an observation point from an object as d, the standard deviation of bearing for 1°, the radius of the 95 per cent probability circle of a ship's position fixed by cross bearing method is expressed as $0.03023K'd/\sqrt{\sin^2\theta_1+\sin^2\theta_2+\sin^2\theta_3}$, and if he substitutes the values of K' shown in Table 4.3 into this equation and calculates by affording θ_1, θ_2, θ_3, the radii of the circles are indicated in Table 4.6.

Table 4.6. *Radius of 95 per cent probability circle.* (unit: d)

θ_2 \ θ_1	10°	20°	30°	40°	50°	60°	70°	80°	90°
10°				0.0556	0.0473	0.0421	0.0390	0.0375	0.0375
20°			0.0580	0.0491	0.0433	0.0396	0.0375	0.0369	0.0375
30°		0.0580	0.0498	0.0440	0.0400	0.0375	0.0364	0.0364	0.0375
40°	0.0556	0.0491	0.0440	0.0401	0.0375	0.0360	0.0356	0.0360	0.0375
50°	0.0473	0.0433	0.0400	0.0375	0.0359	0.0352	0.0352	0.0359	0.0375
60°	0.0421	0.0396	0.0375	0.0360	0.0352	0.0349	0.0352	0.0360	0.0375
70°	0.0390	0.0375	0.0364	0.0356	0.0352	0.0352	0.0356	0.0364	0.0375
80°	0.0375	0.0369	0.0364	0.0360	0.0359	0.0360	0.0364	0.0369	0.0375
90°	0.0375	0.0375	0.0375	0.0375	0.0375	0.0375	0.0375	0.0375	

Figures such as 3.5~5.8% which are indicated in the table are very simple and convenient, however, these are radii of circles concerning the case when three position lines are all equal. Accordingly, the figures are applicable in practice to the combinations in which the distances of an observation point from the three objects are almost equal, but if the distances have large differences it is impossible to show any error boundaries simply by means of a single quantity. But if objects such as the intersecting angles of the position lines are extremely small are not chosen, the radii of the circles are almost within 4% of distances; accordingly, even if an indicated radius is treated as the ratio to the distance of an observation point from the farthest object, an error of radius in itself is small and the probability exceeds 95% undoubtedly, therefore in practice the means is considered to be admitted.

4.4.3 *In the case of unequally accurate position lines*[32]

(1) Error boundary of a determined position by horizontal sextant angles
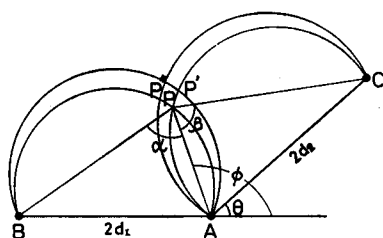

Fig. 4.7. Relation between observation point and three objects.

In Fig. 4.7, a ship's position is determined as the intersection P of two circular arcs by observing the horizontal angles α between object A and B and β between A and C; now if the observed value α includes an error $\Delta\alpha$, the intersection shifts from P to P' and similarly if β includes $\Delta\beta$ the intersection shifts to P''. Then the lengths of $\widehat{PP'}, \widehat{PP''}$ are expressed by equations (3.7) (3.8) as follows,

$$\widehat{PP'} = \frac{2d_1 d_2 \sin^2 \phi \Delta\alpha}{(d_1+d_2 \cos\theta - d_2 \cot\beta \sin\theta)\sin^2\alpha \sin\beta}\,,$$

$$\widehat{PP''} = \frac{2d_1 d_2 \sin\phi \sin(\phi-\theta)\Delta\beta}{(d_1+d_2 \cos\theta - d_2 \cot\beta \sin\theta)\sin\alpha \sin^2\beta}$$

where if he puts $d_1=d_2$, $\Delta\alpha=\Delta\beta$ to simplify the relations,

$\dfrac{\widehat{PP'}}{\widehat{PP''}} = \dfrac{\sin \beta}{(\cos \theta - \sin \theta \cot \phi) \sin \alpha}$ is led, then the relation ϕ and d_1, d_2, α, β, θ is expressed by equation (3.6) such as $\cot \phi = \dfrac{\cot \alpha - \sin \theta - \cot \beta \cos \theta}{1 + \cos \theta - \cot \beta \sin \theta}$. And by substituting this relation into the former equation

$$\frac{\widehat{PP'}}{\widehat{PP''}} = \frac{(1 + \cos \theta - \cot \beta \sin \theta) \sin \beta}{(\cos \theta + \cos^2 \theta - \cot \beta \sin \theta \cos \theta - \sin \theta \cot \alpha + \sin^2 \theta + \cot \beta \sin \theta \cos \theta) \sin \alpha}$$

$$= \frac{(1 + \cos \theta - \sin \theta \cot \beta) \sin \beta}{(1 + \cos \theta - \sin \theta \cot \alpha) \sin \alpha}$$

is obtained.

Next, as the most typical arrangement of three objects, the case of $\theta = 0°$ which is a combination of three objects lying on a straight line is studied. In that case, the accuracy ratio $(\widehat{PP'}/\widehat{PP''})$ of each position line is expressed as $\sin \beta / \sin \alpha$, and the lengths of $\widehat{PP'}$, $\widehat{PP''}$ are respectively $d \sin^2 \phi \varDelta \alpha / \sin^2 \alpha \sin \beta$, $d \sin^2 \phi \varDelta \beta / \sin \alpha \sin^2 \beta$, and $\sin^2 \phi$ is obtained as $4/\{4 + (\cot \alpha - \cot \beta)^2\}$ based on the equation $\cot \phi = (\cot \alpha - \cot \beta)/2$.

Therefore

$$\widehat{PP'} = \frac{4d\varDelta \alpha}{\{4 + (\cot \alpha - \cot \beta)^2\} \sin^2 \alpha \sin \beta} \ ,$$

$$\widehat{PP''} = \frac{4d\varDelta \beta}{\{4 + (\cot \alpha - \cot \beta)^2\} \sin \alpha \sin^2 \beta}$$

are gotten. When the standard deviations of each position line are pursued from these $\widehat{PP'}$, $\widehat{PP''}$, if the observation of α and β is carried out at the same time, σ_1 and σ_2 are expressed as follows:

$$\sigma_1 = \frac{4d \sin (\alpha + \beta) \varDelta \alpha}{\{4 + (\cot \alpha - \cot \beta)^2\} \sin^2 \alpha \sin \beta} \ , \ \sigma_2 = \frac{4d \sin (\alpha + \beta) \varDelta \beta}{\{4 + (\cot \alpha - \cot \beta)^2\} \sin \alpha \sin^2 \beta}$$

And if he substitutes these relations into the indicating equation of the radius, $R = K\sqrt{\sigma_1^2 + \sigma_2^2} \ \mathrm{cosec} \ \varphi$, then

$$R = K \sqrt{\left[\frac{4d \sin (\alpha + \beta) \varDelta \alpha}{\{4 + (\cot \alpha - \cot \beta)^2\} \sin^2 \alpha \sin \beta} \right]^2 + \left[\frac{4d \sin (\alpha + \beta) \varDelta \beta}{\{4 + (\cot \alpha - \cot \beta)^2\} \sin \alpha \sin^2 \beta} \right]^2} \ \mathrm{cosec} \ (\alpha + \beta)$$

$$= \frac{4Kd\varDelta \alpha \sqrt{\sin^2 \alpha + \sin^2 \beta}}{\{4 + (\cot \alpha - \cot \beta)^2\} \sin^2 \alpha \sin^2 \beta}$$

is given. (where $\varDelta \beta$ was treated as being equal to $\varDelta \alpha$)

Since $\varDelta \alpha$ differs from the shape of the three objects and from the distances of an observation point from the objects on a chart, it is impossible to reach a uniform conclusion; now if he puts $\varDelta \alpha$ as $20'$ and d for 1,

$$R = \frac{0.02327 K \sqrt{\sin^2 \alpha + \sin^2 \beta}}{\{4 + (\cot \alpha - \cot \beta)^2\} \sin^2 \alpha \sin^2 \beta}$$

is given, according to the above-mentioned equation. Accordingly, if α and β are given at will, K corresponding to them is determined and R is computed, and consequently the epitome is indicated in Table 4.7.

Table 4.7. *Radius of 95 per cent probability circle. (unit: $d/100$, $\theta=0°$)*

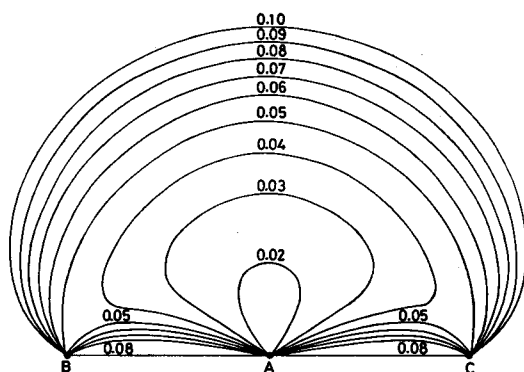| β \ α	10°	20°	30°	40°	50°	60°	70°	80°	90°	100°	110°	120°	130°	140	150°
10°	305	38.9	16.2	10.0	7.3	5.9	5.0	4.5	4.2	4.0	4.0	4.1	4.3	4.8	5.4
20°	38.9	38.6	17.8	10.1	6.9	5.3	4.4	3.8	3.5	3.2	3.2	3.2	3.3	3.5	3.9
30°	16.2	17.8	11.8	7.7	5.4	4.2	3.5	3.0	2.8	2.6	2.6	2.6	2.7	2.9	
40°	10.0	10.1	7.7	5.4	4.1	3.3	2.8	2.5	2.3	2.2	2.2	2.2	2.3		
50°	7.3	6.9	5.4	4.1	3.2	2.7	2.3	2.1	2.0	2.0	1.9	2.0			
60°	5.9	5.3	4.2	3.3	2.7	2.3	2.0	1.9	1.8	1.8	1.8				
70°	5.0	4.4	3.5	2.8	2.3	2.0	1.9	1.8	1.7	1.7					
80°	4.5	3.8	3.0	2.5	2.1	1.9	1.8	1.7	1.6						
90°	4.2	3.5	2.8	2.3	2.0	1.8	1.7	1.6							

Fig. 4.8. Accuracy contours for horizontal sextant angles. (unit: d)

Further combinations of α and β in which R takes 2, 3, $\cdots$, 10 per cent of d are pursued from the R-curve; those combinations are shown in Fig. 4.8 as accuracy contours. Moreover as these figures are computed and constructed, putting $\Delta\alpha$ for 20', if $\Delta\alpha$ is regarded as 30', 40', the numerical values in the figures can be read with a good understanding of the content only by multiplying by 1.5, 2.0.

Next is the problem concerning the ratio between area (S_1) of the 95% probability circle and area (S_2) of the 95% probability ellipse, where they are expressed as

$$S_1 = \frac{16\pi K^2 d^2 (\Delta\alpha)^2 (\sin^2 \alpha + \sin^2 \beta)}{\{4 + (\cot \alpha - \cot \beta)^2\}^2 \sin^4 \alpha \sin^4 \beta}, \quad S_2 = \frac{16(2.4477)^2 \pi d^2 (\Delta\alpha)^2 \sin(\alpha+\beta)}{\{4 + (\cot \alpha - \cot \beta)^2\}^2 \sin^3 \alpha \sin^3 \beta},$$

therefore the ratio is as follows:

$$\frac{S_1}{S_2} = \frac{0.1669 K^2 (\sin^2 \alpha + \sin^2 \beta)}{\sin \alpha \sin \beta \sin(\alpha+\beta)}$$

and the epitome is indicated in Table 4.8.

(2) Error boundary of a ship's position fixed by the Loran position lines

If the author puts the included angles formed at an observation point by the

Table 4.8.   *Ratio of areas. (95% probability circle/95% probability ellipse)*

β \ α	10°	20°	30°	40°	50°	60°	70°	80°	90°	100°	110°	120°	130°	140°	150°
10°	3.7	3.1	3.1	3.2	3.4	3.5	3.6	3.7	3.8	3.9	4.1	4.3	4.6	5.1	6.0
20°	3.1	1.8	1.6	1.6	1.7	1.7	1.8	1.9	2.1	2.3	2.5	2.8	3.4	4.5	
30°	3.1	1.6	1.2	1.2	1.2	1.3	1.4	1.5	1.7	1.9	2.3	2.9	4.0		
40°	3.2	1.6	1.2	1.0	1.1	1.1	1.2	1.4	1.7	2.0	2.6	3.9			
50°	3.4	1.7	1.2	1.1	1.0	1.1	1.3	1.6	1.9	2.6	3.8				
60°	3.5	1.7	1.3	1.1	1.1	1.2	1.5	1.9	2.5	3.7					
70°	3.6	1.8	1.4	1.2	1.3	1.5	1.8	2.5	3.7						
80°	3.7	1.9	1.5	1.4	1.6	1.9	2.5	3.7							
90°	3.8	2.1	1.7	1.7	1.9	2.5	3.7								

master station and the slave stations as φ_1, φ_2 and the standard deviation of measurement of time difference for 1.5 μ.s., the radius of the 95 per cent probability circle is expressed as

$$R(\text{n.m.}) = 0.121K \cosec \frac{1}{2}(\varphi_1+\varphi_2) \sqrt{\cosec^2 \frac{\varphi_1}{2} + \cosec^2 \frac{\varphi_2}{2}}$$

and K are coefficients fixed by $(\varphi_1+\varphi_2)/2$ and $\cosec (\varphi_2/2) \sin (\varphi_1/2)$.

Accordingly, if φ_1 and φ_2 are given at one's will, R is calculated, and if the points of the radii which take 0'.5, 1', 2', 3', 4' founded on curves of the radii gotten by such a method are connected, they take the form of accuracy contours such as Fig. 4.9 (a)(b)(c)(d)(e). This is considered appropriate for ground wave observations (Loran A): contours for sky wave observations (Loran A) and for observations by Loran C would have to be appropriately scaled.

Next, as to the ratio of areas, area (S_1) of the 95% probability circle is expressed as $\pi K^2\sigma^2 \cosec^2\{(\varphi_1+\varphi_2)/2\} \{\cosec^2(\varphi_1/2)+\cosec^2(\varphi_2/2)\}$ while area (S_2) of the 95% probability ellipse is $\pi(2.4477)^2\sigma^2 \cosec (\varphi_1/2) \cosec (\varphi_2/2) \cosec\{(\varphi_1+\varphi_2)/2\}$; accordingly, their ratio is expressed as follows;

$$\frac{S_1}{S_2} = 0.1669K^2 \sin \frac{\varphi_1}{2} \sin \frac{\varphi_2}{2} \cosec \frac{1}{2}(\varphi_1+\varphi_2)\left(\cosec^2 \frac{\varphi_1}{2} + \cosec^2 \frac{\varphi_2}{2}\right)$$

and their outlines are indicated in Table 4.9.

Table 4.9.   *Ratio of areas. (95% probability circle/95% probability ellipse)*

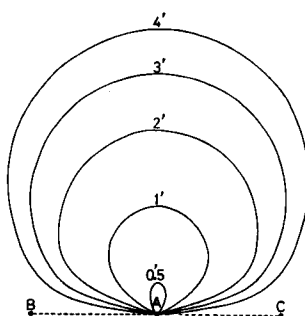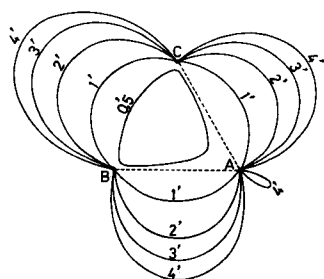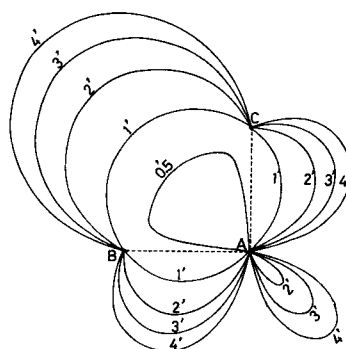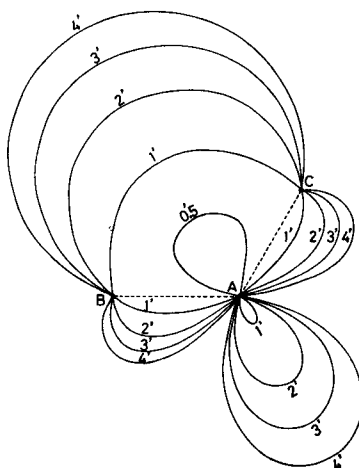| φ_2 \ φ_1	10°	30°	50°	70°	90°	110°	130°	150°	170°	180°
10°	7.3	6.2	6.4	6.7	6.8	7.0	7.1	7.2	7.3	7.4
20°	6.1	3.2	3.1	3.2	3.3	3.4	3.5	3.6	3.7	3.8
30°	6.2	2.4	2.2	2.1	2.2	2.2	2.3	2.4	2.6	2.6
50°	6.4	2.2	1.5	1.4	1.3	1.4	1.5	1.6	1.7	1.8
70°	6.7	2.1	1.4	1.1	1.1	1.1	1.2	1.3	1.5	1.6
90°	6.8	2.2	1.3	1.1	1.0	1.1	1.2	1.4	1.6	1.8

Fig. 4.9(a).　Accuracy contours for Loran position: angle of base line 180°.　$\sigma=1.5\,\mu.\mathrm{s}.$
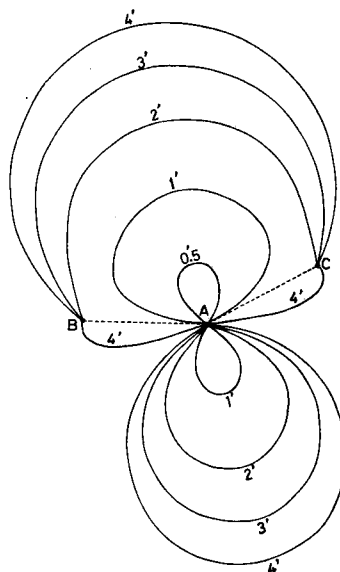

(b)　angle of base line 60°.

(c) angle of base line 90°.

(d)　angle of base line 120°.

(e) angle of base line 150°.

In addition, the author wishes to write that an error of the Loran position line actually includes a certain systematic error besides a random error and this is not clear at present; therefore the discussion concerning the facts of Fig. 4.9 must be done with great care.

4.5   Discussion

a)   The theoretical solution of the error boundary of a determined position is an ellipse.

b)   In the case of indicating an error boundary with a single quantity, if it is expressed by the area of an ellipse it is easy to compare the relative merits and demerits of the respective error boundary but the shape and directions of the axes cannot be known in brief.

c)   Concerning the 95 per cent radial error system, since a combination by which the radius of a circle is larger than the semi-major of an ellipse arises frequently, it is difficult to find and value a practical solution; moreover, as this system is a method to indicate error boundaries concerning determined positions by two position lines, a valuation is still more difficult.

d)   The 95 per cent probability circle system has a weak point, that is its wide region compared with the ellipse as shown in tables of the area ratios, but this question will be solved by considering the selection of objects.   On the other hand it has the advantage of indicating an error boundary by a single quantity.

e)   The case in which the area of a probability circle is by far larger than that of the ellipse is explained by the shape of the ellipse which is lank.   Theoretically if the probability density or the area of an ellipse take the same value, the accuracy of position is treated as equal even if an error boundary draws a lank ellipse or a round shape such as a circle; but in practice if the eccentricity of an ellipse is close to zero, it is more advantageous than the other cases.

This fact arises from the difference in view-point, accordingly, one does not draw any conclusion but it is necessary to consider it in the case of selecting objects.

5.   Conclusion

To conclude his research the author wishes to clarify the relation among the various chapters of his paper from the standpoint of discussing a ship's position.

A fishing boat's position is indicated by two methods.   One of them is by geographical co-ordinates.   When determining the position of a fishing ground and an observation point on the ocean or in the offing, this method is used because no expendient can be found.

The second method is by polar co-ordinates that is a datum point is adopted as a pole.   In case of engaging in trawling in coastal sea or the observation with the close intervals of measuring points, it is effective to install the datum point artifically, and to express the position of each point with the relative point to it. This method has the advantage that the technique is simple and it is also easy to raise the accuracy of each position by an exact determination of the datum point.

In the case of watching a fishing gear (salmon gill-net, tuna long line), after it has been cast, a forecast of the drifting phenomenon and an estimation of the drifting position must be indicated by the relative position to the fishing gear.   Of course it is possible to plot both estimated position on the geographical co-ordinates, but if the absolute positions are omitted, there is no trouble at all, since the necessary matter in the case of watching a fishing gear is the relation between the ship and the gear.

As such, the co-ordinate systems indicating positions are different, but in the end both are the same for the following reason; the former is a method to plot each observation point on the earth directly, and the latter is a method by which each point is determined in relation to a datum point and is replaced in the lump by new co-ordinates, by fixing the datum point on the geographical co-ordinates. The difference is therefore a mere matter of means.

Secondly, the relation between the determination of the position and the confidence degree of a determined position is just similar to it, obversely and reversely.   Namely, as the probability of a determined position has a reciprocal relation to an area of probability ellipse, the accuracy of a determined position is directly related to the size of an ellipse.   Accordingly there is nothing but a difference of expression whether the accuracy of a position is caught qualitatively or quantitatively.   As such, a probability density corresponds to the theoretical solution of an error boundary, and the fact originates a fundamental theory for determining a position.

But in the step of indicating an error boundary practically, some questions arise.   If it is treated as question in the case of a few examples, it is possible to solve it theoretically but when the valuation of many positions is required and has to be materialized, it is almost impossible to solve.   The author advocated the probability circle system as a method to solve the question.   As mentioned previously an error boundary of a determined position need not to be considered and is not considered in practice for a sea-going vessel except for particular cases. Generally speaking, a valuation of the accuracy is required in particular cases, and in such cases, as a determination method is carried out under fair considerations, much contradiction is not felt in replacing an ellipse with a circle.   That is to say, if a weak point of the probability circle system is dissolved by consideration of use, it can be closely akin to the indicating method of probability density.   Conversely speaking, a combination of position lines which does not satisfy such a condition, in other words if the eccentricity of the ellipse is large, such a combination must be avoided to the utmost.

Then the accuracy of an estimated drifting position may be valuated either by a probability density or an error boundary, and in this case an indication by the elements of an error boundary is considered more pertinent, because when a fishing boat closes a drift and starts to move toward a datum point, what is required is the direction and the distance to the point and its accuracy of estimated value. And in this case, the directions of the axes of an error boundary are a primitive line and a rectangular direction to it; accordingly, the shape and direction of the error boundary can be known easily.   The length on the primitive line shows the difference in the time required to arrive at the datum point and the length on the

rectangular direction shows the width of the watching region.   When the angle intersecting the position lines is 90°, as it is in this case, it is easy to express an error boundary by the ellipse system, but it is simpler by the probability circle.   In any event, the effect of using the length on the primitive line brings only small errors to the arrival time, accordingly, it is out of the question in the case of watching a fishing gear.   The length on the rectangular direction to a course shows a priority direction of watching when the datum point enters within visible distance and opens to watch, and an existential probability of the point forms a normal distribution around the direction of the ship's head.

Thus, regardless of estimated position or determined position, and of the means and methods to obtain them, it seems possible to judge the effectiveness and the value of the methods only when the evaluation and the close examination conforming to the probability theory are carried out.

References

1) Yasui, Z. (1940). [On a ship's drifting]. *Umi Sora.* 20, 177–181. (In Japanese).
2) Kosaka, T., Komine, S. and Osugi, I. (1958). On the effect of wind and wave to the observation ship at TANGO POINT. *J. naut. Soc. Japan.* 18, 1–18.
3) Saito, S., Nakane, S. and Fujii, T. (1963). Observation on the drifting of ships due to wind action. *Ibid.* 30, 83–90.
4) Yamaguchi, Y. and Kobayashi, Y. (1967). The way of watching tuna long lines in consideration of drifting of ships due to wind action. *Ibid.* 37, 49–54.
5) Hiraiwa, T., Fujii, T. and Saito, S. (1967). An experimental study of drift and leeway. *J. Inst. Navig.* 20, 131–145.
6) Sameshima, N. and Kawamoto, F. (1950). Probability ellipse of the ship's position, fixed from astronomical position lines. *J. naut. Soc. Japan.* 2, 16–22.
7) Trow, G.H. and Jessel, A.H. (1948). The presentation of fixing accuracy of navigation systems. *J. Inst. Navig.* 1, 313–337.
8) Anderson, E.W. (1952). The treatment of navigational errors. *Ibid.* 5, 103–124.
9) Parker, J.B. (1952). The treatment of simultaneous position data in the air. *Ibid.* 5, 235–249.
10) Hiraiwa, T. (1967). On the 95 per cent probability circle of a vessel's position. *Ibid.* 20, 258–270.
11) Hiraiwa, T., Fujii, T., Yamamoto, S., Masuda, K., Ishii, K. and Sasaki, S. (1971). A method on watching fishing gear by a ship's own characteristic drifting. *J. naut. Soc. Japan,* 45, 47–53.
12) Hiraiwa, T., Fujii, T., Yamamoto, S., Masuda, K., Ishii, K. and Yoneta, K. (1972). Drifting of the Oshoro Maru. *Ibid.* 48, 49–56.
13) Watanabe, Y. (1932). On the effective wave slope and the motion of the centre of gravity of a ship when rolling on waves. *J. Soc. nav. Archit. Japan.* 49, 61–86.
14) Dodimead, A.J., Favorite, F. and Hirono, T. (1963). Review of oceanography of the subarctic Pacific region. *Bull. int. N. Pacif. Fish. Commn.* 11, 1–195.
15) Hiraiwa, T., Saito, S., Ishii, K. and Yoneta, K. (1969). Drift when an anti-rolling tank is in operation and suspension due to wind action. *J. naut. Soc. Japan.* 41, 141–148.
16) Suehiro, K., Sato, N. and Narige, M. (1922). The yawing motion of a ship associated with the rolling amongst waves. *J. Soc. nav. Archit. Japan.* 31, 145–154.
17) Hiraiwa, T., Inaba, Y. and Sakamoto, Y. (1972). Wind tunnel experiments on the Oshoro Maru concerning the drift due to wind action. *J. naut. Soc. Japan.* 48, 43–48.
18) Hiraiwa, T., Saito, S., Ishii, K., Anma, G. and Yoneta, K. (1969). A method of estimating the relative position of a ship to her fishing gear during drifting. *Ibid.*

    42, 101–107.

19) Weinblum, G, Visitor and Denis, M. St. (1950). On the motions of ships at sea. *Trans. Soc. nav. Archit. mar. Engrs, N.Y.* **58**, 184–248.

20) Hiraiwa, T. (1969). Accuracy contours of a ship's position. *J. naut. Soc. Japan.* **41**, 55–60.

21) Hiraiwa, T. (1973). Accuracy contours of a ship's position – II. *Ibid.* **50**, 135–140.

22) Hiraiwa, T. (1955). On the treatment of systematic errors in the horizontal sextant angles method. *Ibid.* **14**, 47–54.

23) Hiraiwa, T. (1954). Study on the determination of ship's position by cross bearings. *Ibid.* **11**, 31–42.

24) Hiraiwa, T. (1955). Study on the determination of ship's position by the horizontal sextant angles method. *Ibid.* **13**, 25–34.

25) Sameshima, N. (1951). [On a ship's error about coastal navigation]. *J. Tokyo Univ. Merc. Mar.* **2**, 3–15 (In Japanese).

26) Akiyoshi, T. (1932). [A certain problem concerning a particular angle observed on the sea]. *Bull. hydrogr. Dep., Tokyo.* **121**, 511–514. (In Japanese).

27) Takigawa, F. (1933). [On a probable error of altitude of heavenly bodies observed by sextant]. *Ibid.* **126**, 219–220. (In Japanese).

28) Shibuya, K. (1941). [On the acurracy of a certain position line by astronomical observation on the sea]. *Ibid.* **225**, 211–217. (In Japanese).

29) Sameshima, N., Kosaka, T., Suzuki, W., Shoji, K. and Kawamoto, F. (1949). [An experimental study of some astronomical observation error in Izu Oshima – I]. *J. naut. Soc. Japan,* **1**, 8–14. (In Japanese).

30) Lejeune, E. (1970). Station de navigation per satellite transit 《Cerci》. *Navigation, Paris.* **18**, 117–122.

31) Hiraiwa, T. (1958). Practical solution of error boundaries of ship's position fixed by three position lines. *J. naut. Soc. Japan.* **19**, 11–18.

32) Hiraiwa, T. (1966). On the error boundaries of ship's positions by the 95% probable circle system. *Ibid.* **36**, 119–125.

33) Hiraiwa, T. (1968). Fundamental studies determining a ship's position. *Ibid.* 20th Anniversary Issue, 75–102.

34) Hiraiwa, T. (1972). On the selection between Loran fix and observed position. *Navigation, Tokyo.* **36**, 22–27.